

https://dspace.org/

Sorption of uranium and arsenic onto iron hydroxide /oxide modified zeolite

Nekhunguni, Pfano Mathews

2017

http://hdl.handle.net/10539/23603

Nekhunguni, Pfano Mathews (2017) Sorption of uranium and arsenic onto iron hydroxide /oxide modified zeolite, University of the Witwatersrand, Johannesburg, <http://hdl.handle.net /10539/23603>

Downloaded from a DSpace repository. https://dspace.org/

Sorption of uranium and arsenic onto iron hydroxide/oxide modified zeolite



By

Pfano Mathews Nekhunguni

A Dissertation submitted to the Faculty of Science, University of the Witwatersrand in fulfilment of the requirements for the award of Master of Science degree.

WITS University, Johannesburg, 2017

Declaration

I declare that this Dissertation is my own unaided work. It is being submitted for the Degree of Master of Science at the University of the Witwatersrand, Johannesburg. It has not been submitted before for any degree or examination at any other University.



Pfano Mathews Nekhunguni

This 27th of February 2017 in Johannesburg

List of publications

This dissertation is based on the following papers:

I. **Investigation of As(V) removal from acid mine drainage by iron (hydr) oxide modified zeolite**.

Pfano Mathews Nekhunguni, Nikita Tawanda Tavengwa, Hlanganani Tutu.

Journal of Environmental Management 197 (2017) 550-558

II. **Adsorption of uranium(VI) from aqueous solution using iron hydr(oxide) modified zeolite**.

Pfano Mathews Nekhunguni, Nikita Tawanda Tavengwa, Hlanganani Tutu.

(*Manuscript in preparation*)

III. **The removal of arsenic and uranium from aqueous solutions by sorption onto iron oxide coated zeolite (IOCZ)**

Bakatula, E.N, Molaudzi, R., Nekhunguni, P. and Tutu, H.

Water, Air, & Soil Pollution 228, no. 1 (2017): 5

Personal contribution to the papers

Paper I. Principal author, involved in planning, performed the sorbent preparation and characterization, sorption experiments, evaluation of the results and writing of the article. Co-authors revised the draft manuscript and made suggestions for improvement.

Paper II. Principal author, involved in planning, performed the adsorbent preparation and characterization, sorption experiments, evaluation of the results and writing of the article. Co-authors revised the draft manuscript and made suggestions for improvement.

Paper III. Principal author, involved in evaluation of the results and writing of the article. Co-author, involved in planning, performed the sorbent preparation and characterization, sorption experiments, evaluation of the results.

Abstract

Mining is an integral sector of most developing countries and it is a highly lucrative industry that has been in existence for centuries, and assumes an essential part in their economies. However, the legacy of mining in these countries has posed a threat to underground and surface water as a result of contamination arising from Acid Mine Drainage (AMD). Bearing in mind the environmental and ecological impairment posed by AMD there is a need for innovation in the treatment of AMD, to enable financially savvy treatment of the contaminated waters.

This research is focused on the extraction of U(VI), As(III) and As(V) from synthetic metal solutions as well as field removal of these metal ions by application of iron hydroxide/oxide-modified zeolite. Batch experiments were performed to evaluate the effectiveness of iron hydroxide/oxide-modified zeolite as a potential low-cost sorbent for extracting As(III), U(VI) and As(V) from AMD. The research approach was based on the possible changes that can occur to a zeolite surface that has been in contact with an iron-laden solution. Zeolite is a commonly used adsorbent, but fewer studies have explored changes that it undergoes as an adsorbent on contact with iron solutions. Thus, the study involved modifying zeolite with iron hydroxide/oxide, which are the main precipitates of iron in the environment and which can possibly alter the adsorption properties of zeolite. Batch extraction studies were performed using the modified zeolite.

In **paper I**, the synthesis of iron (hydr) oxide modified zeolite was achieved through precipitation of iron on the zeolite. The kinetic data for As(V) adsorption by iron (hydr) oxide-modified zeolite model fit well into pseudo second-order and the adsorption capacity was obtained as 0.080 mg g^{-1}. The application of iron (hydr) oxide modified zeolite on AMD for As(V) recovery showed that > 99% of As(V) was extracted from the solution. The high removal efficiency of oxyanionic arsenic species was attributed to arsenic forming complexes with iron oxyhydroxide surface on the surface of the sorbent.

Paper II dealt with adsorption of U(VI) from aqueous solution by application of iron hydro (oxide)-modified zeolite in a single-component system. Parameters such

as: solution pH, contact time, adsorbent dosage, initial concentration and temperature were optimized before field application to real acid mine drainage. The optimum parameters for U(VI) adsorption were: adsorbent dosage (3.0 g), solution pH (6 ±0.1) and contact time (30 min). Optimum parameters where then applied to acid mine drainage were the effluent was found to be cleaner than the influent.

In **Paper III,** iron oxide-coated zeolite (IOCZ) nanocomposite was prepared and fully characterized. This sorbent was then used for extraction of U(VI) and As(III) from aqueous solutions by application of batch techniques. Batch study results were modelled best by the pseudo second-order kinetic model and Freundlich isotherm. The adsorption capacity of both U(VI) and As(II) was dependent on the temperature. The presence of Cd^{2+}, Co^{2+} and Cr^{3+} ions enhance the adsorption of As(III) whereas the opposite trend was observed for U(VI) sorption onto IOCZ nanocomposite.

Dedication

This work is dedicated to my parents Pfananani Donald and Avhashoni Constance Nekhunguni for being very supportive during the course of my postgraduate studies.

A special thank you goes to Marubini Samuel Mudzielwana for being there during the course of my studies.

"Put your heart, mind, and soul into even your smallest acts. This is the secret of success." Swami Sivananda

Acknowledgements

First and Foremost, I would like to acknowledge the almighty God.

I would like to thank my supervisor, Prof Hlanganani Tutu, for his efforts day in and day out despite his tight schedule and other engagements, to scrutinise, peruse my thesis sheet by sheet, and see to the completion of this programme. May the lord bless you and grant you an everlasting joy. You made me a better person.

I would like to thank my mentor Dr Nikita Tawanda Tavengwa whose constructive comments added value to my work.

To my colleagues in the Environmental Analytical Chemistry Research group it was a pleasure to work with in the lab, especially: Mr Smiley Mabape, Ms Xolisiwe Maputsoe, and Mr Chuene Mokghele.

Finally, I want to thank National Research Foundation (NRF) of South Africa for their financial support towards the completion of my research.

Table of Contents

Declaration i

List of publications..... ii

Contribution of the authors iii

Abstract iv

Dedications vi

Acknowledgments vii

Table of contents viii

List of figures x

Chapter 1 xi

1. Background xi

1.1 Brief background 2

1.2 Aims and objectives 2

1.3 Hypotheses 2

1.4 Dissertation layout 4

Chapter 2 5

2. Literature review 5

2.1 Mine water chemistry and Acid Mine Drainage 6

2.1.1 Impact of acid mine drainage on water resource 8

2.1.2 Deleterious effect of AMD acidity 9

2.1.3 Impact of dissolved metals on the aquatic life 9

2.2 Toxic metals present in AMD contamination 10

2.2.1 Arsenic 10

2.2.2 Uranium 11

2.3 Remediation techniques for heavy metals contaminated water 12

2.3.1 Reverse osmosis 13

2.3.2 Electrodialysis 13

2.3.3 Ion exchange 13

2.3.4 Ultrafiltration 13

2.3.5 Chemical precipitation 13
2.3.6 Adsorption 14
2.4 Zeolite 15
Chapter 3 17
3 Research methodology 18
3.1 Chemical 18
3.2 Instrumentation 18
3.2.1 Power x-ray diffraction 18
3.2.2 X-ray fluorescence 18
3.2.3 Fourier transform infrared (FT-IR) spectra 19
3.2.4 Scanning electron microscopy (SEM) 19
3.2.5 Inductively coupled plasma-optical emission spectrometry (ICP-OES) 19
3.3 Batch Adsorption Experiments 20
3.4 Data modelling 21
3.4.1 Kinetic modelling 21
3.4.2 Isotherm modelling 21
3.5 Data Validation 22
Chapter 4 23
4 List of publications 23
Paper I 24
Paper II 34
Paper III 65

Chapter 5 80

5 General conclusion and future work 80

5.1 Conclusion 81

5.2 Future work.....82

References 83

List of figures

Fig 1: Impact of low pH on the river.....8

Fig 2: A Google earth map of the Central and East rand Basin (26° 14′13.67″ S, 28° 07′ 34.00″ E) (Elevation 1659 m, eye alt 59.69 km) 10

List of abbreviations and acronyms

AMD	Acid Mine Drainage
GDP	Gross Domestic Product
USEPA	United States Environmental Protection Agency
IHOMZ	Iron (hydr) oxide modified zeolite
SEM	Scanning Electron Microscopy
FT-IR	Fourier transforms infrared
ICP-OES	Inductively Coupled Plasma Optical Emission Spectrometry
PXRD	Powered X-ray diffraction
LOI	Loss of ignition

Chapter 1

1.0 Background

This chapter gives a background on the mining industry, mine tailings and acid mine drainage

1.1 Background

In the minerals sector of the world, South Africa is renowned for its overwhelming deposits of several minerals and mining industry contribute significantly to the country Gross Domestic Product (GDP) (Cawthorn, 2010; Adler et al., 2007). However, one of the negative impacts from the industry is a legacy of contamination to the environment in the form of mine tailings and acid mine drainage (AMD) (Rösner and Van Schalkwyk 2000).

Mining industries have contributed immensely to the volumes of waste materials handled worldwide (Blowes et al., 2003). The important environmental concern associated with mine wastes is the production of acidic water and the outflow of water containing high concentration of dissolved trace and radionuclide elements from these wastes are a global environmental issue (Blowes et al., 2003; Johnson and Hallberg, 2005).

The process of extracting precious metal from the mineral bodies proceeds through a sequence of the steps: from mining to pulverizing and mineral recuperation. Each of these steps generate a stream of waste material and these waste materials are incorporated together resulting in the formation of mine tailings which are the main source of pollution and primary component of mining industry (Blowes et al.,2003). These wastes are made of generally sand sized molecule, and lack macronutrients for common development of plants (N, P, K), and accommodate essentially no organic matter (Blowes et al., 2003; Ye et al., 2002; Rosario et al., 2007; Mendez et al., 2007).

Mine wastes are primary composed of sulphide mineral with pyrite and pyrrhotite being the principal sulphide mineral, and other sulphide mineral liable to oxidation, releasing toxic elements which are incorporated in minute percentage (Blowes et al., 2003; Rösner and Van Schalkwyk, 2000). In the Witwatersrand basin, more than 270 mine tailing has been identified and covers a total area of about 180 km^2 (Rösner and Van Schalkwyk, 2000).

The mine tailings in the Witwatersrand Basin run from exceedingly acidic (pH ≤ 2) to basic (pH ≥9) depending upon the carbonate content and acid-generating capability of the tailings (Gitari et al., 2006). In mine tailings, rain water percolates through the finely divided tailings encountering sulphide minerals that are experiencing oxidation resulting in the formation of highly acidic (pH 2–4), sulphate-rich water which solubilise high context of transition metal, heavy metal and low concentration of radionuclide which are adequately environmentally harmful to require exclusive storage, remediation and disposal technique (Gitari et al., 2006). Mine drainage can have significant adverse effects on the freshwater communities, starting from direct lethal effects through to interfere with the ecosystem processes due to the toxicity of trace elements (Johnson and Hallberg, 2005).

The extreme low pH levels promote weathering of tailing resulting in leaching of toxic trace elements such as Al, Fe, As, Cd, Cu, Mn, Pb, and Zn contained in the tailings (Masindi et al.,2016). These elements leaching from tailing amass in living organism and are non-biodegradable, causing numerous diseases, death and disorders (Sprynskyy et al., 2006). The increase in solvency of trace elements associated with gold correlates with the increase in the acidity of the water. Trace elements concentrations such as: As, Cd, Cu, Mn, Pb, and Zn are as low as 1 g kg^{-1} in present day tailings and can be more prominent than 50 g kg^{-1} in historic tailings (Ye et al., 2002; Rosario et al., 2007; Mendez et al., 2007; Rösner and Van Schalkwyk, 2000; Mendez et al., 2008). However, the bioavailability of these metals is controlled by other natural component such as: pH, temperature and the dissolved organic carbon in the tailings (Peng et al., 2008).

The unfavourable repercussion of AMD in South African was documented in a case study based on coal mine located in Middleburg colliery near Witbank (Bell at al., 2001). The case study illustrated the effects of AMD generated from a mine decommissioned in 1947, and in 1996 the mine was still discharging water with sulphate level in excess of 1000 mg L^{-1} and a pH< 3. The water from the mine entered the Blesbokspruit River reducing the upstream pH from pH > 7 to a pH

value of approximately 3.2 and sulphate concentration ranging between 185-2250 mg L^{-1}(Bell at al., 2001).

In-order to avoid the undesirable impact of AMD on the environment, the decommissioned mines and mine tailing should be managed properly and the water contaminated by AMD must be collected, treated to remove toxic metal and increase the pH before being released into the streams (Neculita et al., 2007). Since AMD represents a substantial source of water if properly treated (Enslin et al., 2010).

1.2 Aims and objectives

The study considered the synthesis and the performance evaluation of iron hydroxide/oxide-modified zeolite adsorbent in the removal of arsenic and uranium from acid mine drainage. This aim will be achieved by addressing the following objectives:

- To conduct batch studies to assess the effect of pH, concentration, time, temperature and competing and other ions on the adsorption of arsenic and uranium.
- To conduct desorption studies based on various desorbing solutions to establish the potential release of the pollutants back to the solution.

1.3 Hypotheses

The hypothesis put forward in this research is that the iron hydroxide in the AMD will coat the natural zeolite altering the sorptive characteristics of the readily available natural zeolite.

1.4 Dissertation layout

This dissertation is made up of three chapters, each explaining the investigations performed on this research in detail. The summary of the chapters is given below:

Chapter One: A general background to water pollution by heavy metal due to acid mine drainage generated from mine tailing and decommissioned mines.

Chapter Two: A concise literature review on the impact of AMD on the environment, ecosystem and water system is given.

Chapter Three: The methodology is outlined in this section

Chapter Four: This chapter list all the manuscripts (**Paper I-III**) submit for this dissertation examination. The work carried out, results and discussion are presented in each paper.

Chapter Five: General conclusions and future work based on experimental findings are discussed in this section

References*:* The references arising from the introduction and literature review (Chapter 1 and 2) are listed at the end of the dissertation.

Chapter 2

2.0 Literature review

This chapter commences with an in-depth literature review on the impact of AMD on the environment, ecosystem and water system. This chapter is concluded by the concise review on the possible treatment techniques.

2.1 Mine water chemistry and Acid Mine Drainage

In the aqueous environments two utmost important reactions that occur involve either protons or electrons (Stumm and Morgan, 1996). The transfer of electrons and protons affect the redox potential, signified as the 'Eh' or 'pe' and the pH of the system, respectively. In summary, in a chemical reaction protons and electrons are interdependent of each other and govern the oxidising power and acidity of the solution (Stumm and Morgan, 1996).

Metal rich seepage can be produced through a combination of physical and chemical processes by which sulphide minerals are converted to iron oxyhydroxides and sulphates (Neculita et al., 2007). When either surface or groundwater encounters sulphide minerals at mine sites under oxic conditions, problematic mine drainage generally develops as dissolution reactions between the water and the ore or rock forming minerals (Akcil and Koldas, 2006). The characteristics of mine waters vary considerably relying upon the geochemical conditions at point source and the chemistry of the host rocks and gangue minerals (Espana et al., 2005). These characteristics determine whether waters will be acidic and ferruginous, net alkaline and ferruginous, circumneutral or saline (Gitari et al., 2006). The Witwatersrand basin, in which the sites of primary focus of this study are located, is generally characterised by acidic mine drainage because of the high content of pyrite in the ores (Tutu et al., 2008; Naicker et al., 2003).

In general terms, AMD is generated through a reaction of pyrite or marcasite (FeS_2) with water and an oxidant such as dissolved O_2 or Fe(III). Occasionally, this reaction is supported by a catalyst, for example MnO_2 or microorganisms (Blowes et al., 2003; Tutu et al., 2008). Depending on the oxidant present, reactions occur in both oxygenated and anoxic systems. Furthermore, the commonly complex process involves chemical, biological and electrochemical reactions.

The steps are as follows:

Oxidation of pyrite in the presence of water and oxygen

$$FeS_2(s) + {}^{7}/_{2}\, O_2 + H_2O \rightarrow Fe^{2+} + 2H^{+} + 2SO_4^{2-} \quad (1)$$

Oxidation of Fe(II) to Fe(III)

$$Fe^{2+} + {}^{1}/_{4}\,O_2 + H^+ \rightarrow Fe^{3+} + {}^{1}/_{2}\,H_2O \quad (2)$$

Conversion of Fe(III) to Ferric Hydroxide

$$Fe^{3+} + 3H_2O \leftrightarrow Fe(OH)_3 + 3H^+ \quad (3)$$

The overall equation for the oxidation of pyrite by atmospheric oxygen is given as:

$$4FeS_2(s) + 15O_2 + 14H_2O \rightarrow 4Fe(OH)_3(s) + 16H^+ + 8SO_4^{2-} \quad (4)$$

Furthermore, the precipitation of iron oxide and oxyhydroxide forms the characteristics orange staining (yellow boy) that can be seen coating river beds and streams (Neculita et al., 2007; Johnson and Hallberg, 2005; Gray, 1997.). The four moles of proton released for each mole of pyrite oxidized, reduces the pH of the stream or drainage, pose great threat to the ecological system and facilitate the oxidation process of other minor sulphide minerals present in the tailings releasing trace elements such as: Cu, As, Ni, Zn, Cr, Pb and Co to the environment (Akcil and Koldas, 2006). The presence of carbonates as natural buffering system may neutralize the pH and reduce the detrimental effect of posed. At a pH of 4.2, the buffering system becomes inadequate for neutralization. The water drainage suddenly becomes acidic, and therefore posed a great threat to ecosystem life. This leads to the precipitation out of amorphous, orange, yellow or red deposit (yellow boy) $Fe(OH)_3$ on the surface of the stream in Figure 1 (Neculita et al., 2007).



Figure 1: Impact of low pH on the trench.

2.1.1 Impact of acid mine drainage on water resource

AMD poses a major environmental threat to clean water bodies throughout the world (Nganje et al., 2010; Johnson and Hallberg, 2005). South Africa is one of the nations confronted with water insecurity, resulting from the release of mineral wastes such as AMD, fluoride. The country is confronted with disproportionately distributed water resources with low and inconsistent rainfalls with an average yearly rainfall of around 464 mm and erratic climate conditions. With limited water resources, the water resources of the country are being contaminated by leachates from mine tailing and decommissioned mine (Johnson and Hallberg, 2005).

AMD enters streams and rivers altering the ecosystem by reducing the pH into unnaturally low value (< 3), introducing elevated levels of toxic trace elements, and inducing the formation of metal hydroxide precipitates (Fig. 1) (Sprynskyy et al., 2006). Thus, the metal solubilised enters the food chain through the aquatic system (Gitari, 2006).

2.1.2 Deleterious effect of AMD acidity

The damaging effect of AMD on the environment is controlled by the pH of the drainage, since solution pH is a principal variable for metal ion mobility, sorption and precipitation which all influence the bioavailability (Simate and Ndlovu, 2014). The lower the pH value, the more extreme the impacts of the AMD will be on the aquatic life (Johnson and Hallberg, 2005; Sprynskyy et al., 2006; Motsi, 2010).

A drop-in pH below the tolerance level may results in death due to respiratory or osmo regulatory failure (Motsi, 2010; Simate and Ndlovu, 2014). At low pH levels, sodium, which is vital for normal body operation is replaced by hydrogen ions in the cell. Sodium is essential in the function of the nerve, muscle and in the regulation of body fluids (Motsi, 2010; Simate and Ndlovu, 2014).

The acidity effect of AMD does not end on the aquatic life, it also affects the man-made structure through corrosion. In overall the high acidity reduce the ability of a stream to buffer other chemical change, reduction in habitant, food chain breakdown and accumulation of toxic metal in the food chain (Motsi, 2010).

2.1.3 Impact of dissolved metals on the aquatic life

Trace elements solubilized by AMD not only increase the poisonous quality of the drainage but also acts as metabolic toxins to aquatic life. These elements amass in living organism and are non-biodegradable, causing numerous disease and disorders (Demirbas, 2008; Bailey et al., 1998). With appropriate conditions, precipitation of dissolved heavy metal as metal oxide or hydroxide occurs (Johnson and Hallberg, 2005; Kumari et al., 2010). The precipitation of different metal oxide or hydroxide consumes oxygen, resulting in diminishing the dissolved oxygen content. creating an inhospitable ecosystem for aquatic life (Simate and Ndlovu, 2014; Motsi, 2010) and small animal that feed on the bottom of the stream can no longer feed, resulting in their demise.

Metal like aluminium rarely occurs naturally in water systems at elevated levels but significant amount of aluminium introduced to aquatic system through AMD coupled with low pH increase the rate of sodium ions depletion from tissue and

blood resulting in death (Kumari et al., 2010). According to Brown and Sadler (1980) the death of fish in AMD contaminated water reservoirs was due to loss of sodium ions and oxygen from blood and tissue, respectively.

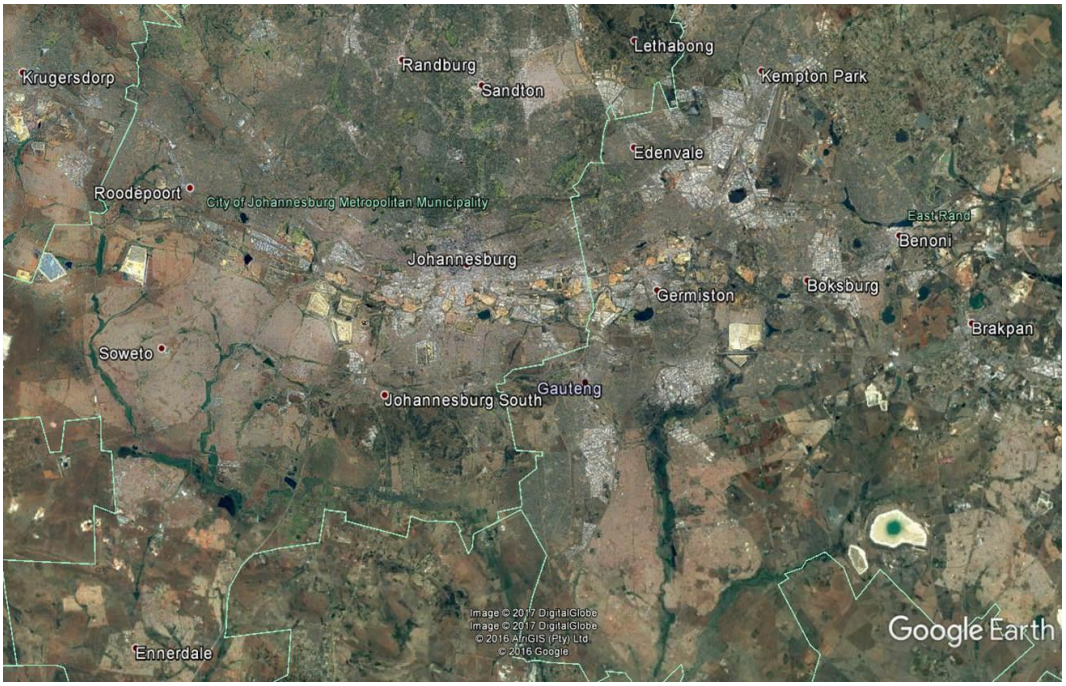


Figure 2: A Google earth map of Central and East rand Basin (26° 14′13.67″ S, 28° 07′ 34.00″ E) (Elevation 1659 m, eye alt 59.69 km)

2.2 Toxic metal present in AMD contamination

Gold tailings in the Witwatersrand Basin contribute significantly to the heavy metal released into the water system in this region (Winde and Van der Walt, 2004; Nengovhela, 2006). Heavy metals form part of the most common pollutant in the ecosystem and are non-degradable. They bio-accumulate throughout the food chain, giving rise to ecological instabilities and posing health risk to human (Akpor and Muchie, 2010). The toxicity of heavy metals in the ecosystem depends on their solubility at varying different pH state, which consequently determines the phase of occurrence of the metal (Gadd and Griffiths, 1977). At near-neutral pH heavy metals are generally less toxic, since this represent the range of minimum solubility of most metal hydroxides (Gitari, 2006).

Tailing dams in the Witwatersrand Basin remains a major source of high concentrations of radioactive and chemical toxic heavy metals (Winde and Van der

Walt, 2004). A lot of literature has reported the existence trace elements such as U and As in high levels in the Witwatersrand basin, which represent the source of severe potential hazard on the aquatic system when leached to the streams (Bakatula et al.,2017: Winde and Van der Walt, 2004; Tutu, et al., 2008).

2.2.1 Arsenic

Arsenic (As) is a toxic metalloid widely distributed throughout soils, natural water bodies and in trace levels in all-living matter. Elevated arsenic concentrations in water bodies have resulted from both natural and anthropogenic activities and represent a noteworthy threat to human wellbeing (Wang and Mulligan, 2006; Morin and Calas, 2006; Wong et al., 1999). Arsenic is commonly associated with volcanic and sedimentary rocks, especially with sulfidic minerals of copper, lead and gold (Rathinasabapathi et al., 2006; Cheng et al., 2009).

Arsenic prevails in the environment in numerous oxidation states (−3, 0, +3, +5), with the trivalent and pentavalent oxidation state being the most stable (Mohan and Pittman, 2007; Khaodhiar et al., 2000; Stanić et al., 2009). In natural water bodies, inorganic arsenic enerally found as trivalent arsenite or pentavalent arsenate (Morin and Calas, 2006; Payne et al., 2005). The mobility of arsenic is governed by the bacterial activity and its speciation is affected by the pH and seasonal changes, even at extreme concentrations (Morin and Calas, 2006).

The trivalent arsenite is considered more toxic and more potent in chronic toxicity than the pentavalent arsenate. Arsenic is toxic to plants and aquatic life: in humans, chronic exposure can cause bladder and kidney cancer. Chemically, arsenic has very similar chemical properties to its predecessor, phosphorus, and it can partially substitute for phosphorus in biochemical reactions (Cheng et al., 2009; Mohan and Pittman, 2007).

One of the more widespread problems is leaching of elevated amount of arsenic into water aquifer through AMD which has been reported in many countries including South Africa in the Witwatersrand basin, due to high affinity of arsenic

to sulfidic ores (Cheng et al., 2009; Simate and Ndlovu, 2014; Hansen, 2015; Nengovhela, 2006).

2.2.2 Uranium

The auriferous ores of the Witwatersrand Basin contain up to 1000 mg/kg of uranium (Tutu et al., 2009). In the Witwatersrand Basin uranium is discharged to the environment as a by-product of gold mining industry, and close to 6000 tons of uranium waste was reported to be annually disposed into tailing dams and seepage from such deposits frequently leads to diffuse contamination of nearby streams (Winde et al., 2004; Sprynskyy et al.,2011).

Uranium is a life-threatening radionuclide due to its high toxicity and radioactivity, and occurs in diverse oxidation states (+2, +3, +4, +5, and +6), with the hexavalent as the most commonly found in environment. In natural environments, uranium exits as the mobile hexavalent uranyl ion (Krestou, 2004; Wade and Coetzee, 2008; Bakatula et al., 2017; Winde et al., 2004).

The mobility of uranium ions depends on the presence of chelating agents which forms soluble complexes with the uranyl ions (Winde et al., 2004). Uranium, it is known to cause intense toxicological consequences for human and living life form, and its compounds are potential occupational carcinogens according to USEPA (Rahmati et al., 2012). In human uranium can induce nephritis chemically when consumed (Das et al., 2010; Sureshkumar et al., 2010; Rahmati et al., 2012).

Leachates from mine tailings containing uranium pose a threat to surface and ground waters (Winde et al., 2004; Parab et al., 2005).

2.3 Remediation techniques for trace elements in contaminated water

Numerous processes have been developed to purify water contaminated by dissolved trace elements from mining industry both locally and globally. The most common processes developed for AMD treatment involve either chemical or biological remediation strategies to remove the metal and elevate the water pH to values between 6 and 9 prior to mixing with surface waters. These processes include reverse osmosis (Zhong et al., 2007), electrodialysis (Martí-Calatayud et al., 2014),

ultrafiltration (Al Abdulgader et al., 2013), chemical precipitation (Matlock et al., 2002; Wei et al., 2005), ion exchange (Hubicki and Kołodyńska, 2012) and adsorption (Yavuz et al., 2003).

Most of these techniques are costly, require high levels of expertise and generate secondary wastes requiring further treatment and disposal, which restricts their application in pilot scale (Febrianto et al., 2009). Compared to many other developed techniques, adsorption is the most frequently applied technique in wastewater treatment because its application is simple, safe and environmental friendly (Yavuz et al., 2003).

2.3.1 Reverse osmosis

This treatment system utilizes semi-permeable film to treat AMD. AMD effluent is pressurized through a membrane which permits passage to solvent not solute (Zhong et al., 2007). The highly concentrated AMD is left on the other side of the membrane. The high operating and setting cost limit the application in pilot scale.

2.3.2 Electrodialysis

In Electrodialysis systems, ions are separated by imposing an electromagnetic field difference across the membrane resulting in selective migration of positively and negatively charged ions through ion-exchange membrane as a result of an electrical driving force (Simate and Ndlovu, 2014; Martí-Calatayud et al., 2014).

2.3.3 Ion exchange

Ion exchange treatment involves the interchange of ions between a liquid phase and porous materials, which maybe be synthetic or natural such as zeolite or resins (Simate and Ndlovu, 2014; Hubicki and Kołodyńska, 2012). In ion exchange remediation of AMD toxic metal present in solution substitute for the harmless metal ions in the pores of the porous solid which can either be zeolite or resins (Hubicki and Kołodyńska, 2012).

2.3.4 Ultrafiltration (UF)

In ultrafiltration (UF) process, semi-permeable polymeric membrane and high pressure are used to separate molecules on the premise of molecular size, shape, surface electric charge and chemical structure (Al Abdulgader et al.,2013). This technique separates relatively high molecular weight solutes such as protein, polymer and colloidal materials. The permeability and retention characteristics are the most important characteristic of ultrafiltration (UF) process.

2.3.5 Chemical precipitation

In chemical precipitation wastewater treatment process the state of dissolved material is change into solid particles (Matlock et al., 2002; Wei et al., 2005). The phase change is induced by addition of counter-ion to reduce the solubility of the metallic cation (Wei et al., 2005).

2.3.6 Adsorption

"Adsorption has been defined by many authors but conventionally it is accepted as a phenomenon where molecules of the contaminants dissolved in water attach themselves to the surface of individual soil particles". The adsorption process can occur in two forms and according to the type of adsorbate- adsorbent interactions bonds are formed.

The two forms of adsorption are:

- Physisorption

  In this process, the adsorbate is attached to the adsorbent micro-pores through weak van der Waal forces. This makes the Physisorption process reversible because the adsorption bonds between adsorbate and adsorbent are easily formed and broken, due to the low energy of adsorption for such system.

- Chemisorption

This process is a result of chemical interaction between analyte and sorbent in solution. Interactions between adsorbate and adsorbent surface results in the formation of ionic and covalent bonds and high adsorption energy is liberated. This process is usually irreversible as the bonds formed are semi-permanent; thus, for desorption to occur, the adsorbate undergoes a chemical change.

2.4 Zeolite

Zeolites are hydrated aluminosilicate minerals occurring naturally with a 3D structure composed of AlO_4 and SiO_4 tetrahedral (Motsi et al., 2009; Erdem et al., 2004; Wang and Peng, 2010). The AlO_4 and SiO_4 tetrahedral are linked together by sharing an oxygen atom to form cages and channels which are interconnected (Erdem et al., 2004).

The negative charge on the surface is generated from isomorphic substitution of Si by Al in the lattice is counterbalanced by the exchangeable cation present on the cages and channels (Erdem et al., 2004; Wingenfelder et al., 2005). These exchangeable cation ions are relatively innocuous which makes the suitable for extracting toxic elements from contaminated waters (Erdem et al., 2004).

In contrast to synthetic zeolites, natural occurring zeolite exhibits higher resistance towards acidic solutions (Wingenfelder et al., 2005; Wang and Peng, 2010). To date, more than forty types of natural occurring and over 170 synthetic zeolites have been reported in literature. Among the natural occurring zeolites, clinoptilolite is one of the most abundant (Wingenfelder et al., 2005; Polat et al., 2004). Due to its extraordinary properties clinoptilolite is widely used in waste water treatment, contaminated soils and in agronomical applications (Wingenfelder et al., 2005; Polat et al., 2004; Wang and Peng, 2010).

The earliest application of clinoptilolite was the in the decontamination of cesium and strontium radioisotopes (Erdem et al., 2004). The high selectivity of clinoptilolite towards toxic trace elements makes it a promising material for the treatment of mine waste waters (Wingenfelder et al., 2005). Several studies have

been conducted on the utilization of natural and surfactant-modified clinoptilolite for removing and/or exchanging trace elements from mine waste waters (Motsi et al., 2009; Li et al., 2008; Bowman, 2003).

Even though considerable research has been conducted on the utilization of zeolite as a low-cost absorbent for AMD, the main gaps exist in the field application of zeolites, mainly the fact that most studies are simply based on the properties as used at the laboratory scale. However, field application leads to the coating of the zeolite with hydroxides and oxides of Fe, largely influencing the adsorptive properties as the zeolite surfaces become modified and can be viewed as mixtures of zeolitic and Fe hydroxide surfaces. The investigations into the effects of these changes have not been widely reported. Thus, the aim of this study was to gain insight into the effect of the hydroxides and oxides (resulting from maturation of hydroxides) of Fe coating will have on the adsorptive properties of zeolite.

Chapter 3

3 Research Methodology

3.1 Chemicals

All the chemical reagents used were analytically pure and were purchased from Sigma-Aldrich, South Africa. Standard solutions of 1000 mg L^{-1} of U(VI), As(III) and As(V) were prepared by dissolving appropriate amount of $UO_2(NO_3) \cdot 6H_2O$,

$NaAsO_2$ and $Na_2HAsO_4 \cdot 7H_2O$ respectively, .in Millipore-Q water with resistivity of 18.2 MΩ cm, which was used for preparation of standard solutions and cleaning of glassware. Working solutions were prepared by serial of dilution of the stock solutions. Initial solution pH values were adjusted by the addition of 0.1 mol L^{-1} NaOH or HNO_3 solutions.

3.2 Instrumentation

All metal ions measurements were performed on a Spectro Genesis inductively coupled plasma optical emission spectrometry (ICP-OES) (Kleve, Germany). Solution pH measurements were performed on a Five easy FE20 pH meter from Mettler Toledo (Johannesburg, South Africa). All instruments used for sorbent characterization are briefly described below:

3.2.1 Powder X-ray diffraction

Powder diffractograms were collected with a Bruker D2 diffractometer (Bruker, Germany) coupled with Cu Kα radiation (1.5418 Å). Continuous scans from 10° to 90° were obtained at a scan speed of 0.020°/step and 17.7 s/step. The reflection positions and intensities peaks were used to identify the underlying structure of the material.

3.2.2 X-ray fluorescence (XRF) spectroscopy

Chemical composition of natural zeolite was determined using WD X-ray fluorescence (XRF) spectrometer (Almelo, Netherlands). Only major elements were determined in their oxide form.

3.2.3 Fourier transform infrared (FT-IR) spectra

Fourier transform infrared (FT-IR) spectra were recorded using a Tensor 27 spectrophometer (Bruker, Germany). The spectra were recorded in the frequency range of 400 – 4000 cm^{-1} at a resolution of 2 cm^{-1} and in solid state.

3.2.4 Scanning electron microscopy (SEM)

The microphotographs of the sorbent were recorded using a FEI Quanta 200 ESEM electron microscope (Oregon, USA). Small amount of the sorbent was sprinkled onto the carbon tape on the specimen stub. The small was coated with Chromium and then loaded into the SEM microscope where the microphotographs were viewed.

3.2.5 Inductively coupled plasma-optical emission spectrometry (ICP-OES)

A Spectro Genesis inductively coupled plasma-optical emission spectrometry (ICP-OES) (Kleve, Germany) was used to determine the concentration of metals in solutions with operating conditions shown in Table 1.

Table 1: Operating condition of the ICP-OES

Instrumental parameter	Setting
RF power	1400 W

Coolant Gas Flow	14.00 L min^{-1}
Auxiliary Gas Flow Rate	1.00 L min^{-1}
Nebulizer Gas Flow Rate	1.00 L min^{-1}
Sample Pump Flow Rate	2.00 L min^{-1}
Sample Aspiration Rate	2.00 L min^{-1}
Flush Pump Rate	100 rpm
Replicates	3
Plasma Torch	Quartz
Spray Chamber	Single pass
Nebulizer	Cross-flow
Processing Mode	Area

3.3 Batch Adsorption Experiments

In batch experiments, various factor such as: solution pH, sorbent dosage, contact time and initial metal concentration were optimized. Each factor was optimized independently. The experiments were executed in triplicates. The influence of these parameters on the adsorption of the metal ions was evaluated by calculating the extraction efficiency as shown in Eq. 5.

$$\text{Extraction efficiency } (\%) = \frac{C_i - C_f}{C_i} \text{ X } 100 \quad (5)$$

The adsorption capacity, q_e (mg g^{-1}) of a sorbent is defined as the amount of the adsorbate sorbed on a gram of the adsorbent at equilibrium. It can be calculated mathematical from equation 6.

$$q_e = \frac{(C_i - C_f)V}{m} \quad (6)$$

where $C_o(\text{mg L}^{-1})$ and $C_e(\text{mg L}^{-1})$ are the concentration of metal ions in the solution before and after adsorbent addition respectively, V(mL) the volume of the

aqueous solution and m (g) is the weight of the iron hydro (oxide) modified zeolite. The procedure for each optimization is detailed in chapter 3 under each manuscript.

3.4 Data modelling

3.4.1 Kinetic modelling

Batch kinetic data was modelled using the two most commonly utilized kinetic models namely the Lagergren pseudo first-order equation (Eq. (7)) and the pseudo second-order equation (Eq. (8)) (Oke et al., 2008; Pokhrel and Viraraghavan, 2008):

$$\log(q_e - q) = \log q_e - \frac{k_1}{2.303} t \quad (7)$$

$$\frac{t}{q_t} = \frac{1}{k_2 q_e^2} + \frac{t}{q_e} \quad (8)$$

Where k_1 (min^{-1}) and k_2 (g mg^{-1} min^{-1}) are the rate constant for Lagergren pseudo first-order and the pseudo second-order, respectively. q_t (mg g^{-1}) is the adsorption capacity of the adsorbent at time "t".

3.4.2 Isotherm modelling

The affinity of the adsorbate-adsorbent was assessed using three isotherm model namely the Langmuir (Eq. (9)), Freundlich (Eq. (10)), and Dubinin–Radushkevich (D-R) (Eq. (11)) isotherm models (Martinson and Reddy, 2009: Chutia et al., 2009; Saada et al., 2003).

$$\frac{C_e}{q_e} = \frac{C_e}{q_m} + \frac{1}{k_l q_m} \quad (10)$$

$$\log(q_e) = \log k_f + \frac{1}{n} \log(C_e) \quad (11)$$

$$\ln q_e = \ln x_m + \beta \varepsilon^2 \quad (12)$$

where for Eqs. (10) and (11) C_e (mg L^{-1}) is the equilibrium concentration, q_m is the monolayer sorption capacity, k_l (L mol^{-1}) is the Langmuir adsorption constant related with the free energy adsorption and k_f (mg g^{-1}) is the Freundlich constant, n is the heterogeneity factor and varies with adsorbent, respectively.

For Eq. (12) x_m is the maximum sorption capacity and K ($mol^2 kJ^{-2}$) is related to the mean free energy of sorption per mole of the sorbate.

3.5 Data validation

In all scientific investigations, it is essential to know the quality of the data used for decision-making purposes. The limit of detection (LOD) is defined as the lowest concentration of the measured that can be detected at a specified level of confidence. Equation (13) shows the mathematical equation for calculating the limit of detection (LOD)

$$\mathrm{LOD} = \mathrm{Blank} + 3\mathrm{sd}(\mathrm{blank}) \quad (13)$$

The validity of each model was evaluated using the normalized standard deviation Δq (%) which can be calculated from the following Eq. 14:

$$\Delta q(\%) = 100\sqrt{\frac{\sum_{i=1}^{n}\left[\frac{q_{\exp} - q_{calc}}{q_{\exp}}\right]^2}{n-1}} \quad (14)$$

where q_{exp} is the experimental metal ion removal, q_{cal} is the calculated amount of metal ions adsorbed and n is the number of data points. The significance difference between the experimental values was evaluated by the p value using one way ANOVA at the 95% confidence level.

Chapter 4

List of publications

This chapter list all the three manuscripts submitted for examination. Each manuscript is formatted according to the style required per journal. Note also that the reference styles are different. **Paper I** and paper **III** have already been published, while **Paper II** is a manuscript to be submitted soon.

Paper I

This paper “Investigation of As(V) removal from acid mine drainage by iron (hydr) oxide modified zeolite” was published by *Journal Environmental Management*. It explores the use of iron (hydr) oxide modified zeolite as an alternative adsorbent for As(V) removal from acid mine drainage.

Journal of Environmental Management 197 (2017) 550–558

Contents lists available at ScienceDirect

Journal of Environmental Management

journal homepage: www.elsevier.com/locate/jenvman

Research article

Investigation of As(V) removal from acid mine drainage by iron (hydr) oxide modified zeolite

Pfano Mathews Nekhunguni, Nikita Tawanda Tavengwa, Hlanganani Tutu*

Molecular Sciences Institute, School of Chemistry, University of the Witwatersrand, Private Bag X3, WITS 2050, Johannesburg, South Africa

ARTICLE INFO

Article history:
Received 20 February 2017
Received in revised form
10 April 2017
Accepted 11 April 2017

Keywords:
Arsenic
Adsorption
Isotherm model
Modified zeolite
Thermodynamics
Acid mine drainage

ABSTRACT

In this work, the synthesis of iron (hydr) oxide modified zeolite was achieved through precipitation of iron on the zeolite. The structure and surface morphology of iron (hydr) oxide modified zeolite (IHOMZ) was studied by scanning electron microscopy (SEM), coupled with an energy-dispersive X-ray spectroscopy (EDX), and Fourier transform infrared (FT-IR) spectra. The efficiency of IHOMZ was then investigated through batch technique for the extraction of As(V) from mine waste water. The optimum parameters for maximum As(V) adsorption were: an initial As(V) concentration (10 mg L^{-1}), adsorbent dosage (3.0 g), contact time (90 min) and temperature (53 °C). The initial pH of the solution had no compelling effect on As(V) adsorption by IHOMZ. However, adsorption capacity was significantly affected by the solution temperature with 53 °C registering the maximum removal efficiency. The thermodynamic parameters: Entropy (ΔS° = 0.00815 kJ (K mol)$^{-1}$), variation of the Gibbs free energy (ΔG°) and enthalpy (ΔH° = 9.392 kJ mol^{-1}) of As(V) adsorption onto IHOMZ system signified a non-spontaneous and endothermic process. It was noted that Freundlich isotherm model exhibited a better fit to the equilibrium experimental data, implying that the adsorption process occurred on a heterogeneous surface. The kinetic data from As(V) adsorption experiments was depicted by the pseudo-second-order kinetic model (R^2 > 0.999), suggesting a chemisorption adsorption process. The experimental batch equilibrium results indicated that IHOMZ could be used as an effective sorbent for As(V) ion extraction from acid mine drainage.

© 2017 Published by Elsevier Ltd.

1. Introduction

Water pollution by arsenic is a worldwide problem (Sun et al., 2006). Arsenic is discharged into the environmental water bodies through a combination of natural and anthropogenic processes (Kanel et al., 2005; Alam et al., 2002). These processes can either be due to weathering of As-containing minerals, mining, and application of arsenic containing herbicides and pesticides (Alam et al., 2002).

Arsenic exists in two forms, namely as inorganic and organic arsenic, though the organic form is uncommon (Sarı and Tuzen, 2009). In natural water environment such as lakes, the inorganic form occurs primarily as As(III) and As(V) (Kanel et al., 2005). Arsenite (H_3AsO_3) species is the most toxic form of arsenic, although arsenate (H_3AsO_4) is the mobile species (Macedo-Miranda and Olguin, 2007; Bonnin, 2000). At near neutral pH, As(V) predominately exists as divalent ($HAsO_4^{2-}$) and monovalent ($H_2AsO_4^-$) species, whereas As(III) occurs as neutral species (H_3AsO_3) (Sun et al., 2006; Joshi and Chaudhuri, 1996; Ghimire et al., 2003).

Elevated concentrations of arsenic above the recommended standard in drinking water level of 10 μg L^{-1} can cause adverse effects on human health and ecological balance (Baskan and Pala, 2011; Katsoyiannis and Zouboulis, 2004). Chronic subjection to arsenic can cause skin, lung, and kidney cancer (Ng et al., 2003; Wang et al., 2014; Mohan and Pittman, 2006; Simsek et al., 2014). Quite a lot of literature studies have reported that arsenic's harmful effects are primarily due to the consumption of arsenic contaminated water. When ingested, arsenate replaces phosphate in biochemical reactions, whereas arsenite react with thiol in the protein and inhibit their activity (Ng et al., 2003; Payne and Abdel-Fattah, 2005).

Several remediation methods have been used in the extraction of arsenic from water, such as filtration (Beolchini et al., 2006), lime softening (Vahedi and Gorczyca, 2011), reverse osmosis (Kang et al.,

* Corresponding author. Tel.: +27 11 7176713.
E-mail address: hlanganani.tutu@wits.ac.za (H. Tutu).

http://dx.doi.org/10.1016/j.jenvman.2017.04.038
0301-4797/© 2017 Published by Elsevier Ltd.

2000), and coagulation (Guo et al., 2009). However, most of these techniques are encumbered by problems associated with high operating costs, technical difficulties in the preparation of material, and treatment and disposal of the waste sludge generated (Guo et al., 2009). In-order to overcome these hurdles, adsorption among others, has emerged as the preferred method. Adsorption offers a more convenient route for metal recovery, removal and recycling from wastewater (Shuibo et al., 2009).

In literature, there are reports about arsenic removal from contaminated water using Fe(II-III) bearing materials such as haematite, goethite, and Fe(III) loaded resins due to their selectivity and affinity towards inorganic arsenic species (Sun et al., 2006; Stanić et al., 2009; Jeon et al., 2009; Guan et al., 2008a). Even though these materials are efficient and selective, their application in a pilot scale is limited due to operational costs (Elizalde-González et al., 2001).

Hence, the use of a naturally occurring material such as zeolite in adsorption of arsenic has emerged as a viable option (Sarı and Tuzen, 2009; Chowdhury and Yanful, 2010). These naturally occurring materials main advantages are their low cost, simple modification and availability in huge amounts (Sarı and Tuzen, 2009). However, these materials have low affinity for anionic pollutants so by improving their surface characteristics; their affinity for anionic pollutants can be improved (Macedo-Miranda and Olguin, 2007).

Therefore, the objectives of this research were (1) to alter the sorptive characteristics of the readily available natural zeolite using iron hydroxide to adsorb anionic arsenic species from aqueous solution, (2) to investigate the adsorption of arsenic on iron (hydr) oxide modified zeolite under different experimental conditions *viz*., pH, arsenic concentration, temperature, contact time and selectivity and (3) to examine the reusability of iron (hydr) oxide modified zeolite. An insight view of these aspects of adsorption process is helpful in elucidating the adsorption mechanism.

2. Experimental

2.1. Chemical and reagents

Sodium hydroxide (NaOH), nitric acid (HNO_3), ferric nitrate ($Fe(NO_3)_3 \cdot 9H_2O$), sodium arsenate dibasic heptahydrate ($Na_2HAsO_4 \cdot 7H_2O$), calcium carbonate ($CaCO_3$), magnesium sulphate ($MgSO_4$) and sodium hydrogen phosphate (NaH_2PO_4) were purchased from Sigma-Aldrich (Johannesburg, South Africa). All chemicals used were of analytical grade and no further purification was needed. The natural zeolite was obtained from Johannesburg fields in South Africa. An appropriate amount of sodium arsenate dibasic heptahydrate was dissolved in ultrapure water to prepare As(V) stock solutions. A solution of 0.1 M HNO_3 and/or 0.1 M NaOH was used to adjust the initial pH of the working solutions, and was measured using a Mettler Toledo pH meter (Johannesburg, South Africa). Fresh dilutions were used for each experiment, and samples were analysed by a Spectro Genesis inductively coupled plasma optical emission spectrometry (ICP-OES) (Kleve, Germany). The solutions were centrifuged using a ROTOFIX 32A benchtop centrifuge obtained from Hettich (Massachusetts, United States).

2.2. Preparation of iron hydro (oxide) modified zeolite

Initially, the natural zeolite was immersed in distilled water for 24 h to reduce its alkalescency, and dried at room temperature. A sample of 100 g of natural zeolite was transferred to a flask containing 1000 mL of 2.0 M NaCl solution. The mixture was agitated for 24 h at ambient temperature and the phases were separated by decantation. The natural zeolite sample was then washed with deionized water until elimination of chloride ions was achieved, silver nitrate ($AgNO_3$) was used to test the presence of chloride ions. Finally, the sodium-treated zeolite (NaZ) was air-dried.

For the preparation of iron hydro (oxide) modified zeolite (IHOMZ), a sample of 100 g of NaZ was transferred to a flask containing 1000 mL of 0.5 M $Fe(NO_3)_3$ solution, the pH of the solution was adjusted to a value between 2 and 3 using 0.1 M NaOH and/or 0.1 M HNO_3. The mixture was shaken with an overhead shaker (150 rpm) for 24 h. The liquid phase was then decanted off and the remaining solid phase was washed exhaustively with deionized water and then air-dried.

2.3. Characterization of the prepared sample

Powder X-ray diffraction analysis was performed on both NaZ and IHOMZ to identify the mineralogy. Powder diffractograms of both samples were collected with a Bruker D2 diffractometer (Bruker, Germany) coupled with Cu Kα radiation. Continuous scans from 10° to 90° were obtained at a scan speed of 0.020°/step and 17.7 s/step. Fourier transform infrared (FT-IR) spectra were obtained using a Tensor 27 spectrophometer (Bruker, Germany). The FT-IR spectra ranged from 400 to 4000 cm^{-1} at a resolution of 2 cm^{-1}. For scanning electron microscopy observation, the sample was mounted on the sample holder and coated with chromium. The microphotographs were observed at 30 keV by FEI Quanta 200 ESEM electron microscope (Oregon, USA). The elemental composition of the zeolite sample was determined by an EDX system coupled to the microscope.

2.4. As(V) adsorption experiments

Batch scale experiments were conducted to study the impact of pH, contact time, adsorbent dosage, temperature and initial concentration on the adsorption of As(V) by IHOMZ. To study the influence these parameters on the removal of As(V) by IHOMZ, different conditions of pH (3.0–8.0), adsorbent dose (0.5–3.0 g), contact time (0.5–1080 min), initial concentration (0.5–220 mg L^{-1}), and temperature (23–53 °C) were evaluated. The aqueous solution was filtrated before analysis with ICP-OES. All sorption experiments were done in triplicates at 150 rpm.

The amount of As(V) adsorbed in (mg g^{-1}) at equilibrium (q_e) was calculated from mass balance of its concentrations in test solution and in the supernatant liquid after adsorption. The amount of As(V) adsorbed at equilibrium was calculated from mass balance using Eq. (1) and the adsorption percentage of As(V) adsorbed was calculated using Eq. (2).

$$q_e = \frac{(C_o - C_e)V}{m} \quad (1)$$

$$\text{Adsorption } (\%) = \frac{(C_o - C_e)}{C_0} \times 100 \quad (2)$$

where C_o (mg L^{-1}) and C_e (mg L^{-1}) are the concentrations of As(V) in solution before and after adsorbent addition respectively, V (mL) is the volume of the aqueous solution and m (g) is the weight of the IHOMZ. The initial and final concentrations of arsenic were determined by using ICP-OES.

2.5. Influence of co-existing anions

To determine the influence of co-existing anions on the performance of the adsorbent; batch equilibrium experiments were performed with sulphate, carbonate and phosphate (10, 100 and 250 mg L^{-1}) at optimized conditions. After shaking and

centrifugation at ambient temperature, the remaining As(V) concentration was evaluated using ICP-OES.

2.6. Reusability studies

For the regeneration of spent IHOMZ, the best desorbing eluent (0.1 M HNO_3) investigated by Pushpa et al. (2006) was used. Firstly, batch equilibrium experiments were performed on IHOMZ; A 30 mL As(V) solution with an initial concentration of 10 mg L^{-1} was added and contacted with 3.0 g sorbent in a 50 mL polyethylene tube. The spent IHOMZ was alienated from the solution through centrifugation, thoroughly washed with 30 mL ultrapure water four times to remove unsorbed As(V), and dried at 100 °C in an oven. As(V) ions loaded IHOMZ samples were taken and equilibrated at ambient temperature, with 30 mL of 0.1 M HNO_3 solution. The HNO_3 extract was collected and analysed for As(V) ions. Three consecutive adsorption-desorption cycles were performed on the spent IHOMZ. The recovery efficiency of As(V) from the solid phase was calculated using Eq. (3):

$$\text{Recovery efficiency} = \frac{C_{des}}{C_{ads}} \times 100 \quad (3)$$

where C_{des} (mg L^{-1}) and C_{ads} (mg L^{-1}) are the amount of As(V) released into the solution and the amount of As(V) adsorbed onto the IHOMZ sorbent, respectively. Statistical analyses and inferences were conducted using MS Excel 2010.

3. Results and discussion

3.1. Characterization of the adsorbent

The surface characteristic of NaZ and IHOMZ was examined by scanning electron microscopy (SEM). The SEM microphotograph of NaZ and IHOMZ were characterized by plate and laths which are morphologies characteristic of clinoptilolite family of zeolite (Charkhi et al., 2010; Mozgawa et al., 2009a; Jha and Hayashi, 2009) and the crystal morphology were not altered after coating with iron hydroxide (Fig. 1(a) and (b)). Jiménez-Cedillo et al. (2009) observed similar morphology when investigating the adsorption kinetic of arsenate by iron, manganese and a combination of iron-manganese-modified clinoptilolite.

The elemental composition on the surface of IHOMZ was performed by qualitative EDX analysis. The EDX results were as follows: O (51.59%), Na (0.76%), Mg (0.53%), Al (6.62%), Si (33.22%), K (4.0%), Ca (2.09%) and Fe (1.19%) on the surface of IHOMZ. Clinoptilolite-rich tuffs are aluminium silicate materials

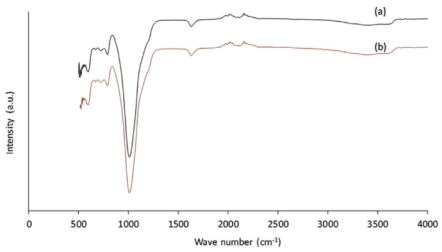


Fig. 2. FT-IR spectrum of (a) natural zeolite and (b) IHOMZ.

characterized by high silica content confirmed by high silica percentage obtained from EDX analysis. Han et al. (2009) observed similar results on the high content of silica when investigating iron oxide-coated zeolite as new composite sorbent for extracting Cu(II) from aqueous solution.

The FT-IR spectra of NaZ and IHOMZ are shown in Fig. 2. The characteristic peaks of natural zeolite observed were: peaks of water deformation at 1627.68 cm^{-1}, sorbed water molecules 671 cm^{-1}, vibration bands of the zeolite framework between 719.77 and 1009.65 cm^{-1}, and stretching vibration band of hydroxyl group Si – OH or Al – OH at 3410.11 cm^{-1} (Mozgawa et al., 2009b; Mozgawa, 2000). Similar FT-IR results for natural clinoptilolite zeolite were reported by Mozgawa et al. (2009a). The spectra of IHOMZ maintained the basic characteristic peaks of NaZ with a minute shift on the peaks; stretching vibration band of hydroxyl group was shifted to 3409.03 cm^{-1}. The vibration band of water deformation was shifted to 1632.41 cm^{-1}. The stretching bands of tetrahedral framework were shifted to the range of 725.25–1007.04 cm^{-1}. The iron (hydr) oxide bands were masked by the zeolite peak. The minute shifts on the bands indicated the presence of small content of iron. Han et al. (2009) reported similar minute shift on the FT-IR bands of iron oxide-coated zeolite as compared to that of the raw zeolite.

Fig. 3 illustrates the powder diffractograms of natural clinoptilolite zeolite and IHOMZ. X-ray powder diffraction pattern showed that the position of the intense reflections observed corresponds to reported literature data of clinoptilolite (Vasylechko et al., 2003; Korkuna et al., 2006; Olad and Naseri, 2010; Kurama et al., 2002; Li et al., 2011). Examination of IHOMZ by X-ray powder diffraction revealed that modification of natural clinoptilolite resulted in no significant structural change but comparative evaluation of the

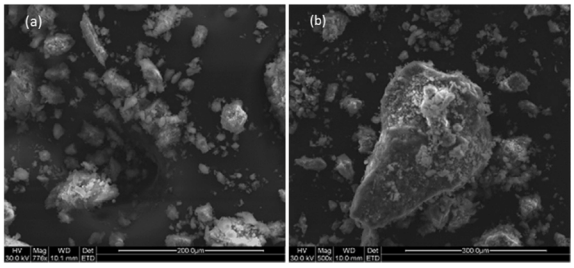


Fig. 1. SEM image of (a) natural zeolite and (b) IHOMZ.

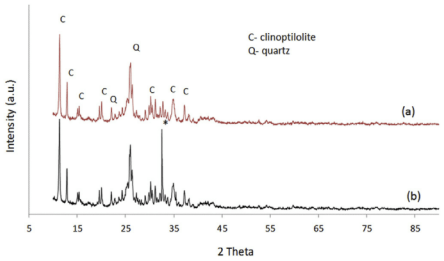


Fig. 3. X-ray powder diffraction pattern of (a) natural zeolite and (b) IHOMZ.

diffractograms revealed that there was no visible change on the reflection position, although the bernalite peak was observed at $2\theta = 33°$. Furthermore, a decrease in the reflection intensities was observed, except for the peak at $2\theta = 26°$, which represent silicon oxide. The reflection position at ($2\theta = 11°, 13°, 22°, 26°, 35°, 37°$, and $38°$) corresponds to clinoptilolite (Korkuna et al., 2006; Ren et al., 2014). A similar change in the intensity of most reflections was observed by Vasylechko et al. (2003) after treating clinoptilolite with 1.0 M HCl solution.

3.2. Effect of initial solution pH

The surface charge of IHOMZ is controlled by the protonation and deprotonation reaction of the iron-hydroxide grafted on the surface of the zeolite (Jeon et al., 2009). Depending on the solution pH, the surface charge can either be positive or negative. At acidic pH (pH< pH_{pzc}), the material is positive because of the protonation of the hydroxyl groups around the sorbent by the excess proton in solution, providing more active site for arsenate adsorption which exists as an oxyanion. At pH > pH_{pzc}, the surface of IHOMZ is negatively charged. The adsorption of As(V) onto IHOMZ was insignificantly affected by the initial pH of the solution. As illustrated in Fig. 4, the adsorption capacity of As(V) by IHOMZ remained constant at pH studied (3–8) indicating that adsorption likely followed a surface complexation process and was thus independent of pH. At pH range 3–8 the speciation of As(V) was found to remain constant (as As(V)) throughout this pH range with $H_2AsO_4^-$ as the dominant species. Thus, the reaction of As and the surface before and after the pH_{PZC} did not change. Jeon et al. (2009) observed a similar trend in pH range 3 < pH < 9 when investigating the adsorption of As(V) by iron coated zeolite. The possible mechanism for As(V) adsorption by iron (hydr) oxide modified zeolite was therefore proposed to proceed *via* inner sphere complexation and could be presented as:

$$Fe - OH(s) + H_2AsO_4^- \rightleftharpoons Fe - OAsO_3H_2 + OH^-$$

The mechanism put forward is well in agreement with the observed pH increase in the equilibrium solution an increase in pH of 0.10–0.40 for the initial As(V) concentrations of 10–212 mg L^{-1}. This observation could be due to the fact that arsenic forms complexes with the iron attached to the surface of the zeolite, displacing the hydroxyl group, resulting in an increase observed while conducting the batch experiments. The formation of inner sphere complexes between iron(III) hydroxide on the surface of the zeolite and arsenate would enhance As(V) removal from aqueous solution. An increase in the equilibrium pH from an initial pH of 3.10–3.30 supports the proposed mechanism of As(V) adsorption by IHOMZ.

3.3. Effect of adsorbent dosage

The influence of sorbent dosage on the removal efficiency of As(V) by IHOMZ is illustrated in Fig. 5. The adsorption capacity of As(V) decreased from 0.175 mg g^{-1} to 0.108 mg g^{-1} with an increase in IHOMZ dosage. The increase in the dosage resulted in an increase in the number of vacant active sites available for adsorption, thus an increase in removal efficiency of As(V) by IHOMZ. After 2.0 g, the adsorption reached a plateau value, and 3.0 g was taken as an optimum dosage for further experiments.

3.4. Effect of contact time on As(V) uptake and kinetic modelling

The effect of contact time on the adsorption of As(V) onto by IHOMZ was studied and the results are shown in Fig. 6. The plot shows that the adsorption of As(V) increased with time, reaching a plateau at 240 min. After that, no significant change was observed in the adsorption of As(V), suggesting that equilibrium was reached. This may be attributed to lower availability of active sites onto the surface of IHOMZ as time progressed. The amount of As(V) sorbed at equilibrium point reflects the maximum removal by the sorbent under the operating conditions applied. Similar time dependence results were obtained by Li et al. (2011) who used Fe-modified zeolite to adsorb arsenic.

The two most commonly utilized kinetic models; pseudo-first-order and pseudo-second-order kinetic models were employed to explore the characteristic adsorption behaviour of As(V) onto IHOMZ, and the suitability of the models was judged by coefficient

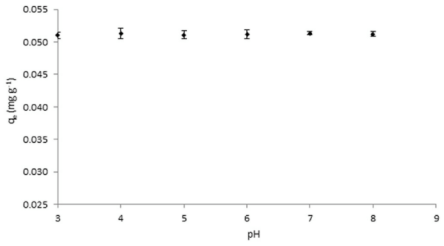


Fig. 4. Effect of pH on the adsorption of As(V) onto IHOMZ. (Experimental conditions: As(v) concentration = 10 mg L^{-1}, mass = 3.0 g, volume = 30 mL and contact time = 90 min) (n = 3, RSD < 5%).

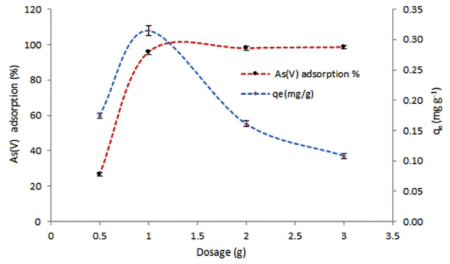


Fig. 5. Effect of adsorbent dose of IHOMZ on the adsorption of As(V). (Experimental conditions: As(V) concentration = 10 mg L^{-1}, mass = 3.0 g, volume = 30 mL and contact time = 90 min) (n = 3, RSD < 5%).

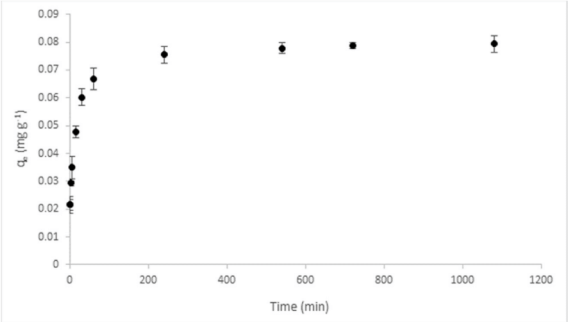


Fig. 6. Effect of contact time on the adsorption of As(V) by IHOMZ. (Experimental conditions: As(V) concentration = 10 mg L^{-1}, mass = 3.0 g and volume = 30 mL) (n = 3, RSD < 5%).

of determination (R^2) and the closeness of the experimental q_m to the calculated q_{cal}. The pseudo-first model was used in the linearized form Eq. (4):

$$\log(q_e - q) = \log q_e - \frac{k_1}{2.303}t \quad (4)$$

where q_e (mg g^{-1}) and q (mg g^{-1}) are the amounts of arsenic adsorbed at per unit mass of adsorbent at equilibrium and time 't' (min), respectively. k_1 (min^{-1}) is the rate constant of pseudo-first-order adsorption. The rate constants, k_1 and q_e were computed from the straight-line plot of $\log(q_e - q)$ versus t. The linearized form of the pseudo-second-order is expressed as Eq. (5).

$$\frac{t}{q_t} = \frac{1}{k_2 q_e^2} + \frac{t}{q_e} \quad (5)$$

where k_2(g mg^{-1} min^{-1}) is the rate constant of second-order adsorption. The intercept and slope of the kinetic plot of $\frac{t}{q_t}$ versus t were used to determine the value of k_2 and q_e.

The values of k_2, k_1 and q_e and coefficients of determination obtained from the linear plots are presented in Table 1. The pseudo-second-order model gave a good linear regression coefficient ($R^2 > 0.99$). Consequently, the good agreement between the modelled and experimentally observed equilibrium adsorption capacity value, and the large correlation coefficients, suggested that As(V) adsorption by IHOMZ followed the pseudo-second-order kinetic model and adsorption occurred *via* a chemical interaction. Ren et al. (2014) reported similar findings when investigating the sorption of As(V) onto modified montmorillonite. The pseudo-second-order kinetic model is the more probable kinetic model to predict the behaviour of the adsorption process with chemical adsorption as a rate controlling step.

3.5. Effect of initial As(V) concentration and isotherm modelling

The dependence of the adsorption on the initial As(V) concentration is shown in Fig. 7. The adsorption percentage decreased with an increase in the initial As(V) concentration. At lower initial As(V) concentration, the number of unoccupied active site on the surface of IHOMZ is higher than the number of As(V) ions so most of As(V) ions are adsorbed onto the sorbent sufficiently. As the initial As(V) concentration increased, the ratio decrease, resulting in the decrease in the adsorption efficiency. Correspondingly, the adsorption capacity increased with an increase in the initial As(V) concentration.

In-order to gain insight on the adsorption mechanism, surface properties and affinity of the sorbent, the equilibrium isotherm models were applied to the equilibrium adsorption data. The experimental adsorption equilibrium information was examined with three most commonly utilized isotherm models, namely the Langmuir, Freundlich, and Dubinin–Radushkevich (D-R) isotherm models. The applicability of the models was judged by the closeness of q_m to the calculated value q_{calc} and the correlation coefficients, R^2.

The Langmuir model assumes a homogeneous surface within the sorbent. The model can be expressed in its linear form, Eq. (6):

$$\frac{C_e}{q_e} = \frac{C_e}{q_m} + \frac{1}{k_l q_m} \quad (6)$$

where q_e (mg g^{-1}) is the maximum sorption capacity of a sorbent, q_m(mg g^{-1}) is the monolayer capacity of the adsorbent, and k_l (L mol^{-1}) is the equilibrium constant. The coefficient of determination (R^2) was found to be 0.947, indicating that the adsorption of As(V) fitted the Langmuir model. The monolayer adsorption capacity and the k_l values of the IHOMZ were found to be 1.69mg g^{-1} and 7626.3 L mol^{-1}, respectively.

The Freundlich model was assessed in the linearized form, Eq. (7):

$$\log(q_e) = \log\left(\text{pg } k_f\right) + \frac{1}{n}\log(C_e) \quad (7)$$

where k_f (mg g^{-1}) is the Freundlich constant, n is the heterogeneity factor and varies with adsorbent. The Freundlich constants k_f

Table 1
Calculated kinetic parameters of pseudo-first and second orders for initial As(V) concentration of 10 mg L^{-1}.

Pseudo-first-order				Pseudo-second-order		
$q_{e,exp}$ (mg g^{-1})	k_1 (min^{-1})	q_e (mg g^{-1})	R^2	k_2 (g mg^{-1} min^{-1})	q_e (mg g^{-1})	R^2
0.113	0.008	0.992	0.899	6.902×10^{-5}	0.080	0.999

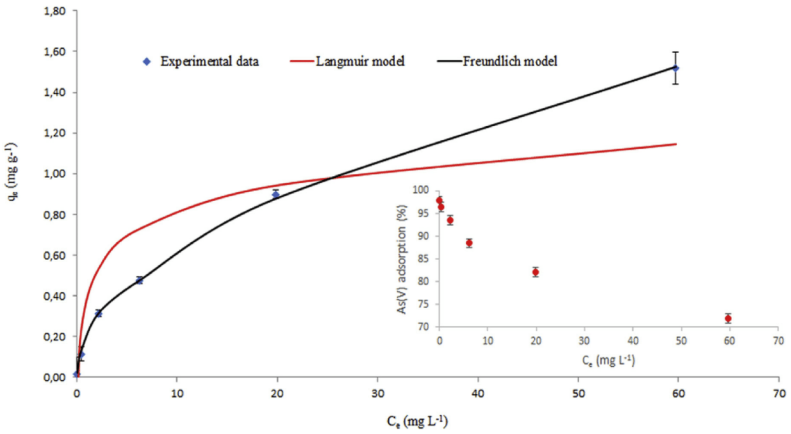


Fig. 7. (a) Effect of initial concentration, Langmuir and Freundlich isotherm on the adsorption of As(V) by IHOMZ. (Experimental conditions: mass = 3.0 g, volume = 30 mL and contact time = 90 min) (n = 3, RSD < 5%). In the insert is the % removal versus initial concentration.

and n were calculated to be 0.152 and 1.637 for As(V) adsorption by IHOMZ, respectively. The value of n > 1 indicated that the adsorption of As(V) was favourable at the operating conditions studied.

With the use of the correlation coefficients, the applicability of different isotherms was assessed. The Freundlich model ($R^2 = 0.984$) was more suitable in describing the equilibrium data, since the coefficient of determination (R^2) for the model was higher than that of the Langmuir model ($R^2 = 0.947$). The modelled results concur with studies executed by other scientist which revealed that the Freundlich model gave a superior fit compared to the Langmuir model for the adsorption of As(V) on different sorbents such as iron modified pottery granules (Dong et al., 2009), nanocrystal line titanium dioxide (Pena et al., 2005), *L. nigrescens* (Hansen et al., 2006), montmorillonite-supported nanoscale zero-valent iron (Bhowmick et al., 2014), granular ferric hydroxide (Guan et al., 2008b), granular activated carbon (Mondal et al., 2008) and iron–chitosan-modified sand (Gupta et al., 2013). Consequently, the comparison between the measured and modelled data for both the Freundlich, and Langmuir isotherm showed that the Freundlich isotherm is a better fit.

Lastly, the Dubinin–Radushkevich isotherm model was employed on the equilibrium data to determine the nature of the adsorption processes. The linearized form of the Dubinin–Radushkevich model can be expressed as Eq. (8):

$$\ln q_e = \ln x_m + \beta\varepsilon^2 \tag{8}$$

where x_m (mg g^{-1}) is the maximum sorption capacity of sorbent, q_e (mg g^{-1}) is the amount adsorbed at equilibrium, β is a constant (mol^2 kJ^{-2}) related to the mean sorption energy, and ε is the Polanyi potential ($\varepsilon = RT\ln\left(1+\frac{1}{C_e}\right)$). The mean free energy (E_{DR}) (kJ mol^{-1}) can be expressed as Eq. (9):

$$E_{DR} = \frac{1}{\sqrt{-2\beta}} \tag{9}$$

The D–R model fitted the experimental data well, since the coefficients of determination value was 0.998 and the x_m value was calculated to be 0.465 mg g^{-1} for As(V) adsorption by IHOMZ (Table 2). The magnitude of E_{DR} is a useful parameter for assessing the type of adsorption process (physical or chemical). E_{DR} value between 8 and 16 kJ mol^{-1} implies that the adsorption process proceeds *via* a chemical ion exchange, and E_{DR} < 8 kJ mol^{-1} implies a physical nature of adsorption on the sorbent. The mean free energy for As(V) adsorption by IHOMZ was computed to be 10.56 kJ mol^{-1}, implying the adsorption process was taking place *via* a chemical ion exchange mechanism.

3.6. Adsorption thermodynamics

The temperature of the solution is important for energy dependent adsorption process. In order to describe the thermodynamic behaviour of As(V) adsorption, thermodynamic parameters Gibbs free energy (ΔG°) was calculated from Eq. (10):

$$\Delta G^\circ = -RT\ln K_d \tag{10}$$

where ΔG° is the standard free energy change, R (J K^{-1} mol^{-1}) is the universal gas constant, T (K) is the absolute temperature and K_d is the distribution coefficient. The values of ΔH° and ΔS° were computed from Eq. (11):

$$\ln K_d = \frac{\Delta S^\circ}{R} - \frac{\Delta H^\circ}{RT} \tag{11}$$

The slope and intercept of the Van't Hoff plot were used to calculate ΔH° and ΔS°, respectively (Fig. 8). The adsorption capacity of As(V) onto IHOMZ increased with increasing solution temperature from 23 to 53 °C for a constant initial concentration, indicating that the adsorption process was endothermic in nature. It is known that the increase in temperature results in a decrease in the viscosity of the solution, resulting in an increase in the rate of diffusion of the As(V) ions across the boundary layer (Tan et al., 2008; Al-Ghouti et al., 2005).

Table 2
Langmuir, Freundlich, and Dubinin–Radushkevich isotherm model constants and their correlation coefficients.

Langmuir constant			Freundlich constant			D-R constant		
k_l (L mol^{-1})	q_m (mg g^{-1})	R^2	n	k_f (mg g^{-1})	R^2	x_m (mg g^{-1})	E_{DR} (kJ mol^{-1})	R^2
7626.3	1.69	0.947	1.64	0.152	0.984	0.465	10.43	0.998

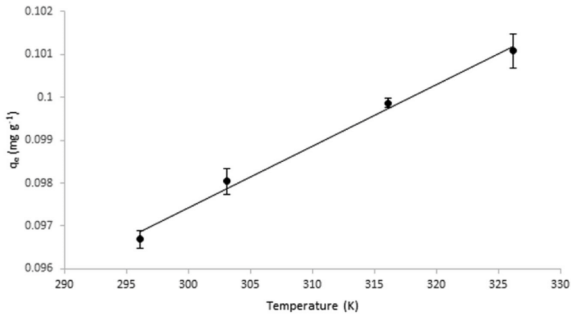


Fig. 8. Effect of temperature on the adsorption of As(V) by IHOMZ. (Experimental conditions: As(V) concentration = 10 mg L^{-1}, mass = 3.0 g, volume = 30 mL, and contact time = 90 min) (n = 3, RSD < 5%).

The variations of ΔG° were calculated to be 6.98, 6.92, 6.82, and 6.74 kJ mol^{-1} for As(V) adsorption at 296.15, 303.15, 316.15 and 326.15 K, respectively (Table 3). The positive value of ΔG° indicated a non-spontaneous adsorption process at the temperatures studied, and may be attributed to a chemisorption process. This is usually associated with a large activation energy (E_a) barrier or irreversible reaction. The decrease in the variation of ΔG° as the temperature increased showed the feasibility of the adsorption process at higher temperature. The enthalpy (ΔH°) and entropy (ΔS°) values were calculated to be 9.392 kJ mol^{-1} and 0.00815 kJ K^{-1} mol^{-1}, respectively. The positive value of enthalpy (ΔH°) indicated the endothermic nature of adsorption at the sorbent. The positive entropy (ΔS°) value was indicative of the increase in randomness at the IHOMZ and As(V) solution interface during the adsorption process, implying that this process probably by favoured complexation.

3.7. Influence of co-existing oxyanions

The effect of other anions (SO_4^{2-}, CO_3^{2-} and HPO_4^{2-}) on the adsorption of As(V) was examined (Table 4). The presence of SO_4^{2-}, HPO_4^{2-} and CO_3^{2-} anions had insignificant effect on the adsorption of As(V) up to 250 mg L^{-1}. However, the HPO_4^{2-} anion had the highest effect compared to the other two oxyanions, and reduced the adsorption efficiency of As(V) from 98.4 to 94.5%. The decrease in the adsorption efficiency in the presence of hydrogen phosphate ions was due to the competitive reaction with phosphate. The chemical characteristics of phosphate are very similar to those of arsenic thus; this anion competed with arsenic for the active sites on the adsorbent. Another reason to this behaviour could be that phosphate sorb strongly onto mineral surfaces and forms inner-sphere complexes, therefore affecting the sorption of arsenate (Gao and Mucci, 2001). Similarly, Su and Puls (2001) reported that the removal of As(III) and As(V) by zero-valent was severely inhibited in the presence of phosphate. Despite the effect of these common anions, especially the phosphate anion, it can be concluded that these anions would not interfere significantly with the uptake of arsenic as they were at low concentrations in this study. The observed trend on the adsorption of As(V) in the presence of common co-existing oxyanions anion was as follows: $H_2PO_4^{2-} > SO_4^{2-} > CO_3^{2-}$.

Table 4
Percentage of As(V) removal in the presence of competing anions.

Concentration (mg L^{-1})	Percentage uptake of As(V) in the presence of anions		
	SO_4^{2-}	CO_3^{2-}	HPO_4^{2-}
0	98.4	98.4	98.4
50	98.0	98.1	96.5
100	97.8	98.1	96.2
250	97.4	97.6	94.5

3.8. Application of the adsorbent

The adsorbent was applied to a sample of mine waste water obtained from an abandoned mine site in Johannesburg, South Africa. The mine water had a pH of 2.23, oxidation reduction

Table 3
Thermodynamic parameters for adsorption of As(V) by IHOMZ.

					ΔS° (kJ (mol K)$^{-1}$)	ΔH° (kJ mol^{-1})	R^2
T (K)	297.15	303.15	316.15	326.15	0.00815	9.392	0.999
ΔG° (kJ mol^{-1})	6.98	6.92	6.82	6.74			

Table 5
Recovery of arsenic and other metal ions from acid mine drainage water.

		As	Cr	Fe	Mn	Cu	U	Pb	Zn
Raw AMD	Mean (mg L^{-1})	0.38	0.32	557.25	32.50	1.35	0.54	0.42	9.58
	RSD	5.26	3.13	0.25	0.18	0.07	0.19	0.71	0.09
Treated AMD	Mean (mg L^{-1})	<DL	0.14	35.93	10.06	0.36	0.21	0.25	1.82
	RSD	0.01	7.14	0.04	0.60	0.28	0.48	1.20	0.55
	Recovery (%)	>99	56.9	93.6	68.6	73.5	60.8	41.7	81.0
	RSD	5.26	7.79	0.25	0.18	0.29	0.52	1.39	0.56

RSD – relative standard deviation.
AMD – Acid mine drainage.

Table 6
Maximum adsorption capacities of some adsorbents reported in the literature.

Adsorbent	pH	q (mg g^{-1})	References
Iron (hydr) oxide modified zeolite	3.5	1.69	This study
Iron oxide coated sand	7	0.018	Thirunavukkarasu et al. (2001)
F400-M[a]	7	0.847	Vitela-Rodriguez and Rangel-Mendez (2013)
CAZ-M[a]	7	0.431	Hlavay and Polyák (2005)
Iron hydroxide-coated alumina	4.0	14.98	Hlavay and Polyák (2005)
Iron coated rice husk	4.0	2.472	Pehlivan et al. (2013)
Iron oxide coated quartz (IOCQ)	6	0.097	Mostafa et al. (2010)
Iron oxide-coated perlite (IOCP)	6.5–7	0.390	Mostafa et al. (2011)

[a] Activated carbons modified with iron hydro (oxide) nanoparticles.

potential of 496 mV and electrical conductivity of 3.06 mS cm^{-1}. The water sample was subjected to batch equilibrium experiments using the optimum conditions: amount of adsorbent (3.0 g), contact time (90 min) and volume (30 mL). The results for the batch adsorption experiments are presented in Table 5. Arsenic was not detected after batch equilibrium adsorption, indicating that it was below the detection limit of 0.006 mg L^{-1}. This suggested that the removal exceeded 99%. This result proved the suitability of IHOMZ to selectively extract arsenic ions from aqueous matrices as other recoveries of metal ions were below 100%. The method was also good as it had good repeatability (RSD < 10%)

3.9. Comparison of iron (hydr) oxide modified zeolite with other adsorbents

A comparison of adsorption capacity for As(V) adsorption by IHOMZ with various other adsorbents reported in the literature is shown in Table 6. The maximum adsorption capacity for As(V) adsorption by IHOMZ was found to be 1.69 mg g^{-1} (Table 6). In comparison, the maximum As(V) adsorption capacity of iron (hydr) oxide modified zeolite is superior to most of the adsorbents reported in the literature (Table 6). It appears that IHOMZ has a realistic prospective as an adsorbent for the removal of As(V) from environmental water samples.

3.10. Reusability studies

Disposal of the exhausted adsorbent loaded with toxic pollutants can create another environmental problem as it is potentially a hazardous material (Mostafa et al., 2011). The feasibility of regenerating the spent adsorbent is of utmost importance in the application of a sorbent on a large scale. To elute the As(V) sorbed on IHOMZ and regeneration of the adsorbent, 0.1 M HNO_3 was used as an eluent (Pushpa et al., 2006). Three consecutive adsorption-desorption cycles were performed on the spent IHOMZ to test its reusability. The specific recovery efficiency for three adsorption-desorption cycles performed on IHOMZ were 77.5%, 70.3% and 68.4%. These recovery efficiencies were found to be significantly different ($p < 0.000016$). Moreover, it can be seen from the three cycle a decrease of about 9.1% was observed in the recovery of As(V) after three cycles of sorption-desorption processes.

4. Conclusion

Batch equilibrium study results showed that IHOMZ can be used as an efficient adsorbent for the removal of As(V) from contaminated water sources. The adsorption process has been shown to be dependent on the initial As(V) concentration, adsorbent dosage, and the solution temperature. The adsorption of As(V) by IHOMZ was insignificantly affected by the initial solution pH. The Freundlich isotherm model was found to describe the equilibrium adsorption data adequately. The kinetic data revealed that a pseudo-second-order kinetic model was more appropriate in describing the adsorption process. The results obtained from batch experiments showed that the adsorption of As(V) proceeds via inner-sphere ligand ion exchange mechanism. This inner-sphere ligand replacement by $H_2AsO_4^-$ was also substantiated by the thermodynamic results (sorption energy (E_{DR}) of 10.43 kJ mol^{-1}) that showed that the reaction proceeded via a chemisorption process. The positive enthalpy (ΔH°) value indicated that the adsorption process was endothermic in nature, and followed a chemisorption process. The most common oxyanions such as sulphate carbonate and phosphate had insignificant effect on the adsorption of As(V). The results from this study suggested that IHOMZ has potential as an effective sorbent for As(V). Furthermore, this adsorbent can be regenerated, making its reuse possible.

Conflict of interest

The authors declared no conflict of interest.

Acknowledgement

The authors would like to thank the National Research Foundation (NRF) South Africa for funding Pfano Nekhunguni through the innovation Masters Scholarship [grant ID number SFH150624120802].

References

Al-Ghouti, M., Khraisheh, M.A.M., Ahmad, M.N.M., Allen, S., 2005. Thermodynamic behaviour and the effect of temperature on the removal of dyes from aqueous solution using modified diatomite: a kinetic study. J. Colloid Interface Sci. 287, 6–13.

Alam, M.G.M., Allinson, G., Stagnitti, F., Tanaka, A., Westbrooke, M., 2002. Arsenic contamination in Bangladesh groundwater: a major environmental and social disaster. Int. J. Environ. Res. 12, 235–253.

Baskan, M.B., Pala, A., 2011. Removal of arsenic from drinking water using modified natural zeolite. Desalination 281, 396–403.

Beolchini, F., Pagnanelli, F., De Michelis, I., Vegliò, F., 2006. Micellar enhanced ultrafiltration for arsenic (V) removal: effect of main operating conditions and dynamic modelling. Environ. Sci. Technol. 40, 2746–2752.

Bhowmick, S., Chakraborty, S., Mondal, P., Van Renterghem, W., Van den Berghe, S., Roman-Ross, G., Chatterjee, D., Iglesias, M., 2014. Montmorillonite-supported nanoscale zero-valent iron for removal of arsenic from aqueous solution: kinetics and mechanism. Chem. Eng. J. 243, 14–23.

D. Bonnin, Method of removing arsenic species from an aqueous medium using modified zeolite minerals, U.S. Patent 6,042,731, issued March 28, 2000.

Charkhi, A., Kazemian, H., Kazemeini, M., 2010. Optimized experimental design for natural clinoptilolite zeolite ball milling to produce nano powders. Powder Technol. 203, 389–396.

Chowdhury, S.R., Yanful, E.K., 2010. Arsenic and chromium removal by mixed magnetite–maghemite nanoparticles and the effect of phosphate on removal. J. Environ. Manag. 91, 2238–2247.

Dong, L., Zinin, P.V., Cowen, J.P., Ming, L.C., 2009. Iron coated pottery granules for arsenic removal from drinking water. J. Hazard. Mater. 168, 626–632.

Elizalde-González, M.P., Mattusch, J., Einicke, W.D., Wennrich, R., 2001. Sorption on natural solids for arsenic removal. Chem. Eng. J. 81, 187–195.

Gao, Y., Mucci, A., 2001. Acid base reactions, phosphate and arsenate complexation, and their competitive adsorption at the surface of goethite in 0.7 M NaCl solution. Geochim. Cosmochim. Acta 65, 2361–2378.

Ghimire, K.N., Inoue, K., Yamaguchi, H., Makino, K., Miyajima, T., 2003. Adsorptive separation of arsenate and arsenite anions from aqueous medium by using orange waste. Water Res. 37, 4945–4953.

Guan, X.H., Wang, J., Chusuei, C.C., 2008a. Removal of arsenic from water using granular ferric hydroxide: macroscopic and microscopic studies. J. Hazard. Mater 156, 178–185.

Guan, X.H., Wang, J., Chusuei, C.C., 2008b. Removal of arsenic from water using granular ferric hydroxide: macroscopic and microscopic studies. J. Hazard. Mater 156, 178–185.

Guo, X., Wu, Z., He, M., 2009. Removal of antimony (V) and antimony (III) from drinking water by coagulation–flocculation–sedimentation (CFS). Water Res. 43, 4327–4335.

Gupta, A., Yunus, M., Sankararamakrishnan, N., 2013. Chitosan-and Iron–chitosan-coated sand filters: a cost-effective approach for enhanced arsenic removal. Ind. Eng. Chem. Res. 52, 2066–2072.

Han, R., Zou, L., Zhao, X., Xu, Y., Xu, F., Li, Y., Wang, Y., 2009. Characterization and properties of iron oxide-coated zeolite as adsorbent for removal of copper (II) from solution in fixed bed column. Chem. Eng. J. 149, 123–131.

Hansen, H.K., Ribeiro, A., Mateus, E., 2006. Biosorption of arsenic (V) with Lessonia nigrescens. Miner. Eng. 19, 486–490.

Hlavay, J., Polyák, K., 2005. Determination of surface properties of iron hydroxide-coated alumina adsorbent prepared for removal of arsenic from drinking water. J. Colloid. Interface Sci. 284, 71–77.

Jeon, C.S., Baek, K., Park, J.K., Oh, Y.K., Lee, S.D., 2009. Adsorption characteristics of As(V) on iron-coated zeolite. J. Hazard. Mater 163, 804–808.

Jha, V.K., Hayashi, S., 2009. Modification on natural clinoptilolite zeolite for its NH4+ retention capacity. J. Hazard. Mater. 169, 29–35.

Jiménez-Cedillo, M.J., Olguín, M.T., Fall, C., 2009. Adsorption kinetic of arsenates as water pollutant on iron, manganese and iron–manganese-modified clinoptilolite-rich tuffs. J. Hazard. Mater. 163, 939–945.

Joshi, A., Chaudhuri, M., 1996. Removal of arsenic from ground water by iron oxide-coated sand. J. Environ. Eng. 122, 769–771.

Kanel, S.R., Manning, B., Charlet, L., Choi, H., 2005. Removal of arsenic (III) from groundwater by nanoscale zero-valent iron. Environ. Sci. Technol. 39, 1291–1298.

Kang, M., Kawasaki, M., Tamada, S., Kamei, T., Magara Kang, Y., 2000. Effect of pH on the removal of arsenic and antimony using reverse osmosis membranes. Desalination 131, 293–298.

Katsoyiannis, I.A., Zouboulis, A.I., 2004. Application of biological processes for the removal of arsenic from groundwaters. Water Res. 38, 17–26.

Korkuna, O., Leboda, R., Skubiszewska-Zie, J., Vrublevs'ka, T., Gun'ko, V.M., Ryczkowski, J., 2006. Structural and physicochemical properties of natural zeolites: clinoptilolite and mordenite. Microporous Mesoporous Mater. 87, 243–254.

Kurama, H., Zimmer, A., Reschetilowski, W., 2002. Chemical modification effect on the sorption capacities of natural clinoptilolite. Chem. Eng. Technol. 25, 301–305.

Li, Z., Jean, J.S., Jiang, W.T., Chang, P.H., Chen, C.J., Liao, L., 2011. Removal of arsenic from water using Fe-exchanged natural zeolite. J. Hazard. Mater. 187, 318–323.

Macedo-Miranda, M.G., Olguin, M.T., 2007. Arsenic sorption by modified clinoptilolite–heulandite rich tuffs. J. Incl. Phenom. Macrocycl. Chem. 59, 131–142.

Mohan, D., Pittman, C.U., 2006. Activated carbons and low cost adsorbents for remediation of tri-and hexavalent chromium from water. J. Hazard. Mater. 137, 762–811.

Mondal, P., Majumder, C.B., Mohanty, B., 2008. Effects of adsorbent dose, its particle size and initial arsenic concentration on the removal of arsenic, iron and manganese from simulated ground water by Fe3+ impregnated activated carbon. J. Hazard. Mater. 150, 695–702.

Mostafa, M.G., Chen, Y.H., Jean, J.S., Liu, C.C., Teng, H., 2010. Adsorption and desorption properties of arsenate onto nano-sized iron-oxide-coated quartz. Water Sci. Technol. 62, 378–386.

Mostafa, M.G., Chen, Y.H., Jean, J.S., Liu, C.C., Lee, Y.C., 2011. Kinetics and mechanism of arsenate removal by nanosized iron oxide-coated perlite. J. Hazard. Mater. 187, 89–95.

Mozgawa, W., 2000. The influence of some heavy metals cations on the FTIR spectra of zeolites. J. Mol. Struct. 555, 299–304.

Mozgawa, W., Krol, M., Pichor, W., 2009. Use of clinoptilolite for the immobilization of heavy metal ions and preparation of autoclaved building composites. J. Hazard. Mater 168, 1482–1489.

Mozgawa, W., Król, M., Bajda, T., 2009b. Application of IR spectra in the studies of heavy metal cations immobilization on natural sorbents. J. Mol. Struct. 924, 427–433.

Ng, J.C., Wang, J., Shraim, A., 2003. A global health problem caused by arsenic from natural sources. Chemosphere 52, 1353–1359.

Olad, A., Naseri, B., 2010. Preparation, characterization and anticorrosive properties of a novel polyaniline/clinoptilolite nanocomposite. Prog. Org. Coat. 67, 233–238.

Payne, K.B., Abdel-Fattah, T.M., 2005. Adsorption of arsenate and arsenite by iron-treated activated carbon and zeolites: effects of pH, temperature, and ionic strength. J. Environ. Sci. Health 40, 723–749.

Pehlivan, E., Tran, E.T.H., Ouédraogo, W.K.I., Schmidt, C., Zachmann, D., Bahadir, M., 2013. Removal of As(V) from aqueous solutions by iron coated rice husk. Fuel Process. Technol. 106, 511–517.

Pena, M.E., Korfiatis, G.P., Patel, M., Lippincott, L., Meng, X., 2005. Adsorption of As(V) and As(III) by nanocrystalline titanium dioxide. Water Res. 39, 2327–2337.

Pushpa, K., Sharma, P., Srivastava, S., Srivastava, M.M., 2006. Biosorption studies on shelled Moringa oleifera Lamarck seed powder: removal and recovery of arsenic from aqueous system. Int. J. Miner. Process. 78, 131–139.

Ren, X., Zhang, Z., Luo, H., Hu, B., Dang, Z., Yang, C., Li, L., 2014. Adsorption of arsenic on modified montmorillonite. Appl. Clay Sci. 97, 17–23.

Sarı, A., Tuzen, M., 2009. Biosorption of As(III) and As(V) from aqueous solution by macrofungus (Inonotus hispidus) biomass: equilibrium and kinetic studies. J. Hazard. Mater. 164, 1372–1378.

Shuibo, X., Chun, Z., Xinghuo, Z., Jing, Y., Xiaojian, Z., Jingsong, W., 2009. Removal of uranium (VI) from aqueous solution by adsorption of hematite. J. Environ. Radioact. 100, 162–166.

Simsek, E.B., Özdemir, E., Tuna, A.O.A., Beker, U., 2014. Factorial design analysis of as (V) adsorption onto iron-aluminum binary oxide-doped clinoptilolite. Desalin. Water Treat. 52, 7812–7821.

Stanić, T., Daković, A., Živanović, A., Tomašević-Čanović, M., Dondur, V., Milićević, S., 2009. Adsorption of arsenic (V) by iron (III)-modified natural zeolitic tuff. Environ. Chem. Lett. 7, 161–166.

Su, C., Puls, R.W., 2001. Arsenate and arsenite removal by zerovalent iron: effects of phosphate, silicate, carbonate, borate, sulfate, chromate, molybdate, and nitrate, relative to chloride. Environ. Sci. Technol. 35, 4562–4568.

Sun, H., Wang, L., Zhang, R., Sui, J., Xu, G., 2006. Treatment of groundwater polluted by arsenic compounds by zero valent iron. J. Hazard. Mater 129, 297–303.

Tan, I.A.W., Ahmad, A.L., Hameed, B.H., 2008. Adsorption of basic dye on high-surface-area activated carbon prepared from coconut husk: equilibrium, kinetic and thermodynamic studies. J. Hazard. Mater 154, 337–346.

Thirunavukkarasu, O.S., Viraraghavan, T., Subramanian, K.S., 2001. Removal of arsenic in drinking water by iron oxide-coated sand and ferrihydrite-batch studies. Water Qual. Res. J. Can. 36, 55–70.

Vahedi, A., Gorczyca, B., 2011. Application of fractal dimensions to study the structure of flocs formed in lime softening process. Water Res. 45, 545–556.

Vasylechko, V.O., Gryshchouk, G.V., Kuz'ma, Y.B., Zakordonskiy, V.P., Vasylechko, L.O., Lebedynets, L.O., Kalytovs'ka, M.B., 2003. Adsorption of cadmium on acid-modified Transcarpathian clinoptilolite. Microporous Mesoporous Mater. 60, 183–196.

Vitela-Rodriguez, A.V., Rangel-Mendez, J.R., 2013. Arsenic removal by modified activated carbons with iron hydro (oxide) nanoparticles. J. Environ. Manag. 114, 225–231.

Wang, C., Luo, H., Zhang, Z., Wu, Y., Zhang, J., Chen, S., 2014. Removal of As(III) and As(V) from aqueous solutions using nanoscale zero valent iron-reduced graphite oxide modified composites. J. Hazard. Mater 268, 124–131.

Paper II

This paper “Adsorption of uranium (VI) from aqueous solution by application of iron hydro (oxide) modified zeolite” is still in preparation. It investigates the extraction of U(VI) from aqueous solution by application of iron modified zeolite as a sorbent.

Adsorption of uranium(VI) from aqueous solution by application of iron hydro (oxide) modified zeolite.

Pfano Mathews Nekhunguni, Nikita Tawanda Tavengwa, Hlanganani Tutu*

Molecular Sciences Institute, School of Chemistry, University of the Witwatersrand, Private Bag X3, WITS 2050 Johannesburg, South Africa,

**Corresponding author. Email: hlanganani.tutu@wits.ac.za, Tel.: +27 11 717 6753*

Abstract

Iron hydro (oxide)-modified zeolite was prepared by precipitation of iron onto zeolite. The prepared iron hydro (oxide) modified zeolite was then assessed as the adsorbent for uranium(VI) removal from aqueous solution. The concentration of uranium in solution was determined using ICP-OES. The prepared adsorbent material was characterized by scanning electron microscope (SEM), and Fourier transform infrared spectroscopy (FTIR). Various parameters such as solution pH, initial concentration, sorbent dosage and rate of adsorption were investigated using batch adsorption experiments and the optimum conditions were: solution pH (6 ± 0.1), initial U(VI) concentration (10 mg L^{-1}), mass (3.0 g) and contact time (30 min). The kinetic data was better correlated by the pseudo-second-order kinetic model ($R^2 > 0.999$). The adsorption experimental equilibrium data was best defined by Freundlich isotherm model ($R^2 > 0.933$). The adsorption of U(VI) onto iron hydro (oxide) modified zeolite was non-spontaneous and exothermic.

Keywords: PHREEQC, Uranium, Iron hydro (oxide) modified zeolite, Modelling, Thermodynamics

1. Introduction

Contamination of water bodies by operational and out of commission gold mining operation is a renowned environmental predicament in mining industry around the world (Chisholm-Brause *et al*., 2001). Mining operation exposes pyrite and non-pyritic sulfidic minerals to atmospheric conditions resulting in the formation of acidic and sulphate rich waste-water (Akcil and Koldas, 2006). Waters infiltrating through active and abandoned mines are often net acidic, allowing the transport of metal in soluble forms (Akcil and Koldas, 2006).

Such waters characteristically pose an additional threat to the environment as they are characterized by elevated concentrations of aluminium, iron, manganese and low concentrations of toxic trace metals (Johnson and Hallberg, 2005). The metal load in the waters is of superior concern as compared to its acidity when it comes to environmental damage (Sheoran and Sheoran, 2006). Uranium is one of the most severe contaminants of concern in gold and uranium mining industry, because of its radioactivity and toxicity. The toxicity of uranium compounds poses a threat to the human health and ecosystem balance (Weihau *et al*., 2009; Shimin *et al*., 2013).

The toxicity effect of uranium when consumed in water is similar to that of heavy metal like cadmium, lead and arsenic, accumulates in kidneys causing irreparable damage to the main filtering mechanism in the body (Medvidović and Trgo, 2006; Johnson and Hallberg, 2005; Choy *et al*., 2005). The World Health Organization (WHO) has classified uranium as a carcinogen and with a concentration limit of 50 $\mu g\, L^{-1}$ in water. The U.S. Environmental Protection Agency (US EPA) has recommended a limit of 20 $\mu g\, L^{-1}$ in drinking water (Camacho *et al.*, 2010; Wang *et al.*, 2009).

Under standard environmental conditions, uranium predominately exists in its hexavalent form as the mobile, linear dioxo uranyl cation or with its hydroxyl complexes. However, in the presence of commonly occurring oxyanions, uranyl forms complexes and therefore its speciation is affected (Matijasevic *et al.*, 2006; Katsoyiannis, 2007; Katsoyiannis and Zouboulis, 2012).

Several processes are available for uranium removal in waste water such as chemical precipitation (Fu and Wang, 2011)**,** ion exchange (Dabrowski *et al*., 2004), membrane separation (Mavrov *et al*., 2003) and coagulation (Feryal and

Camcı, 2010). However, most of these methods suffer from some disadvantage such as incomplete metal recovery, generation of toxic sludge and immense cost (Shuibo *et al.*, 2009).

Adsorption has been reported to be an effective and economic method for metal recovery from wastewater (Wang *et al.*, 2009). Various materials, such as activated carbon (Yi *et al*., 2016), synthetic polymer (Tavengwa *et al.*, 2014), zeolite (Akyil and Eral, 2004), and biomass (Bhat *et al*., 2008) have been used for uranium recovery.

Among them, zeolite as low cost adsorbent, have gained significant interest in the removal of heavy and trace metal from contaminated water, attributed to their strong affinity for toxic heavy metals (Wang *et al.*, 2009; Kreston *et al*., 2004). The uranyl ion has been shown to be strongly sorbed onto metal oxide/hydroxide under appropriate chemical conditions. Therefore, such material can be used for the removal of uranium from aqueous solution (Shuibo *et al.*, 2009; Sharma and Tomar, 2008).

As far as the authors are concerned, there is no investigation reported in literature on the use of iron hydro (oxide) supported on zeolite as a sorbent for U(VI) recovery from acid mine drainage. The purpose of this work was to study the possibility of utilizing iron hydroxide modified zeolite as an adsorbent for the removal of U(VI) from acid mine drainage water. Sorption of uranium onto iron hydro (oxide) modified zeolite was investigated under various experimental conditions i.e. pH, uranium concentration, temperature, contact time and contents of other heavy metals in solution. The adsorption isotherms, kinetic, thermodynamic studies and pH Redox Equilibrium Code (PHREEQC) code were used for data modelling to gain insight of the equilibrium adsorption mechanisms

2. Materials and methods

2.1. Chemical and Reagents

All chemical used in this study were purchased as analytically pure, and no further purification was done. Uranyl nitrate ($UO_2(NO_3)_2.6H_2O$), ferric nitrate ($Fe(NO_3)_3.9H_2O$), sodium hydroxide ($NaOH$) and nitric acid (HNO_3), were purchased from Sigma-Aldrich (Johannesburg, South Africa). The raw zeolite

sample used in this study was obtained from the field in Johannesburg, South Africa. Stock solution of 1000 mg L^{-1} of U(VI) was prepared by dissolving a desired amount of uranyl nitrate($UO_2(NO_3)_2.6H_2O$) obtained from Sigma-Aldrich (Johannesburg, South Africa) in ultrapure water obtained from Millipore water system (Massachusetts, USA). The initial pH of the working solutions was adjusted by addition of 0.1 M HNO_3 and/or 0.1 M NaOH solution, and was measured using a Mettler Toledo pH meter (Johannesburg, South Africa). A Spectro Genesis inductively coupled plasma optical emission spectrometry (ICP-OES) from Spectro (Kleve, Germany) was used to analyse the sample. The solutions were centrifuge using a Hettich ROTOFIX 32A benchtop centrifuge (Massachusetts, United States)

2.2. Characterization techniques

Powered X-ray diffraction (PXRD) analyses were performed on both iron treated and natural zeolite to identify the mineralogy of the zeolite materials. Powder diffractograms of both samples were obtained with a Bruker D2 diffractometer (Bruker, Germany) couple with a copper anode x-ray tube. Fourier transform infrared (FT-IR) spectra were obtained using Tensor 27 spectrophometer (Bruker, Germany). The FT-IR spectra ranged from 400 – 4000 cm^{-1} at a resolution of 2 cm^{-1}. The chemical composition of natural zeolite was determined using WD X-ray fluorescence (XRF) spectrometer (Almelo, Netherlands). Only major elements were determined in their oxide form. For morphological observation, scanning electron microscopy (SEM), a FEI Quanta 200 ESEM electron microscope (Oregon, USA) at 30 KV was used.

2.3. Preparation of iron hydro (oxide) modified zeolite

Prior to modification, the natural zeolite was washed with 1000 mL of deionized water and air-dried. A sample of 100 g of natural zeolite (Z) was then transferred to a flask containing 1000 mL of 2.0 M NaCl solution. The mixture was shaken for 24 h at ambient temperature, and then separated by decantation. The zeolitic material was washed with 1500 mL deionized water until elimination of chloride ions was achieved, $AgNO_3$ was used to test the presence of chloride ions. Finally, the sodium-treated zeolite (NaZ) was air-dried.

The iron hydro (oxide) modified zeolite was prepared by adding 100g of NaZ to a flask containing 1000 mL of 0.5 M $Fe(NO_3)_3$ solution, the pH of the solution was adjusted to pH value between 3-4 by adding 0.1 M NaOH and /or 0.1 M HNO_3 to create an iron precipitate. The mixture was shaken with an overhead shaker (150 rpm) for 24 h. The solid phase was separated by decantation and was washed exhaustively with 500 mL of distilled water and then air-dried.

2.4. U(V) batch adsorption studies

The adsorption of U(VI) by iron hydro (oxide) modified zeolite was investigated by batch technique in polyethylene tube at ambient temperature. Sorption experiments were conducted at different condition viz., pH (3-10), mass (0.5 - 5.0 g), initial U(VI) concentration (1.0 - 50 mg L^{-1}) and temperature (20 - 53°C). The pH of U(VI) solution was adjusted by adding 0.1 M HNO_3 and/or 0.1 M NaOH solution. The mixtures were shaken on an overhead shaker. The samples were centrifuge before analysis by ICP-OES.

The amount of adsorbed U(VI) in (mg g^{-1}) at equilibrium (q_e) was calculated from mass balance of its concentrations initially in the test solution and that detected in supernatant liquid after adsorption. The amount of U(VI) at time t (min) was calculated from mass balance equation Eq. 1 and the adsorption percentage of U(VI) ions adsorbed were calculated by the difference of initial and final concentration using Eq. 2:

$$q_e = \frac{(C_o - C_e)V}{m} \quad (1)$$

$$\text{Adsorption } (\%) = \frac{(C_o - C_e)}{C_o} \times 100 \quad (2)$$

where C_o(mg L^{-1}) and C_e(mg L^{-1}) are the concentration of U(VI) in the solution before and after adsorbent addition respectively, v(mL) the volume of the aqueous solution and m(g) is the weight of the iron hydro (oxide) modified zeolite. The initial and final concentrations of U(VI) were determined by ICP-OES.

2.5. Point of zero charge (pH_{pzc})

For the point of zero charge (pH_{pzc}) determination the procedure was adopted from Tavengwa et al. (2015) and was followed step by step without any

modification. A 0.01 mol L^{-1} $NaNO_3$ solution was put in contact with 20 mg of iron hydro (oxide) modified zeolite, in duplicate.

2.6. Influence of co-existing anions and cations

In practice, acid mine drainage contains a mixture of different cation ions and anions. Batch experiments were carried out at optimum condition to investigate the influence of the presence of competing cations and anions on the adsorption of U(VI). The adsorption of U(VI) onto iron hydro (oxide) modified zeolite in the presence of SO_4^{2-}, CO_3^{2-} and HPO_4^{2-} anions were assessed through batch technique, and the U(VI) concentration was determined using ICP-OES. A multi-element mixture containing Cr^{3+}, Mn^{2+}, Pb^{2+}, Cu^{2+} and Co^{2+} was used to assess the effect of selected competing cations.

3. Results and discussion

3.1. Characterization of the adsorbent

The chemical compositions of the natural zeolite investigated in this work was determined by XRF elemental analysis and summarized in **Table 1**. XRF measurement showed that the major chemical compositions of the natural zeolite were SiO_2, Al_2O_3, K_2O, Na_2O, and FeO. The Si/Al ratio calculated from the data was found as 6.01 and a loss of ignition of 10.8. Generally, major chemical constituents of the studied clinoptilolite were similar to other natural clinoptilolite zeolite from other countries (Alver *et al*., 2010; Camacho *et al*., 2010(a); Jha *et al*., 2009). **Fig 1** illustrates the XRD diffractogram of (a) zeolite and (b) iron hydro (oxide) modified zeolite, respectively. The most intense reflections observed correspond to the literature data of clinoptilolite zeolite (Baskan *et al*., 2011; Camacho *et al.*, 2011(b)). The two diffraction patterns show that there was no dire change on the crystal-chemistry of the natural clinoptilolite zeolite after modification with iron and but a new intense peak was observed at $2\theta = 33°$ indicating the presence of additional iron hydroxide crystalline phase in the form of bernalite resulting from the iron hydroxide coating of the zeolite. The reflection position at ($2\theta = 11°$, 13°, 22°, 26°, 35°, 37°, and 38°) corresponds to clinoptilolite

(Alver *et al*., 2010; Baskan *et al*., 2011; Camacho *et al*., 2011(b), Mihaly-Cozmuta *et al*.,2014). The surface morphology of the iron hydro (oxide) modified zeolite was investigated by SEM. **Fig. 2** (a) and (b) shows the SEM microphotograph of natural and modified zeolite, respectively. Both SEM micrographs (**Fig. 2**) showed no difference between the natural and modified zeolite, and were characterised by a rough surface. Plates, tabular morphology and laths crystals were observed on the surface, and are typically crystals of clinoptilolite family of zeolite (Charkhi *et al*., 2010; Jiménez-Cedillo *et al*., 2009; Jha and Hayashi, 2009; Díaz-Nava *et al*., 2005). Kragović *et al* (2013) observed similar morphology when investigating adsorption of lead by Fe(III)-modified zeolite. SEM coupled with EDS provides a semi quantitative elemental analysis of the sorbent. In the EDS spectra of natural clinoptilolite zeolite, O (51.59%), Na (0.76%), Mg (0.53%), Al (6.62%), Si (33.22%), K (4.0%), Ca (2.09%) and Fe (0.21%) were detected. Uranium was not detected implying that there was no possibility of it leaching into the solution during application of the sorbent in uranium adsorption. The natural and iron hydro (oxide) modified zeolite was also characterised using Fourier transform infrared spectroscopy (FTIR) technique. The intense peak observed at 3410.11, 1627.68, 1009.65, 788.94, 719.77, 671, and 592.04 cm^{-1} are characteristic peaks of zeolite (**Fig 3**). The peaks at 3410.11 cm^{-1} and 1627.68 cm^{-1} can be assigned to the stretching vibration mode of the hydroxyl groups, lattice water and the OH bending vibration of adsorbed water molecules. The bands 788.94 and 719.77 cm^{-1} represent the symmetric stretch of the zeolite framework. While bands at 1009.65, 671, and 592.04 cm^{-1} represented the asymmetric stretch, water vibration mode and the bending of the framework, respectively (Mozgawa, 2000, Han *et al.*, 2009; Nezamzadeh-Ejhieh and Zabihi-Mobarakeh, 2014). After modification with iron, the characteristic peaks of zeolite were preserved. Thus, indicating that there was no physical alteration on the zeolite framework and the perturbation observed on the characteristic peaks of zeolite indicates the presents of iron on the surface of zeolite. The minute shift observed on the FT-IR, were similar to those reported by Han *et al*. (2009).

Table 1: Chemical composition of natural zeolite

	Percent (% w/w)	Metal oxide	Percent (% w/w)
SiO_2	77.91	Al_2O_3	12.95
Fe_2O_3	0.13	FeO	1.04
MnO	0.02	MgO	0.76
CaO	0.89	Na_2O	2.74
K_2O	3.59	TiO_2	0.153
P_2O_5, NiO, and Cr_2O_3	<1	LOI*	10.8

**LOI loss of ignition*

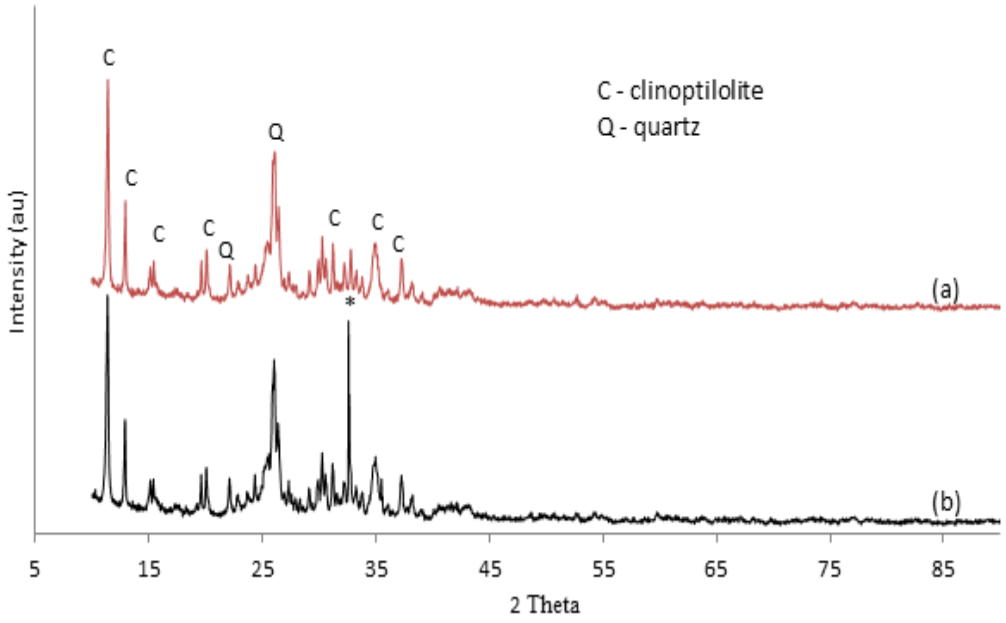


Figure 1: *X-ray powder diffraction pattern of (a) natural zeolite and (b)* iron hydro (oxide) modified zeolite

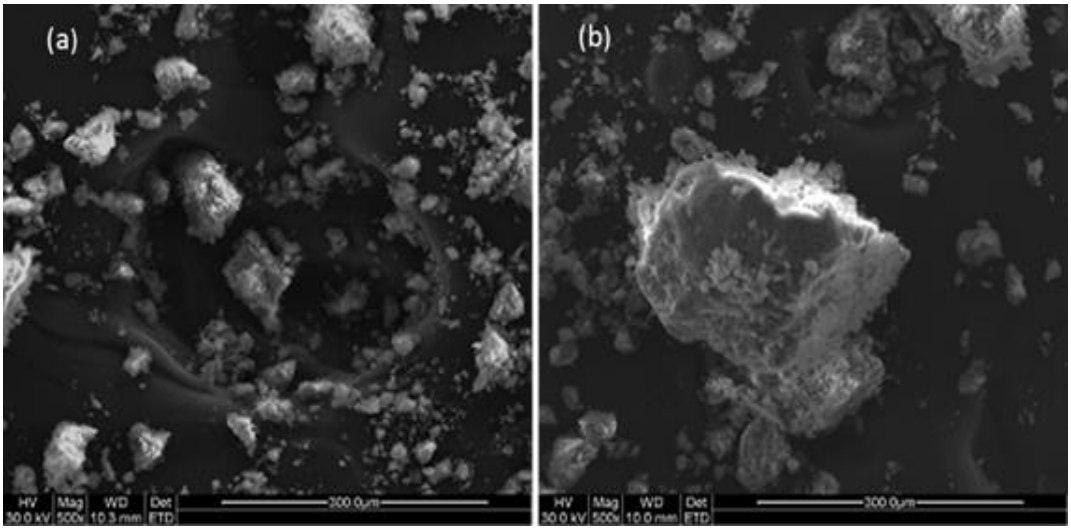


Figure 2: SEM image of (a) natural zeolite and (b) iron hydro (oxide) modified zeolite.

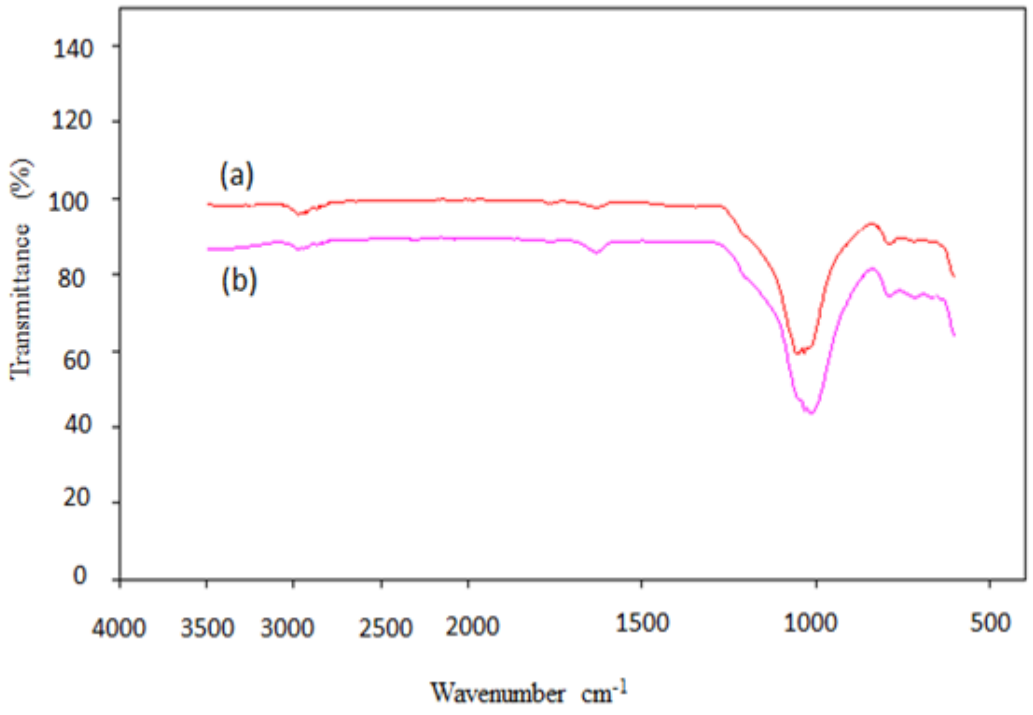


Figure 3: FT-IR spectrum of (a) iron hydro (oxide) modified zeolite and (b) natural zeolite.

3.2. Effect of solution pH

Previous studies on adsorption of U(VI) showed that solution pH is an important parameter affecting the adsorption process (Chegrouche and Barkat, 2005; Bhat *et*

al., 2008, Xiao *et al.*, 2015). It also influences the speciation, precipitation and mobility of metal ions, and the surface charge of the adsorbent. **Fig. 4** illustrates the effect of solution pH on the adsorption of U(VI) by iron hydro (oxide) modified zeolite. As seen from **Fig. 4**, the adsorption efficiency increased steadily with increasing pH values till pH 6. Beyond the optimum pH 6, the extent of U(VI) adsorption efficiency diminishes with further increase in pH. Kütahyalı and Eral (2004) reported similar results when investigating the adsorption of U(VI) by activated carbon. The solution pH affects U(VI) adsorption mechanism through the hydrolysis of the uranyl ions (Han *et al*., 2007). At lower pH values (1- 4) uranium is present in solution predominately in the form of UO_2^{2+} ions, and it is known that at low pH values, concentration of proton (H^+) ions far exceeds that of the metal ions and hence, they compete with U(VI) ions for the active site on surface of the adsorbent. This hinders and limits the U(VI) ions from reaching the active sites of the adsorbent resulting in low adsorption efficiency (Xiao *et al.*, 2015). At pH 4-6, hydrolysis of uranyl ions occurs to produce products such as: $UO_2(OH)^+$, $(UO_2)_2(OH)_2^{2+}$, which are available for uranium adsorption by iron hydro (oxide) modified zeolite, resulting in an increase in the uptake of uranium (Zhou *et al*., 2016). Increasing the solution pH to values beyond 7 results in polymerization of the hydrolysed uranyl ion species such as: $UO_2(OH)_3^-$, $UO_2(OH)_4^{2-}$, and $(UO_2)_3(OH)_7^-$. These negatively charge species have low adsorption affinity and induce repulsion between the adsorbate and adsorbent, since the iron hydro (oxide) modified zeolite point of zero charge (pH_{pzc}) is at 5.6 ±0.1 (**Fig.5**).

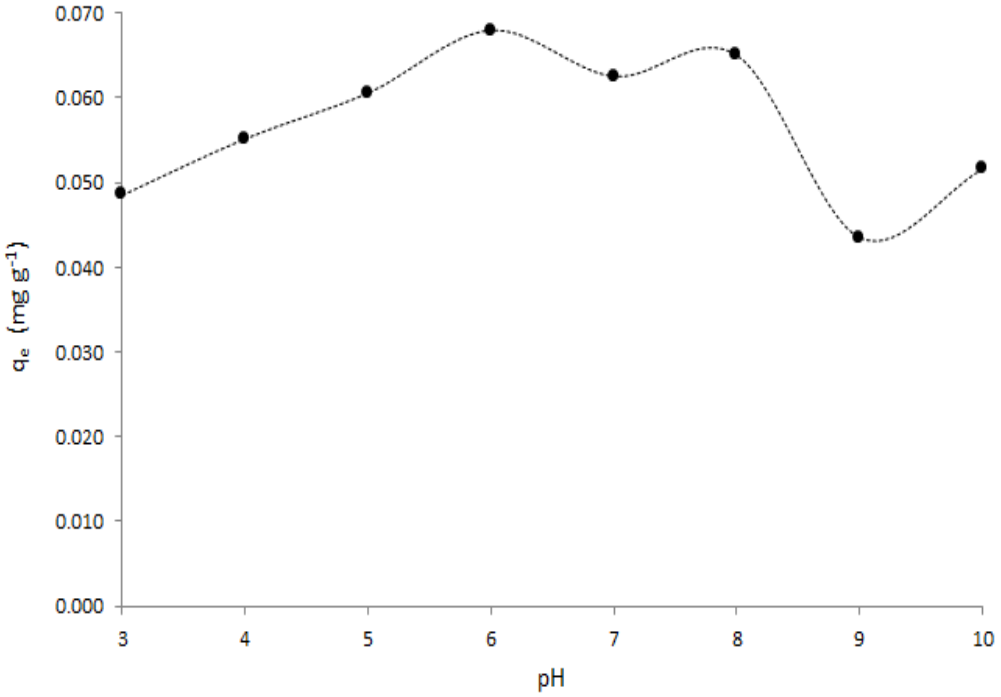


Figure 4: Effect of pH on the adsorption of uranium onto iron hydro (oxide) modified zeolite (U(VI) Concentration = 10 mg L^{-1}, contact time = 30 min and mass =3.0 g) (n = 3, RSD < 10%).

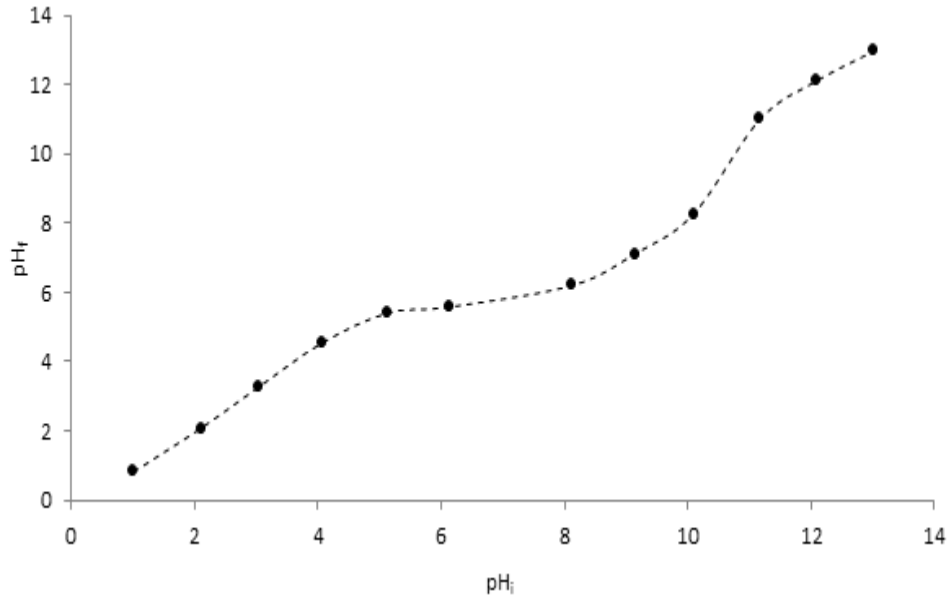


Figure 5: pH_i versus pH_f for point of zero charge determination.

3.3. Effect of adsorbent dosage

The adsorption efficiency of U(VI) by iron hydro (oxide) modified zeolite was investigated as a function of dosage (**Fig. 6**). It was observed that U(VI) adsorption efficiency increased with the increment in the adsorbent dosage from 0.5 to 3.0 g, this could be due to larger surface area and the increment in the available vacant adsorptive sites with increasing adsorbent dosage. Further increase in adsorbent dosage resulted in a slight decrease on the adsorption efficiency of U(VI). The maximum adsorption efficiency of 66% for U(VI) was attained at a dosage of 3.0 g. Therefore, the optimum dosage of 3.0 g was fixed for the subsequent experiments.

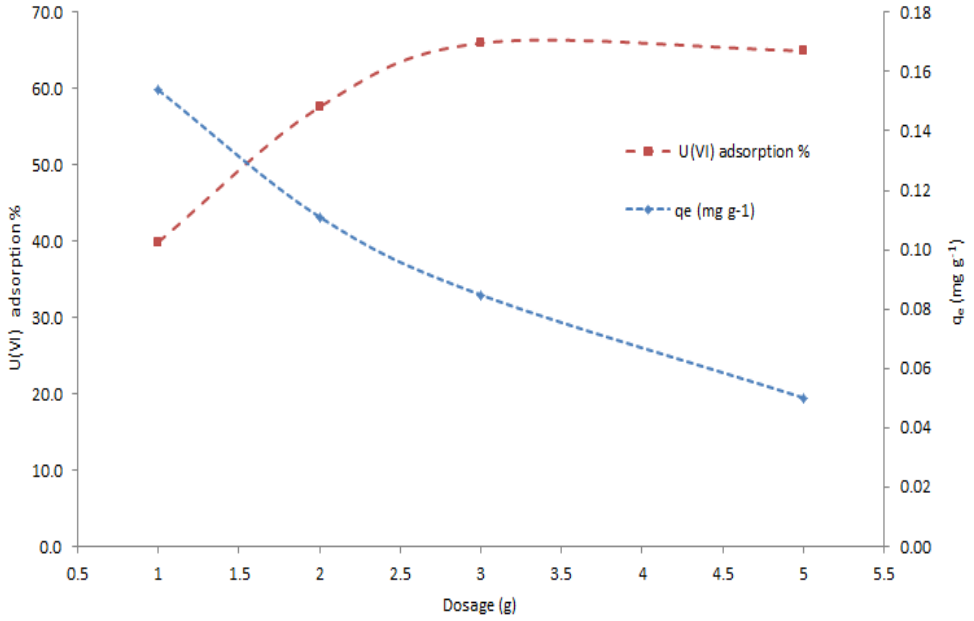


Figure 6: Effect of adsorbent dosage on uranium (VI) adsorption onto iron hydro (oxide) modified zeolite (U(VI) Concentration = 10 mg L^{-1}, contact time = 30 min and pH = 6.01) (n = 3, RSD < 10 %).

3.4. Effect of contact time

Effect of contact time on the adsorption efficiency of U(VI) is illustrated in **Fig. 7**. Kinetic plot of U(VI) adsorption consist of a rapid phase in the beginning where adsorption was fast and contributed significantly to the uptake of U(VI) ions and then became constant. The rapid adsorption of U(VI) in the initial stage could be

attributed to the higher concentration gradient and more available vacant sites for adsorption. The adsorption capacity of U(VI) increases abruptly from 0.040 to 0.139 mg g^{-1} as the time increase from 30 sec to 30 min. Prolonging the contact time to over 30 min gave no improvement in the adsorption efficiency. Therefore, 60 min was chosen as the reaction time required to reach pseudo-equilibrium for U(VI) adsorption by iron hydro (oxide) modified zeolite.

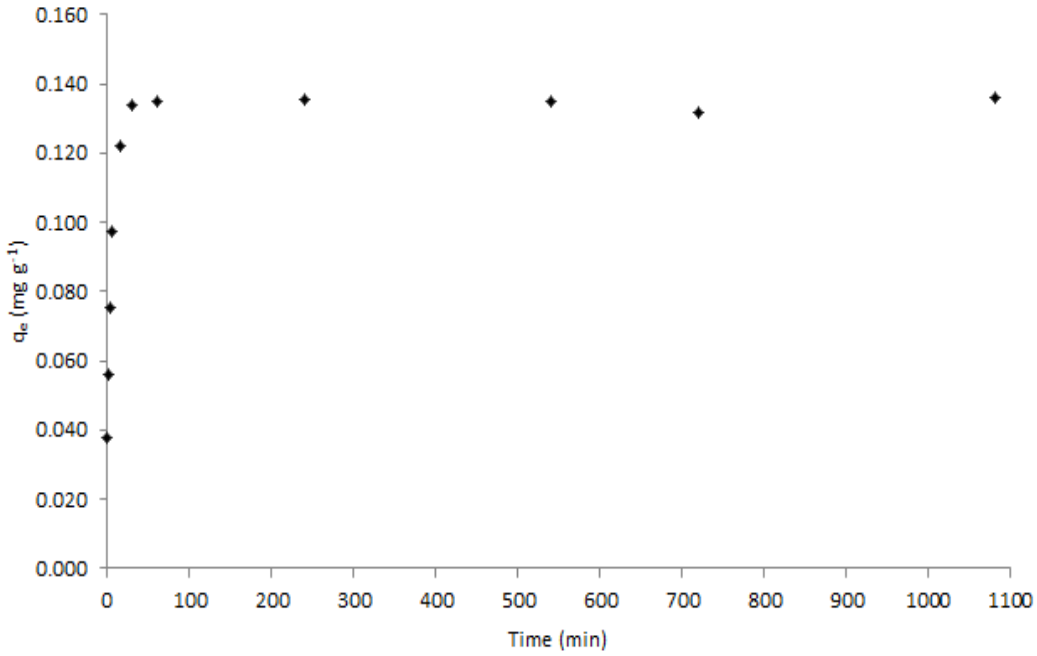


Figure 7: Effect of contact time on uranium (VI) adsorption onto iron hydro (oxide) modified zeolite (U(VI) Concentration = 10 mg L^{-1}, pH = 6.01 and mass =3.0 g) (n = 3, RSD < 10 %).

3.5. Adsorption kinetics

In order to understand the mechanism and potential rate controlling steps, kinetic models were applied to the experimental data. The pseudo-first-order and pseudo-second-order kinetic models were applied to describe the kinetic characteristic of uranyl ions adsorption by iron hydro (oxide) modified zeolite. The pseudo-first order rate equation may be expressed as Eq. (3):

$$\log(q_e - q) = \log q_e - \frac{k_1}{2.303} t \qquad (3)$$

Similarly, the pseudo second order rate can be written as Eq. (4):

$$\frac{t}{q_t} = \frac{1}{k_2 q_e^2} + \frac{t}{q_e} \quad (4)$$

Where $q_e (mg\ g^{-1})$ and, $q_t (mg\ g^{-1})$ signify the mass of U(VI) retained on a unit mass of adsorbent at equilibrium and time t (min), respectively. $k_1 (min^{-1})$ is the rate constant of pseudo-first-order kinetic model and k_2 ($g\ min^{-1}\ mg^{-1}$) is the pseudo-second-order kinetic rate constant. The parameters of the pseudo-first-order and pseudo second order kinetic models were calculated from the linear plots of $\log(q_e - q)$ vs t and $\frac{t}{q_t}$ vs t, respectively. The applicability of the Kinetic model equation to describe the adsorption process was judged by the coefficient of determination (R^2) and the closeness of the experimental q_m to the calculated q_{cal}. The kinetic parameters together with corresponding coefficient of determination (R^2) are shown in **Table 2.** Noticeably, the coefficient of determination (R^2) of the pseudo-second-order kinetic model is higher than that of the pseudo-first-order kinetic model. Moreover, the $q_{e,\ cal}$ value of the pseudo-second-order kinetic model is closer to the experimental value; this model can be adapted to describe the adsorption process of U(VI) by iron hydro (oxide) model zeolite.

These results agree with the studied carried out by other researcher which reported that pseudo-second-order kinetic model gave a better fit than the pseudo-first-order kinetic model when investigating the removal of U(VI) by different adsorbent such as activated carbon (Mellah *et al.,* 2005), hematite (Shuibo *et al.,* 2009), chitosan-tripolyphosphate beads (Sureshkumar *et al.,* 2010), cross-linked magnetic chitosan beads (Huang *et al.,* 2016) and cross-linked chitosan (Wang *et al.,* 2009).

Table 2: Kinetic parameters of U(VI) adsorption on iron hydro (oxide) modified zeolite at 298 K.

Kinetic models	Parameter	
Pseudo-first-order	q_e (mg g^{-1})	0.015
	k_1 (min^{-1})	0.0097
	R^2	0.378
Pseudo-second-order	q_e (mg g^{-1})	0.135
	k_2 (g mg^{-1} min^{-1})	4.864
	R^2	0.999
Experimental	q_e (mg g^{-1})	0.136

3.6. Effect of U(VI) initial concentration

The variation of adsorption capacity of iron hydro (oxide) modified zeolite for U(VI) as affected by initial U(VI) concentration is shown in Fig. 8. With the increase in U(VI) initial concentration, the equilibrium adsorption capacity of the iron hydro (oxide) modified zeolite increased. This could be attributed to the fact that the initial sorbate concentration provides a driving forces to overcome mass transfer resistance between sorbent and solution medium (Ho and Mckay, 2000). The equilibrium adsorption capacity increase with increasing initial U(VI) concentration may also be due to higher interaction between U(VI) and the iron hydro (oxide) modified zeolite.

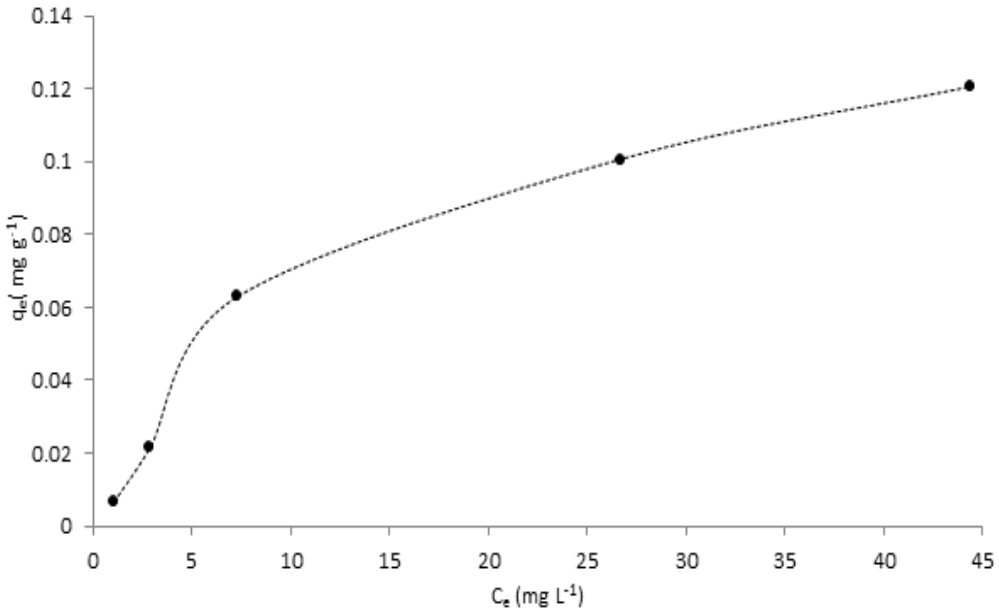


Figure 8: Effect of concentration on uranium (VI) adsorption onto iron hydro (oxide) modified zeolite (Contact time = 30 min pH = 6.01 and mass = 3.0 g) (n = 3, RSD < 10 %).

3.7. Adsorption isotherms study

In order to understand the distribution of the adsorbate on the adsorbent surface at equilibrium, adsorption isotherms are fundamental. It is imperative to establish the most fitting correlation for the equilibrium curves. The applicability of the isotherm equation to describe the adsorption process was judged by the correlation coefficients, R^2 values the closeness of the experimental q_m to the calculated q_{cal}. The experimental data for U(VI) adsorption by iron hydro (oxide) modified zeolite was correlated with the Langmuir isotherm, and Freundlich isotherm model.

The Langmuir isotherm is the simplest adsorption model which assumes that the adsorbate form a monolayer on the surface of the adsorbent and the adsorption energy decreases with an increase in the distance between the adsorbate and surface of the adsorbent. The linear form of the model can be expressed as Eq. (5):

$$\frac{C_e}{q_e} = \frac{C_e}{q_m} + \frac{1}{k_l q_m} \quad (5)$$

where q_e (mg g^{-1}) is the equilibrium metal ion concentration on the adsorbent, C_e (mg L^{-1}) is the equilibrium metal ion concentration in the solution, q_m (mg g^{-1}) is

the monolayer adsorption capacity of the adsorbent, and k_l ($L\,mol^{-1}$) is the Langmuir adsorption constant related with the free energy adsorption.

The essential characteristic of the Langmuir isotherm can be described by the dimensionless parameter R_L:

$$R_L = \frac{1}{1 + bC_0} \tag{6}$$

where C_0 ($mg\,L^{-1}$) is the initial concentration. The factor R_L indicates the affinity of the adsorbate to the investigated adsorbent and can be used to interpret the adsorption types as follows:

$R_L > 1$ (unfavourable), $R_L < 0$ (unfavourable), $0 < R_L > 1$ (favourable) and $R_L = 0$ (Irreversible)

In this study, the R_L value was found to be 2.36×10^{-5} implying favourable adsorption of U(VI) by iron hydro (oxide) modified zeolite.

The Freundlich isotherm which is an empirical model assumes a heterogeneous adsorption surface and active site with different energy. The model can be expressed as Eq. (7):

$$\log(q_e) = \log(q)\frac{1}{n}\log(C_e) \tag{7}$$

where k_f ($mg\,g^{-1}$), is constant indicative of adsorption capacity, and n is an empirical factor relating the adsorption intensity.

The Dubinin–Radushkevich (D–R) isotherm evaluates the nature of sorption based on the Polanyi potential theory assuming heterogeneous surface energies. This model can be written in the following linear form:

$$\ln q_e = \ln x_m + K\varepsilon^2 \tag{8}$$

where ε (Polanyi potential) $= RT\ln(1 + {}^{1}/_{C_e})$, x_m is the maximum sorption capacity and K ($mol^2 kj^{-2}$) is related to the mean free energy of sorption per mole of the sorbate when its transferred to the surface of the solid from infinity in the solution and this energy can be computed using the Eq. (9)

$$E = \frac{1}{\sqrt{2K}} \tag{9}$$

The magnitude of E_{DR} is a useful parameter for estimating the type of adsorption process as physical or chemical, the E_{DR} value was found to be 9.13 kJ mol^{-1} suggesting the adsorption process proceed *via* chemical ion exchange.

The model parameters obtained by applying both Langmuir and Freundlich model to the experimental data are given in **Table 3**. All the three isotherms showed good fit to the experimental data with good correlation coefficients (Table 3). The applicability of the two mostly utilized adsorption isotherms to the sorption of U(VI) shows that both monolayer sorption and heterogeneous energetic distribution of active sites on the surface of the sorbent are possible. The values of k_f and n were found to be 0.105 and 1.315 for U(VI) adsorption, respectively. The value of n > 1 indicated that the adsorption of U(VI) by iron hydro (oxide) modified zeolite was favourable at the operating condition studied. Similarly, Nilchi et al. (2013) reported similar findings when investigating the adsorption of U(VI) by crystalline tin oxide nanoparticles.

Table 3: Langmuir, Freundlich and Dubinin–Radushkevich adsorption isotherm constants for U(VI) adsorption on iron hydro (oxide) modified zeolite.

Isotherm models	Parameter	
Langmuir	q_e (mg g^{-1})	0.24
	k_l (L mol^{-1})	08471
	R^2	0.931
Freundlich	n	1.315
	k_f (g mg^{-1})	0.105
	R^2	0.933
Dubinin-Radushkevich	x_m (mg g^{-1})	0.002
	E_s (kJ mol^{-1})	9.13
	R^2	0.913

3.8. Effect of temperature and thermodynamic study

In order to determine the effect of temperature on the adsorption of U(VI) by iron hydro (oxide) modified zeolite, batch experiments were conducted at four different temperatures. The thermodynamic parameters such as entropy (ΔS°), variation of Gibbs free energy (ΔG°) and enthalpy (ΔH°) were calculated from Eq. (8):

$$\Delta G^{\circ} = -RTlnK_d \quad (8)$$

where ΔG° is the standard free energy change, R (J mol^{-1} K^{-1}) is the universal gas constant, T (K) is temperature in kelvin and K_d is the equilibrium constant. The values of ΔH° and ΔS° parameters can be estimated from Eq. (9):

$$\ln K_d = \frac{\Delta S^{\circ}}{R} - \frac{\Delta H^{\circ}}{RT} \quad (9)$$

The thermodynamic parameters for U(VI) adsorption by iron hydro (oxide) modified zeolite are summarized in **Table 4**. The positive value of (ΔG°) mean that the adsorption process was non-spontaneous and the (ΔG°) values increase as the temperature increased, revealing low adsorption capacity, indicating that the adsorption process was more favourable at low temperature, which agreed with the experimental observation **Fig. 9**.

The negative value of enthalpy (ΔH°) indicates that the adsorption process was exothermic in nature. The negative value of Entropy (ΔS°) confirms the decrease in randomness at the solid-solution interface during adsorption and the reversibility of U(VI) adsorption onto iron hydro (oxide) modified zeolite.

Table 4: Thermodynamic parameters for adsorption of U(VI) on iron hydro (oxide) modified zeolite.

					ΔS° (kJ (mol K)$^{-1}$)	ΔH° (kJ mol^{-1})	R^2
T(K)	297.15	303.15	316.15	326.15	-0.0958	-24.873	0.917
ΔG° (kJ mol^{-1})	3.494	4.164	5.410	6.367			

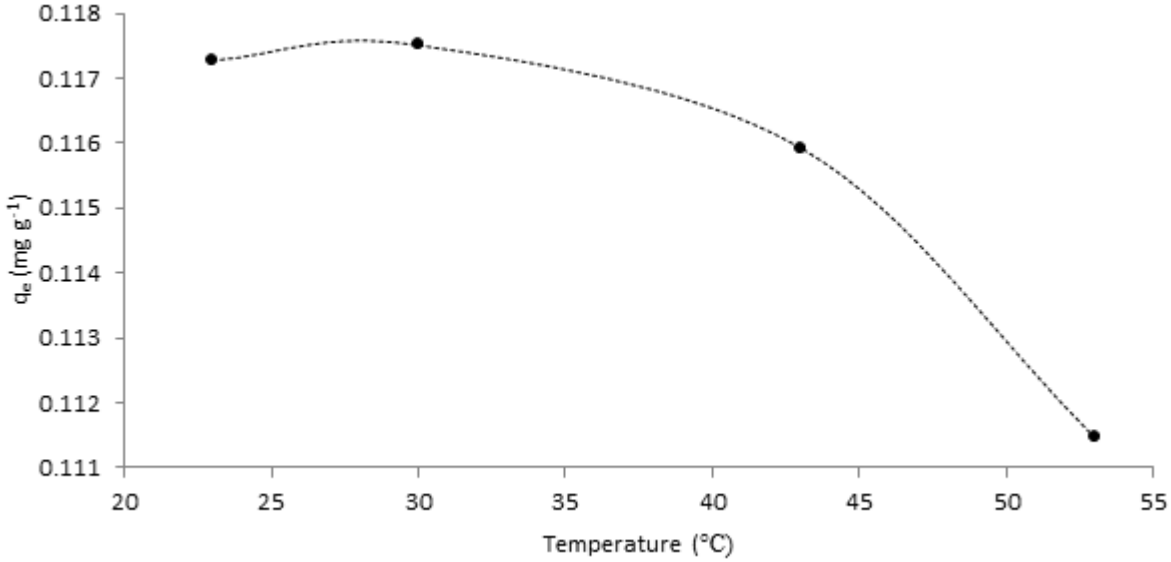


Figure 9: Effect of temperature on uranium (VI) adsorption onto iron hydro (oxide) modified zeolite (U(VI) conc = 10 mg L^{-1}, and m =3.0 g) (n = 3, RSD < 10 %).

3.10. Effect of co-existing cations and anions on the adsorption of uranium (VI) by iron hydro (oxide) modified zeolite

Competitive adsorption of U(VI)/ SO_4^{2-}, U(VI)/ CO_3^{2-}, U(VI)/ HPO_4^{2-}, and U(VI)/ multi-element mixture (Cr^{3+}, Mn^{2+}, Pb^{2+}, and Co^{2+}) were investigated through batch technique at optimum conditions. **Fig. 10** (a) and (b) illustrates the effects of anions and cations on the adsorption of uranyl ion from aqueous solution, respectively. A significant decrease on the adsorption capacity of uranyl ion was observed when the concentration of anions specifically phosphate and carbonate were increased from 100 to 250 mg L^{-1}. According to PHREEQC at pH 5.0, in the absence of competing anions the predominant species of uranium in solution is the cationic uranyl ion (28.6%).With the addition of carbonates ions, the pH of the solution increased resulting in the formation of highly negative charged polynuclear hydroxo carbonato complex that cannot be adsorbed easily on the surface of the iron hydro (oxide) modified zeolite due to their large size and lower mobility in aqueous solution resulting in the reduction of U(VI) adsorption. Interactions between U(VI) and phosphate ions govern the mobility of U(VI) in subsurface and contaminated environments (Cheng et al., 2004). A higher total phosphate concentration resulted in superior decrease in the adsorption capacity of U(VI) by iron hydro (oxide) modified zeolite Fig. 10 (b). The decrease in the adsorption capacity of U(VI) may be attributed to the formation of soluble U(VI)-phosphate complexes such as $UO_2(HPO_4)_2^{2-}$. The presence of UO_2 $(HPO_4)_2^{2-}$ (≈ 100%) species was confirmed by PHREEQC code. Cheng et al., (2004) reported similar effect when investigating the effect of phosphate on U(VI) adsorption by goethite coated sand. The presence of sulphate in solution did not have much effect on U(VI) adsorption, since a lot of sulphate is present as SO_4^{2-} (≈ 99.27%) in solution. When the ratio of competing cations to uranyl ion was increased from 1:1 to 1:5, the adsorption capacity of uranyl ion (q_e) decreased from 0.1329 mg g^{-1} to 0.0151 mg g^{-1}, which resulted in 89% reduction on the maximum adsorption. The decrease on U(VI) adsorption with the increase in cation concentration can be explained on the basis of the dehydration energies and the diffusion coefficients of the competing cations. Thus, metal with low dehydration energy, high mobility and

low hydration radius will be preferred in this case lead is preferred over uranyl ion and other competing metal.

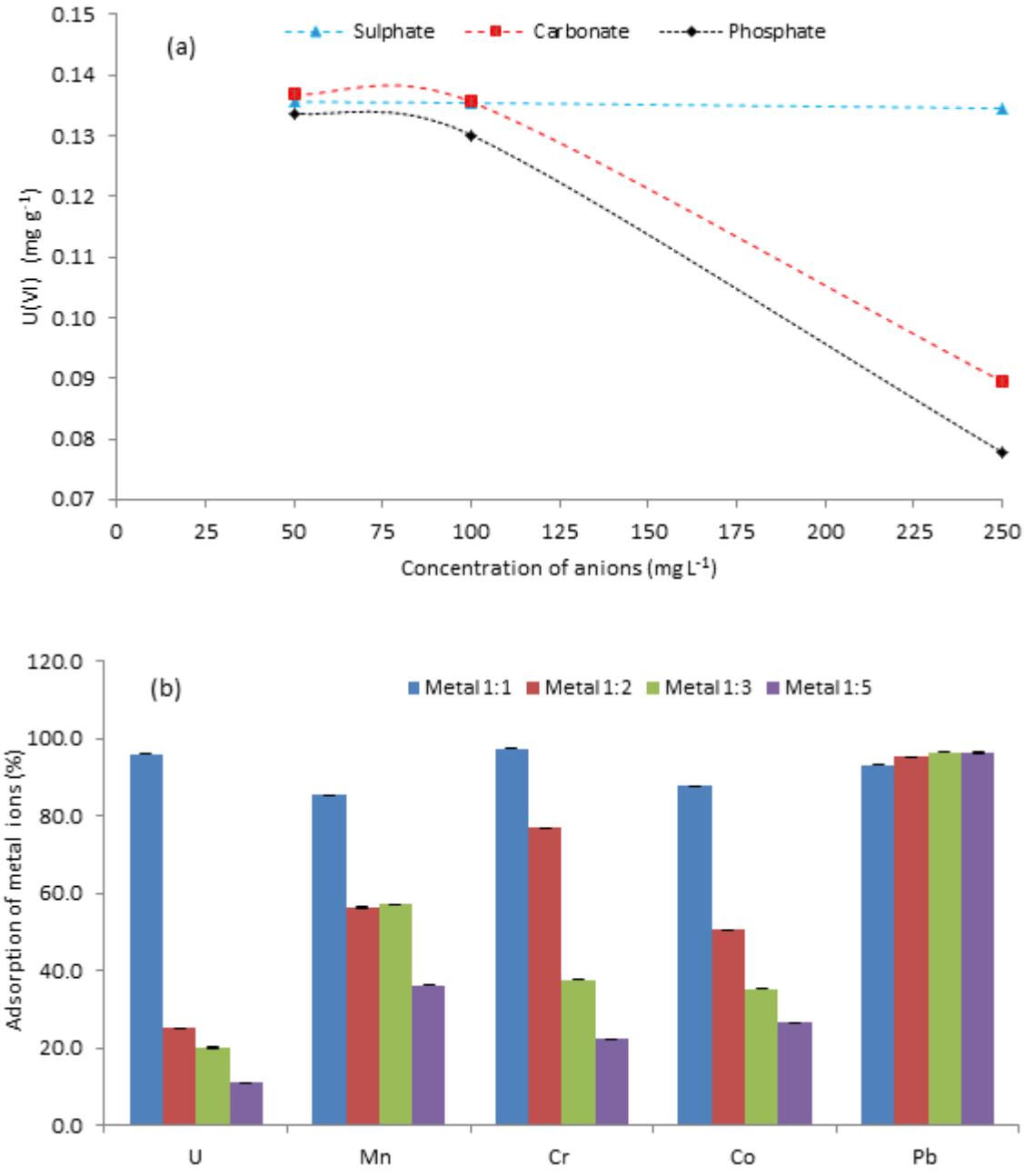


Figure 10: Effect of (a) anions and (b) cations on U(VI) adsorption onto iron hydro (oxide) modified zeolite (U(VI) = 10 mg L^{-1}, Contact time = 90 min and m =3.0 g) (n = 3, RSD < 10 %).

3.11. Application of iron hydro (oxide) modified zeolite

The potential of iron hydro (oxide) modified zeolite as an adsorbent for the recovery of U(VI) from real wastewater in the form of acid mine drainage(AMD) water from the Witwatersrand Basin gold mines was determined by performing batch sorption studies. The AMD water used for this study had a pH of 2.23, oxidation reduction potential of 296 mV and electrical conductivity of 3.06 mS cm^{-1}. The extraction efficiency of U(VI) was determined to be 60.8% from AMD water. This demonstrated the suitability of iron hydro (oxide) zeolite to selectively extract U(VI) ions from aqueous matrices.

3.12 Comparison of iron hydro (oxide) modified zeolite with other adsorbent

The monolayer adsorption capacity ($mg\,g^{-1}$) of iron hydro (oxide) modified zeolite for the removal of U(VI) was compared with other similar adsorbent reported in literature as presented in **Table 3**. In this work, the maximum adsorption capacity was found to be 0.24 $mg\,g^{-1}$ U(VI) for iron hydro (oxide) modified zeolite. It can be seen that the maximum U(VI) adsorption capacity of iron hydro (oxide) modified zeolite is the lowest compared to the reported adsorbent in the literature. This might be due to iron hydro (oxide) particles occupying the pores of the zeolite. This results in the lowering of the adsorption capacity of the sorbent.

Table 3: Maximum adsorption capacities of some adsorbents reported in the literature.

Adsorbent	pH	q_m (mg /g)	References
Iron hydro (oxide) modified zeolite	5	0.24	This study
Magnetite nanoparticles	7	5	Das *et al.*, 2010
Modified clays with titanium oxide	3.5	0.58	Humelnicu *et al.*, 2008
Clinoptilolite zeolite	5.0	1.23	Kilincarslan and Akyil, 2005

4. Conclusion

The removal of uranium from aqueous solution was carried out using classical adsorption techniques. The adsorption of U(VI) ions onto iron hydro (oxide) modified zeolite was fast with equilibrium reached after 30 min, and it was found to be pH dependent. The kinetic data signified that the adsorption of U(VI) ions onto iron hydro (oxide) modified zeolite followed well the pseudo-second-order kinetic model. The adsorption behaviour of U(VI) ions onto iron hydro (oxide) modified zeolite was best described by both Freundlich and Langmuir isotherm model. The fact that the Freundlich isotherm model fits the experimental data confirms the heterogeneous nature and possibly, the multi-layer adsorption of U(VI) ions onto iron hydro (oxide) modified zeolite. The mean free energy obtained from the Dubinin–Radushkevich isotherm model indicated that the adsorption of U(VI) onto iron hydro (oxide) modified zeolite took place via chemical ion exchange on the surface of zeolite. Based on the results of the batch studies conducted with acid mine drainage water, it may be concluded that iron hydro (oxide) modified zeolite cloud be used as a potential adsorbent for U(VI) ions recovery from acid mine drainage water.

Acknowledgement

This research was financially supported by the National Research Foundation (NRF) of South Africa (Grant ID number SFH150624120802).

Conflict of interest

The authors declared no conflict of interest

References

Akbal, Feryal, and Selva Camcı. "Comparison of electrocoagulation and chemical coagulation for heavy metal removal." Chemical Engineering & Technology 33, no. 10 (2010): 1655-1664.

Al Abdulgader, Hasan, Victor Kochkodan, and Nidal Hilal. "Hybrid ion exchange–Pressure driven membrane processes in water treatment: A review." Separation and Purification Technology 116 (2013): 253-264.

Akcil, Ata, and Soner Koldas. "Acid mine drainage (AMD): causes, treatment and case studies." Journal of Cleaner Production 14, no. 12 (2006): 1139-1145.

Aksu, Z. "Determination of the equilibrium, kinetic and thermodynamic parameters of the batch biosorption of nickel (II) ions onto Chlorella vulgaris." Process Biochemistry 38, no. 1 (2002): 89-99.

Alver, Burcu Erdoğan, Meryem Sakizci, and Ertuğrul Yörükoğullari. "Investigation of clinoptilolite rich natural zeolites from Turkey: a combined XRF, TG/DTG, DTA and DSC study." Journal of thermal analysis and calorimetry 100, no. 1 (2010): 19-26.

Akyil, S., M. A. A. Aslani, and M. Eral. "Sorption characteristics of uranium onto composite ion exchangers." Journal of radioanalytical and nuclear chemistry 256, no. 1 (2003): 45-51.

Aytas, S., S. Akyil, and M. Eral. "Adsorption and thermodynamic behavior of uranium on natural zeolite." Journal of Radioanalytical and Nuclear Chemistry 260, no. 1 (2004): 119-125.

Baskan, Meltem Bilici, and Aysegul Pala. "Removal of arsenic from drinking water using modified natural zeolite." Desalination 281 (2011): 396-403.

Bhat, Suman Vikas, J. S. Melo, B. B. Chaugule, and S. F. D'souza. "Biosorption characteristics of uranium (VI) from aqueous medium onto Catenella repens, a red alga." Journal of hazardous materials 158, no. 2 (2008): 628-635.

Camacho, Lucy Mar, Shuguang Deng, and Ramona R. Parra. "Uranium removal from groundwater by natural clinoptilolite zeolite: effects of pH and initial feed concentration." Journal of hazardous materials 175, no. 1 (2010): 393-398.

Cheng, Tao, Mark O. Barnett, Eric E. Roden, and Jinling Zhuang. "Effects of phosphate on uranium (VI) adsorption to goethite-coated sand." Environmental science & technology 38, no. 22 (2004): 6059-6065.

Chisholm-Brause, Catherine J., John M. Berg, Robert A. Matzner, and David E. Morris. "Uranium (VI) sorption complexes on montmorillonite as a function of solution chemistry." Journal of Colloid and Interface Science 233, no. 1 (2001): 38-49.

Dabrowski, A., Z. Hubicki, P. Podkościelny, and E. Robens. "Selective removal of the heavy metal ions from waters and industrial wastewaters by ion-exchange method." Chemosphere 56, no. 2 (2004): 91-106.

Das, Bidus Kanti, Arup Roy, Matthias Koschorreck, Santi M. Mandal, Katrin Wendt-Potthoff, and Jayanta Bhattacharya. "Occurrence and role of algae and fungi in acid mine drainage environment with special reference to metals and sulfate immobilization." water research 43, no. 4 (2009): 883-894.

Das, Debasish, M. K. Sureshkumar, Siddhartha Koley, Nidhi Mithal, and C. G. S. Pillai. "Sorption of uranium on magnetite nanoparticles." Journal of radioanalytical and nuclear chemistry 285, no. 3 (2010): 447-454.

Díaz-Nava, M. C., M. T. Olguín, M. Solache-Rios, M. T. Alarcón-Herrera, and A. Aguilar-Elguezabal. "Characterization and improvement of ion exchange capacities of Mexican clinoptilolite-rich tuffs." Journal of inclusion phenomena and macrocyclic chemistry 51, no. 3-4 (2005): 231-240.

Fu, Fenglian, and Qi Wang. "Removal of heavy metal ions from wastewaters: a review." Journal of environmental management 92, no. 3 (2011): 407-418.

Han, Runping, Weihua Zou, Yi Wang, and Lu Zhu. "Removal of uranium (VI) from aqueous solutions by manganese oxide coated zeolite: discussion of adsorption isotherms and pH effect." Journal of Environmental Radioactivity 93, no. 3 (2007): 127-143.

Han, Runping, Lina Zou, Xin Zhao, Yanfang Xu, Feng Xu, Yinli Li, and Yu Wang. "Characterization and properties of iron oxide-coated zeolite as adsorbent for removal of copper (II) from solution in fixed bed column." Chemical Engineering Journal 149, no. 1 (2009): 123-131.

Huang, Guolin, Lixia Zou, Yu Su, Tingting Lv, and Lele Wang. "Adsorption of uranium (VI) from aqueous solutions using cross-linked magnetic chitosan beads." Journal of Radioanalytical and Nuclear Chemistry 307, no. 2 (2016): 1135-1140.

Humelnicu, Doina, E. Popovici, E. Dvininov, and C. Mita. "Study on the retention of uranyl ions on modified clays with titanium oxide." Journal of Radioanalytical and Nuclear chemistry 279, no. 1 (2009): 131-136.

Ho, Yuh-Shan, and G. McKay. "The kinetics of sorption of divalent metal ions onto sphagnum moss peat." Water research 34, no. 3 (2000): 735-742.

Hsi, Ching-kuo Daniel, and Donald Langmuir. "Adsorption of uranyl onto ferric oxyhydroxides: application of the surface complexation site-binding model." Geochimica et Cosmochimica Acta 49, no. 9 (1985): 1931-1941.

Johnson, D. Barrie, and Kevin B. Hallberg. "Acid mine drainage remediation options: a review." Science of the total environment 338, no. 1 (2005): 3-14.

Katsoyiannis, I. A., and A. I. Zouboulis. "Removal of uranium from contaminated drinking water: a mini review of available treatment methods." Desalination and Water Treatment 51, no. 13-15 (2013): 2915-2925.

Katsoyiannis, Ioannis A. "Carbonate effects and pH-dependence of uranium sorption onto bacteriogenic iron oxides: kinetic and equilibrium studies." Journal of hazardous materials 139.1 (2007): 31-37.

Khani, M. H., H. Pahlavanzadeh, and M. Ghannadi. "Kinetics study of the fluorination of uranium tetrafluoride in a fluidized bed reactor." Annals of Nuclear Energy 35, no. 4 (2008): 704-707.

Kragović, Milan, Aleksandra Daković, Marija Marković, Jugoslav Krstić, G. Diego Gatta, and Nicola Rotiroti. "Characterization of lead sorption by the natural and Fe (III)-modified zeolite." Applied Surface Science 283 (2013): 764-774.

Krestou, A., A. Xenidis, and D. Panias. "Mechanism of aqueous uranium (VI) uptake by hydroxyapatite." Minerals Engineering 17, no. 3 (2004): 373-381.

Kütahyalı, Ceren, and Meral Eral. "Selective adsorption of uranium from aqueous solutions using activated carbon prepared from charcoal by chemical activation." Separation and Purification Technology 40, no. 2 (2004): 109-114.

Mavrov, V., T. Erwe, C. Blöcher, and H. Chmiel. "Study of new integrated processes combining adsorption, membrane separation and flotation for heavy metal removal from wastewater." Desalination 157, no. 1 (2003): 97-104.

Mellah, A., S. Chegrouche, and M. Barkat. "The removal of uranium (VI) from aqueous solutions onto activated carbon: kinetic and thermodynamic investigations." Journal of colloid and interface science 296, no. 2 (2006): 434-441.

Medvidović, N. Vukojević, Jelena Perić, and Marina Trgo. "Column performance in lead removal from aqueous solutions by fixed bed of natural zeolite–clinoptilolite." Separation and Purification Technology 49, no. 3 (2006): 237-244

Mihaly-Cozmuta, L., A. Mihaly-Cozmuta, A. Peter, C. Nicula, H. Tutu, Dan Silipas, and Emil Indrea. "Adsorption of heavy metal cations by Na-clinoptilolite: Equilibrium and selectivity studies." Journal of environmental management 137 (2014): 69-80.

Mozgawa, W. "The influence of some heavy metals cations on the FTIR spectra of zeolites." Journal of Molecular Structure 555, no. 1 (2000): 299-304.

Nilchi, A., T. Shariati Dehaghan, and S. Rasouli Garmarodi. "Kinetics, isotherm and thermodynamics for uranium and thorium ions adsorption from aqueous solutions by crystalline tin oxide nanoparticles." Desalination 321 (2013): 67-71.

Nilsson, Nils, Lars Lövgren, and Staffan Sjöberg. "Phosphate complexation at the surface of goethite." Chemical Speciation & Bioavailability 4, no. 4 (1992): 121-130.

Nezamzadeh-Ejhieh, Alireza, and Hamidreza Zabihi-Mobarakeh."Heterogeneous photodecolorization of mixture of methylene blue and bromophenol blue using CuO-nano-clinoptilolite." Journal of Industrial and Engineering Chemistry 20, no. 4 (2014): 1421-1431.

Sureshkumar, M. K., D. Das, M. B. Mallia, and P. C. Gupta. "Adsorption of uranium from aqueous solution using chitosan-tripolyphosphate (CTPP) beads." Journal of Hazardous Materials 184, no. 1 (2010): 65-72.

Sharma, Pankaj, and Radha Tomar. "Synthesis and application of an analogue of mesolite for the removal of uranium (VI), thorium (IV), and europium (III) from aqueous waste." Microporous and Mesoporous Materials116, no. 1 (2008): 641-652.

Sheoran, A. S., and V. Sheoran. "Heavy metal removal mechanism of acid mine drainage in wetlands: a critical review." Minerals engineering 19, no. 2 (2006): 105-116.

Shuibo, Xie, Zhang Chun, Zhou Xinghuo, Yang Jing, Zhang Xiaojian, and Wang Jingsong. "Removal of uranium (VI) from aqueous solution by adsorption of hematite." Journal of Environmental Radioactivity 100, no. 2 (2009): 162-166.

Tavengwa, Nikita Tawanda, Ewa Cukrowska, and Luke Chimuka. "Preparation, characterization and application of NaHCO3 leached bulk U(VI) imprinted polymers endowed with γ-MPS coated magnetite in contaminated water." Journal of hazardous materials 267 (2014): 221-228.

Tavengwa, Nikita Tawanda, Ewa Cukrowska, and Luke Chimuka. "Sequestration of U (VI) from aqueous solutions using precipitate ion imprinted polymers endowed with oleic acid functionalized magnetite." Journal of Radioanalytical and Nuclear Chemistry 304, no. 2 (2015): 933-943.

Wang, Guanghui, Jinsheng Liu, Xuegang Wang, Zhiying Xie, and Nansheng Deng. "Adsorption of uranium (VI) from aqueous solution onto cross-linked chitosan." Journal of hazardous materials 168, no. 2 (2009): 1053-1058.

Weihua, Zou, Zhao Lei, and Han Runping. "Removal of uranium (VI) by fixed bed ion-exchange column using natural zeolite coated with manganese oxide." Chinese Journal of Chemical Engineering 17, no. 4 (2009): 585-593.

Xiao, Xilin, Jinhua Xue, Dexin Ding, Bo He, Dongxiu He, Li Tan, and Lifu Liao. "Adsorption of low concentration of uranium (VI) from aqueous solution by diethylenetriamine functionalized Cycas revoluta leaves." Journal of Radioanalytical and Nuclear Chemistry 308, no. 3 (2016): 1027-1037.

Yi, Zheng-ji, Jun Yao, Yun-fei Kuang, Hui-lun Chen, Fei Wang, and Jin-sheng Xu. "Uptake of hexavalent uranium from aqueous solutions using coconut husk activated carbon." Desalination and Water Treatment 57, no. 4 (2016): 1749-1755.

Zhou, ShiMin, BaiHua Chen, Yuan Li, JingWei Guo, XiaoJiao Cai, Zhi Qin, Jing Bai, and Ping Na. "Synthesis, characterization, thermodynamic and kinetic investigations on uranium (VI) adsorption using organic-inorganic composites: Zirconyl-molybdopyrophosphate-tributyl phosphate." Science China Chemistry 56, no. 11 (2013): 1516-1524.

Zhou, Limin, Hongbin Zou, Yu Wang, Zhiwei Huang, Yun Wang, Taian Luo, Zhirong Liu, and Adesoji A. Adesina. "Adsorption of uranium (VI) from aqueous solution using magnetic carboxymethyl chitosan nano-particles functionalized with ethylenediamine." Journal of Radioanalytical and Nuclear Chemistry 308, no. 3 (2016): 935-946.

Kilincarslan, A., and S. Akyil. "Uranium adsorption characteristic and thermodynamic behavior of clinoptilolite zeolite." Journal of radioanalytical and nuclear chemistry 264, no. 3 (2005): 541-548.

Paper III

This paper “The Removal of Arsenic and Uranium from Aqueous Solutions by Sorption onto Iron Oxide-Coated Zeolite (IOCZ)” was published in *Water, Air, & Soil Pollution*. Investigate the extraction of Arsenic and Uranium from aqueous solution by Iron Oxide-Coated Zeolite (IOCZ).

Water Air Soil Pollut (2017) 228:5
DOI 10.1007/s11270-016-3190-7

The Removal of Arsenic and Uranium from Aqueous Solutions by Sorption onto Iron Oxide-Coated Zeolite (IOCZ)

E. N. Bakatula · R. Molaudzi · P. Nekhunguni · H. Tutu

Received: 18 August 2016 / Accepted: 22 November 2016
© Springer International Publishing Switzerland 2016

Abstract In this study, an iron oxide-coated zeolite (IOCZ) nanocomposite was synthesized and used for the removal of U(VI) and As(III) from aqueous solutions using a batch system. Parameters such as various contact times, pH, competing ions (Cd^{2+}, Co^{2+}, and Cr^{3+}), temperature, and initial concentrations of uranium(VI) and arsenic(III) were investigated. The experimental results were fitted to the Langmuir, Freundlich, and Dubinin–Radushkevich isotherms to obtain the characteristic parameters of each model. Results suggested that adsorption of U(VI) and As(III) by IOCZ was best modeled with the Freundlich isotherm. The kinetic experimental data fitted the pseudo second-order model better than the pseudo first-order model for both elements. Using the thermodynamic equilibrium constants obtained at different temperatures, various thermodynamic parameters, such as ΔG^{o}, ΔH^{o}, and ΔS^{o}, were calculated. These parameters indicated that the process is spontaneous and exothermic in nature. It was noted that an increase in temperature resulted in a decrease of 8.5 and 27.5% for U and As removal, respectively. An increase in initial concentrations of U(VI) and As(III) from 10 to 100 mg L^{-1} at pH 3 resulted in increased adsorption capacities (q_e) for both elements. The increases were from 1.247 to 20.10 mg g^{-1} for U(VI) and from 3.115 to 54.18 mg g^{-1} for As(V). The presence of competing ions such as Cd^{2+}, Co^{2+}, and Cr^{3+} enhanced the removal of As by 9.2% whereas the adsorption capacity of uranium decreased by 13.8%. This research demonstrated that IOCZ is a potential adsorbent for the removal of U(VI) and As(III) from aqueous solutions.

Keywords Iron oxide-coated zeolite · Arsenic · Uranium · Adsorption · Isotherms

E. N. Bakatula (✉) · R. Molaudzi · P. Nekhunguni · H. Tutu

Molecular Sciences Institute, School of Chemistry, University of the Witwatersrand, Private Bag X3, Wits 2050, South Africa
e-mail: enbakatula@gmail.com

E. N. Bakatula
Civil, Geological and Mining Engineering Department, École Polytechnique de Montréal, Montreal, QC H3C 3A7, Canada

Published online: 05 December 2016

1 Introduction

Aquatic systems are prone to contamination by toxic elements such as Cr, As, Pb, Hg, Cd, and U. Largely, these elements emanate from mining and smelting operations and can find their way into aquatic systems via dust fallout, erosion, and weathering of waste as well as leachate solutions emanating from such sources. In South Africa, for instance, U and As are commonly found in gold mining waste in the Witwatersrand Basin. The basin has contributed immensely to the development of the city of Johannesburg and the economy through vast amounts of gold that have been mined in it, accounting for over half of the gold ever mined in the world (Robb and Robb 1998). The waste from the mining activities is contained in tailing dumps that are scattered along the mining belt stretching in an east–west direction across the south of Johannesburg. Several studies in the basin have reported that the dust and

leachates emanating from the dumps contain significant amounts of contaminants, among them U and As (Winde 2002; Winde and Sandham 2004; Reimold and Gibson 2006; Tutu et al. 2008; Tutu et al. 2009; McCarthy and Pretorius 2009; Winde 2010; Bakatula 2012). U and As occur as uraninite (UO_2), brannerite (UTi_2O_6), arsenopyrite (FeAsS), cobaltite (CoAsS), and gersdofite (NiAsS) in the host ores (Feather and Koen 1975).

In oxidizing environments, uranium occurs as the uranyl ion, UO_2^{2+}, in which it has a valence of VI. Uranium is both chemotoxic and radioactive with the liver and kidneys being the main targets of uranium's toxic effects and with reservoirs of uranium concentrating in the kidneys and bones (WHO 2005; Hakonson-Hayes et al. 2002). This radionuclide makes its way into the human body through eating, drinking, and inhaling dust particles (DWAF 2015; Osborne and Ehrlich 1976). The allowed limit of uranium in drinking water according to South African guideline is 0.07 mg L^{-1} (DWAF 2015). The toxicity of arsenic depends on the specific chemical form. Inorganic trivalent arsenite (As^{III}) is 2–10 times more toxic than pentavalent arsenate (As^{V}) (Ferguson and Gavis 1972), whereas the toxicity of organo-arsenicals is generally lower than that of its inorganic species. Inorganic forms of arsenic most often exist in aqueous systems. Arsenic is sensitive to mobilization at pH between 6.5 and 8.5 and under both oxidizing and reducing conditions (Smedley and Kinniburgh 2003). Contamination with high levels of arsenic is of concern because it can cause a number of human health effects. Several epidemiological studies have reported a strong association between arsenic exposure and increased risks of both carcinogenic and systemic health effects (Tchounwou et al. 2003). Interest in the toxicity of arsenic has been heightened by recent reports of large populations in West Bengal, Bangladesh, Thailand, Inner Mongolia, Taiwan, China, Mexico, Argentina, Chile, Finland, and Hungary that have been exposed to high concentrations of arsenic in their drinking water and are displaying various clinicopathological conditions including cardiovascular and peripheral vascular disease, developmental anomalies, neurologic and neurobehavioral disorders, diabetes, hearing loss, portal fibrosis, hematologic disorders (anemia, leukopenia, and eosinophilia), and carcinoma (Tchounwou et al. 2004; Agency for Toxic Substances and Disease 2000; Centeno et al. 2005; National Research Council 2001).

In South Africa, severe arsenic poisoning has been reported in the Northern Cape and Limpopo provinces where concentrations of 1000 μg/L were found in groundwater (Sami and Druzynski 2003). Another source of arsenic to groundwater and the soil in South Africa is the use of chromated copper–arsenate in the preservation of timber. Arsenic actually protects the timber from wood-destroying insects. Improper disposal of waste from timber plants contaminates the soil and water systems around the plants (Kesunathan et al. 2006). Significant amounts of arsenic have also been reported in mine leachates and tailings in the Witwatersrand Basin (Tutu 2006). The allowed limit of arsenic in drinking water according to South African guideline is 10 μg L^{-1} (DWAF 2015).

Iron oxides have proved to be an effective sorbent for the removal of various contaminants from water, due to their characteristics such as high surface area and surface charge, as well as high affinity towards metals and metalloids. When used by themselves, iron oxides are difficult to remove from water after adsorption and thus need to be placed as a coating onto particles to provide mechanical stability (Thirunavukkarasu et al. 2003; Hsu et al. 2008). Iron-based oxides have been found to adsorb arsenic compounds in drinking water to a significant extent. For instance, Yuan et al. (2002) evaluated several iron-treated natural materials, such as Fe-treated activated carbon (FeAC), Fe-treated gel beads (FeGB), and iron oxide-coated sand (IOCS), for removing arsenic in drinking water for household use (cooking and drinking) and showed that IOCS had a good performance in terms of As(III) and As(V) removal in batch tests, column tests, and field experiments. Yean et al. (2005) evaluated the sorption and desorption behavior of arsenic to magnetite (Fe_3O_4) nanoparticles, and they found that the sorption capacity was dependent on the pH value and surface area of the adsorbent.

Coating iron oxide onto particles with natural affinity for cations (such as zeolites) and high surface area may provide an effective sorption media with the application for both cationic and anionic contaminants from water.

The aim of this work was to assess the performance of iron oxide-coated zeolite (IOCZ) in removing U and As from aqueous solutions. The approach was based on conducting batch studies to assess the effect of pH, initial concentrations of U and As, contact time, temperature, and the presence of competing ions (Cd^{2+}, Co^{2+}, and Cr^{3+}). The insight on the processes gained in this study is useful for systems in which initially

zeolite is used as the adsorbent, but the precipitation of Fe out of the solutions being treated leads to the inadvertent coating of the zeolite.

2 Materials and Methods

2.1 Preparation of Iron Oxide-Coated Zeolite

Natural zeolite was provided by the School of Animal, Plant and Environmental Sciences, University of the Witwatersrand, South Africa. The natural zeolite was treated with NaOH to obtain the activated zeolite–sodium type used for the synthesis of the IOCZ. Na–zeolite was obtained by soaking 100 g of natural zeolite (fraction 2–3 mm) in 1000 mL of 2 mol L^{-1} NaOH for 24 h at room temperature (i.e., 25 ± 1 °C). The zeolitic material was repeatedly washed with deionized water to remove any excess Na and then dried at room temperature.

In the first step, iron oxide (magnetite) particles were prepared by adding a 2 mol L^{-1} NaOH solution drop by drop (with agitation) to a 1000 mL solution containing 4.5 g of ferrous sulfate until the pH reached 11. The resulting slurry (essentially iron hydroxide) was then heated in a water bath to form iron oxide which was then washed with deionized water and dried at room temperature.

In the second step, iron oxide particles (2.0 g) were re-dispersed in deionized water and Na–zeolite (6.0 g) was added slowly with agitation at a ratio of 3:1 (*w*/*w*) zeolite/iron oxide.

The IOCZ obtained was washed with deionized water, dried at room temperature, and crushed to particle size (<2 mm) using a mortar and pestle.

2.2 Physical–Chemical Characterization of the Natural Zeolite and IOCZ

Natural zeolite was characterized using X-ray fluorescence (chemical composition, performed in the School of Geosciences at University of the Witwatersrand, South Africa) and FTIR (Tensor 27, Bruker, Germany) (for the identification of functional groups). The surface area and cationic exchange capacity (CEC) were determined by the Brunauer–Emmet–Teller (BET surface area and porosity analyzer, (Tristar 3000 Analyzer, Micromeritics, USA) and $BaCl_2$ methods Gillman and Sumpter (1986), respectively. The zeolite–iron oxide particles were characterized using the Fourier transform infrared (FTIR) and X-ray diffraction (XRD).

The point of zero charge (PZC) for the IOCZ was determined using the salt addition method (Tan et al. 2008; Mahmood et al. 2011). In the method, a sample mass of 0.200 g was added to 40.0 mL of 0.1 mol L^{-1} $NaNO_3$ solution. The pH was adjusted using a pH Benchtop meter (Thermo Scientific Orion Star A211, Germany) to 2, 3, 4, 5, 6, 7, 8, 9, 10, and 11 (±0.1 pH units), with 0.1 mol L^{-1} HNO_3 and 0.1 mol L^{-1} NaOH as needed in each centrifuge tube. These were then shaken for 24 h in an automated shaker (Labcon, South Africa) at 150 rpm to reach equilibrium. After settling, the final pH of each suspension was measured carefully. The ΔpH (the difference between final and initial pH) values were then plotted against the initial pH values. PZC was the pH value where ΔpH equals zero. Each set of experiments was done in triplicate, and the mean value was recorded.

2.3 Preparation of Stock Solutions

All chemicals used were of analytical grade and were purchased from Merck, South Africa. Uranium(VI) and arsenic(III) stock solutions of 1000 mg L^{-1} were prepared by dissolving appropriate amounts of $UO_2(NO_3)_2{\cdot}6H_2O$ and $NaAsO_2$, respectively, in deionized water. Working solutions were prepared by serial dilution of the stock solutions. Three solutions of 10 mg L^{-1} of co-ions, including Cd^{2+}, Co^{2+}, and Cu^{2+}, respectively, were prepared by the dissolution of known mass of their nitrate salts with deionized water. The initial pH values of the working solutions were adjusted by the addition of 0.5 mol L^{-1} NaOH or HNO_3 solutions.

In order to minimize the contamination of the samples, all glassware and polypropylene vessels were cleaned by soaking in detergent solution then acid bath and in deionized water each for 24 h. Before use, the vessels were rinsed several times with deionized water and air-dried.

2.4 Batch Adsorption Experiments

The setup of the two separate batches of experiments was the same for uranium and arsenic. In each case, elemental concentration, pH, kinetic, temperature, and effect of competing ions were assessed. The different procedures are described in paragraphs below.

2.4.1 Elemental Concentration Study

The effect of elemental concentration was studied by adding 1.0 g of IOCZ into polypropylene bottles containing 50 mL of U or As solutions at concentrations of 10, 20, 50, and 100 mg L^{-1}. The pH level of the solutions was adjusted with 0.1 mol L^{-1} solution $NaOH/HNO_3$ to the given pH value of 3. The mixture was shaken using an automated shaker (Labcon, SA) at 150 rpm for 5 h at a constant temperature (25 ± 1 °C). The optimum contact time evaluated from the kinetic experiments was used to perform these studies. The supernatant was filtered through a 0.45-μm pore cellulose nitrate membrane and then analyzed using an inductively coupled plasma optical emission spectroscopy (ICP-OES) (Kleve, Germany).

2.4.2 pH Study

The effect of varying solutions of pH on adsorbent performance was conducted by adding 1.0 g of IOCZ into polypropylene bottles containing 50 mL of 20 mg L^{-1} U or As solutions. The pH was varied by adding diluted solution of NaOH or HNO_3 dropwise to achieve pH values of 3, 5, and 8. The mixtures were agitated using automated shaker (Labcon, SA) at 150 rpm for 5 h at a constant temperature (25 ± 1 °C). After equilibration, the mixture was filtered through a 0.45-μm pore cellulose nitrate membrane. The supernatant was analyzed using an ICP-OES (Kleve, Germany).

2.4.3 Kinetic Study

The kinetic experiments were performed in a 1-L beaker containing 500 mL of 20 mg L^{-1} U(V) or As(III) solutions and 10.0 g of IOCZ. Solutions of uranium and arsenic were adjusted at pH 3 using diluted HNO_3. The mixture was shaken in an automated shaker (Labcon, SA) at 78 rpm, and the temperature was kept constant at 25 ± 1 °C. Samples were withdrawn at pre-determined time intervals (20, 30, 60, 90, 120, 150, and 180 s). The volume withdrawn at each pre-determined time was 5 mL (i.e., 1% of the total volume) to minimize the change in the ratio of elemental concentration to the adsorbent mass. The supernatant was analyzed using ICP-OES (Kleve, Germany).

2.4.4 Temperature Study

The effect of temperature was studied by adding 1.0 g of IOCZ into polypropylene bottles containing 50 mL of 20 mg L^{-1} U or As solutions at pH 3. The mixture was shaken at 24 and 30 °C (i.e., 297.15 and 303.15 K, respectively) using an automated shaker (Labcon, SA) set at 150 rpm for 5 h. At equilibrium, the mixture was filtered and the filtrate was analyzed by ICP-OES (Kleve, Germany).

2.4.5 The Presence of Competing Ions

The study of the effect of the presence of competing ions was done by adding 1.0 g of IOCZ into polypropylene bottles containing 50 mL of a mixture of Cd^{2+}, Cr^{3+}, and Cu^{2+}. U and As solutions were added to each bottle such that their concentrations were 10 mg L^{-1} while that of competing ions was 5 mg L^{-1}. The obtained mixtures (multi-ion solution and IOCZ) were shaken using an automated shaker (Labcon, USA) for 5 h at 150 rpm, and the temperature was kept constant at 25 ± 1 °C. At equilibrium, the mixture was filtered and the filtrate was analyzed by ICP-OES (Kleve, Germany).

All analyses were based on triplicate measurements with analytical errors (relative standard deviation) less than 10%.

2.5 Modeling of Analytical Results

2.5.1 Adsorption Capacity

The adsorption capacity (q_e) of IOCZ was calculated under various conditions using the following expression (Eq. (1)):

$$q_e = \frac{(C_0 - C_e)V}{M} \quad (1)$$

where C_0 is the initial U or As concentration in milligrams per liter and C_e the U or As concentration at equilibrium in milligrams per liter, V the volume of U or As solution (L), and M the mass of IOCZ adsorbent (g).

2.5.2 Adsorption Isotherms

The equilibrium adsorption isotherm is of importance in the design of adsorption systems (Langmuir 1918; Freundlich 1906; Dada et al. 2012). The equilibrium data obtained in the present study were analyzed using

the linear forms of the expressions of the Langmuir (Eq. (2)), Freundlich (Eq. (3)), and Dubinin–Radushkevich (D-R) (Eqs. (4) and (5)) isotherm models:

$$\frac{C_e}{q_e} = \frac{1}{q_m \cdot b} + \frac{C_e}{q_m} \tag{2}$$

$$\log q_e = \log K_F + \frac{1}{n} \cdot \log C_e \tag{3}$$

$$\ln(qe) = \ln(Xm) + \beta * F^2 \tag{4}$$

$$F = R * T * \ln\left(1 + 1/Ce\right) \tag{5}$$

where forEqs. (2) and (3), C_e is the equilibrium concentration (mg L^{-1}), q_e is the amount adsorbed at equilibrium (mg g^{-1}), q_m is the maximum amount of adsorbate per unit weight of adsorbent to form a complete monolayer on the surface (mg g^{-1}), b is the Langmuir isotherm constant (L mg^{-1}), related to the affinity of the adsorption sites, and K_F ((mg g^{-1}) (L $mg^{-1})^{1/n}$) and n are the Freundlich constants related to adsorption capacity and adsorption intensity of adsorbents, respectively.

For Eq. (4), Xm is the maximum sorption capacity of sorbent (mol/kg), β is a constant related to mean sorption energy (mol^2/kJ^2), F is the Polanyi potential, R is the gas law constant (kJ/(mol K)), and T is the absolute temperature (K).

The constants β and Xm were obtained from the slope and intercept of the plot of ln(qe) vs. F^2. The sorption energy (E_s) (kJ mol^{-1}) is correlated with β (the isotherm constant) by the following relationship:

$$E_s = \frac{1}{\sqrt{-2 \cdot \beta}}. \tag{6}$$

If E_s is less than 8 kJ mol^{-1}, the adsorption process is physisorption (i.e., an ion–ion attraction); if E_s is between 8 and 16 kJ mol^{-1}, the adsorption process is by ion exchange; and if E_s is greater than 16 kJ mol^{-1}, the adsorption process is chemisorption (typically via the formation of strong covalent bonds).

2.5.3 Adsorption Kinetic Study

The study of adsorption kinetics provides information about the mechanism of adsorption, which is important for the efficiency of the process and the prediction of the rate at which contaminants are removed from aqueous solutions. Several kinetic models are available to examine the controlling mechanism of the adsorption process and to test the experimental data.

The rate constants of the adsorbate removal from the solution by IOCZ composites were determined using the Lagergren pseudo first-order equation (Eq. (7)) (Aksu 2002; Fungaro et al. 2012) and the pseudo second-order equation (Eq. (8)) (Ho et al. 1999):

$$\log(q_e - q_t) = \log(q_e) - \frac{k_1 \cdot t}{2.303} \tag{7}$$

$$\frac{t}{q_t} = \frac{1}{k_2 \cdot q_e^2} + \frac{1}{q_e} \cdot t \tag{8}$$

where q_e is the amount of ion adsorbed at equilibrium (mg g^{-1}), q_t is the amount of ion adsorbed at time t (mg g^{-1}), k_1 is the rate constant for the pseudo first-order model (min^{-1}), and k_2 is the rate constant for the pseudo second-order model (g mg^{-1} min^{-1}).

2.5.4 Thermodynamic Study

The thermodynamic parameters, namely the Gibbs free energy change, ΔG^o (kJ mol^{-1}), enthalpy change, ΔH^o (kJ mol^{-1}), and entropy change, ΔS^o (kJ (mol K)$^{-1}$), for the specific adsorption were calculated using Eqs. (9) and (10) (Unlu and Ersoz 2007; Wang and Chen 2006):

$$\Delta G^o = -R.T.\ ln\ K_C \tag{9}$$

$$\Delta G^o = \Delta H^o - T(\Delta S^o) \tag{10}$$

where R is the universal gas constant (8.314 J mol^{-1} K^{-1}), T is the absolute temperature in Kelvin, and K_C is the equilibrium constant (L g^{-1}). Enthalpy change, ΔH^o, and entropy change, ΔS^o, were determined from the slope and intercept of the plot according to Eq. (10).

2.5.5 Mathematical Modeling and Statistical Interpretation

The validity for each model is found by the use of a normalized standard deviation $\Delta q(\%)$ which can be calculated from the following Eq. (11):

$$\Delta q(\%) = 100\sqrt{\frac{\sum_{i=1}^{n}\left[\frac{q_{\exp} - q_{calc}}{q_{\exp}}\right]^2}{n-1}} \tag{11}$$

where q_{exp} is the experimental metal ion removal, q_{cal} is the calculated amount of metal ions adsorbed, and n is the number of data points.

The goodness-of-fit of the models to the experimental data is found by the comparison of the correlation coefficients (i.e., R^2).

2.5.6 Elemental Speciation Study

The speciation of U and As in solution was studied using the Hydra and MEDUSA geochemical modeling code database (Puigdomenech 1999). The code assumes a state of thermodynamic equilibrium for the solutions under consideration and based on this calculates the species distribution under the given solution conditions. It should be noted here that speciation models do not require any calibration as this is done intrinsically in the models.

3 Results and Discussion

3.1 Characterization of Zeolite

The chemical composition of the natural zeolite used in this study was performed using XRF and the results are presented in Table 1.

The cationic exchange capacity was 23.16 meq/100 g, obtained according to the $BaCl_2$ method with Na^+, K^+, Ca^{2+}, and Mg^{2+} being the exchangeable cations in the zeolite cavities (Gillman and Sumpter 1986). The surface area and the average pore volume were 18.07 m^2/g and 0.0968 cm^3/g, respectively.

FTIR and PXRD Analysis of Na–Zeolite and IOCZ Figure 1 shows the FTIR spectra for Na–zeolite (Na-Z) as well as that for the IOCZ. Peaks were depicted at 3434 cm^{-1} (O–H stretch); 1631 cm^{-1} (O–H bend); 1106 cm^{-1} (Si–O) and 795 cm^{-1} (Al–O); and 536 cm^{-1} (O–H bend out of plane). The presence of iron oxide was confirmed by the new peak at 2925 cm^{-1}.

Table 1 Chemical composition of the natural zeolite

Constituent	Value (%)
SiO_2	77.36
Al_2O_3	12.96
CaO	1.42
Fe_2O_3	0.13
Na_2O	1.62
K_2O	4.0
MgO	0.92
LOI	11.96

The powder X-ray diffraction (PXRD) patterns (not shown here) depicted clinoptilolite ($(Na,K,Ca)_{2-3}Al_3(Al,Si)_2\ Si_{13}\ O_{36}12H_2O$) as the predominant mineral in the natural zeolite. The PXRD pattern of IOCZ revealed the presence of 23.98% of Fe_2O_3; an increase of 22.85% compared to natural zeolite confirms the coating of iron oxide on the surface of zeolite.

3.2 Adsorption Studies

3.2.1 Effect of Initial Uranium and Arsenic Concentration

The results for the adsorption of U and As with respect to change in initial concentration are presented in Fig. 2. The results showed an increase of adsorption capacity with an increase in the initial concentration from 10 to 100 mg L^{-1} for both elements. The results indicated that the adsorption capacity of U(VI) and of As(III) increased from 1.247 to 20.10 mg g^{-1} and from 3.115 to 54.18 mg g^{-1}, respectively, as the elemental concentration increased from 10 to 100 mg L^{-1}. The adsorption of As was generally higher (~2 times more) than that of uranium. The saturation point was not reached up to a concentration of 100 mg L^{-1} for both arsenic and uranium.

The increase may be attributed to more elemental ions being available for the adsorption sites as the concentrations increased. The higher adsorption of As compared to U will be explained later when the mechanisms of adsorption are assessed.

3.2.2 Adsorption Isotherms

As aforementioned, Langmuir, Freundlich, and Dubinin–Radushkevich (D-R) isotherms were used to quantitatively describe elemental sorption by IOCZ. The correlation coefficient (R^2) values were used to determine the most fitted model among all the three written above. The isotherm parameters as well as the related correlation coefficients are listed in Table 2.

Based on the correlation coefficient (R^2), the Freundlich model yielded a better fit for both elements ($R^2 = 0.942$ for U and 0.981 for As). The fit to the Freundlich isotherm may be attributed to the heterogenous distribution of active sites on the IOCZ surface (Bakatula et al. 2014). This model assumes adsorption onto a heterogenous surface where different sites could have different energies. The values of the mean free energy (Es) calculated from the D-R isotherm were

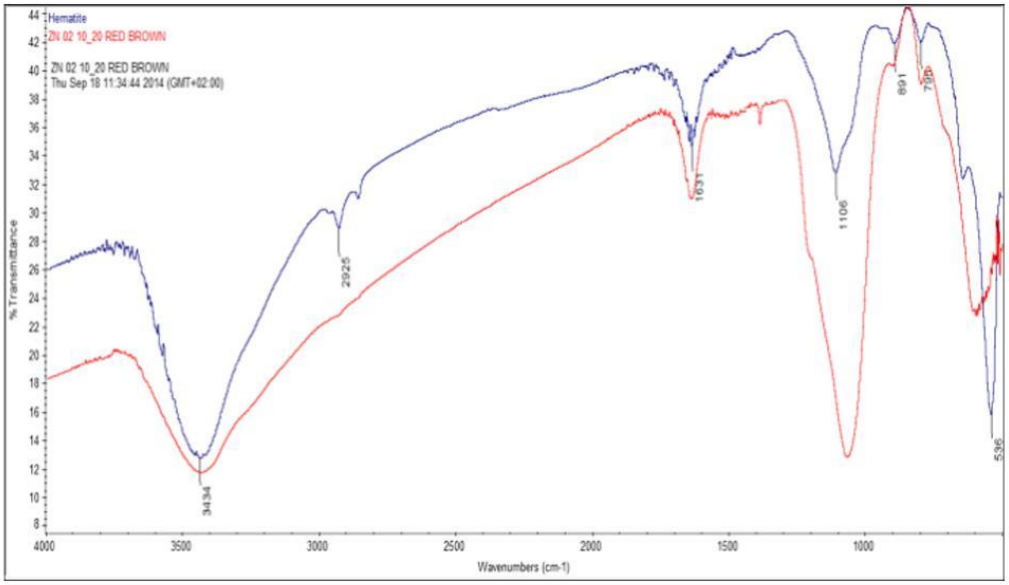


Fig. 1 FTIR spectra of Na–zeolite and IOCZ

8.213 kJ mol^{-1} for uranium and 8.895 kJ mol^{-1} for arsenic, indicating an ion exchange mechanism for both elements. The following mechanism is suggested:

Firstly, the charge on the surface of iron oxides results from the dissociation of the surface hydroxyl groups (Eq. (12)) (Wang et al. 2010).

$$Fe_2O_3 \xrightarrow[H_2O]{\text{Hydroxylation}} \equiv FeOH \begin{cases} \xrightarrow{\text{Protonation}} FeOH_2^+ \\ \xrightarrow{\text{Deprotonation}} FeO^- + H^+ \end{cases}$$

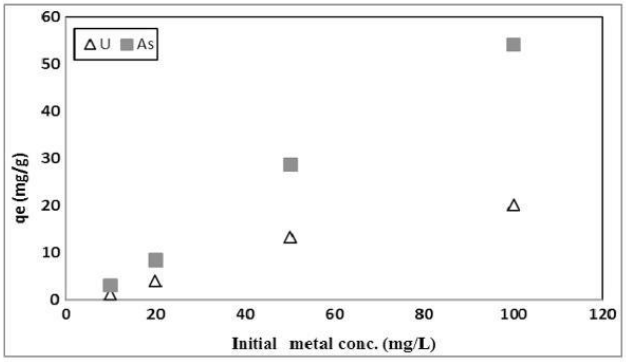


Fig. 2 Effect of U(V) and As(III) concentrations on their adsorption onto IOCZ (pH = 3, temp = 25 °C, contact time = 5 h) ($n = 3$ and RSD <10%)

Table 2 Langmuir, Freundlich, and D-R constant values for the sorption of U and As on IOCZ

	Langmuir constant				Freundlich constant				D-R constant			
	b (L mg^{-1})	q_m (mol kg^{-1})	R^2	Δq (%)	n	K_F (mg g^{-1})	R^2	Δq (%)	Xm (mol kg^{-1})	E_s (kJ mol^{-1})	R^2	Δq (%)
U	21,606	0.019	0.293	26.51	1.999	1.022	0.942	20.77	0.958	8.213	0.928	25.71
As	3889	0.034	0.623	21.24	1.893	1.012	0.981	11.28	0.919	7.295	0.947	36.73

Furthermore, the surface charge of iron oxide coated onto zeolite becomes more positive in acidic conditions due to protonation, resulting in an increase of adsorption sites for As (Jeon et al. 2009).

Secondly, the hydroxyl ion is exchanged with the arsenite ion:

$$Fe{-}OH + H_2AsO_3^- \rightarrow Fe{-}OAsO_2H + OH^-. \quad (13)$$

Previous studies revealed that sorption of As(V) as well as As(III) onto soil constituents, such as aluminum and iron oxides, happens through an inner-sphere complex via a ligand-exchange mechanism (Lumsdon et al. 1984; Sun and Doner 1996; Waychunas et al. 1993). This means that arsenic ions interacted with iron-modified zeolite surfaces in acid/base equilibrium, where underlying Fe ions act as a Lewis acid by exchanging the hydroxyl ion for other ligands to form surface complexes. Interaction between the surface hydroxyl groups and protons as well as ligand exchange provides iron oxides with high affinity to both arsenate and arsenite, both of which are Lewis bases (electron pair donors).

The maximum capacities q_m (mol kg^{-1}) determined from the Langmuir isotherm, defining the total capacity of IOCZ for uranium(VI) as well as As(III), were 0.019 and 0.034, respectively.

The Freundlich constant, K_F, (adsorption capacity, mg g^{-1}) values were 1.022 and 1.012, respectively, for uranium and arsenic. The subunitary values of the ratio $1/n$ suggest that the adsorption was favorable (Taffarel and Rubio 2010) and that the elements were bound with weak sorption energies (Özer et al. 1997). These results indicate that IOCZ has a very strong adsorption capacity for U(VI) and As(III) in the solution. When comparing the statistical results of the three models applied in this work (Table 2), the Freundlich isotherm was found to better predict the adsorption of U(VI) and As(III) onto IOCZ.

In previous studies, the Freundlich isotherm was reported to be suitable to represent arsenic adsorption processes by a wide range of iron containing adsorbents, including iron-pretreated activated carbon (Mondal et al. 2009), granular ferric hydroxide (Badruzzaman et al. 2004), and iron oxide-coated sand (Thirunavukkarasu et al. 2002).

3.2.3 The Effect of Initial pH

The initial pH of the solution is an important factor that must be considered during adsorption studies. The pH has two kinds of influence on elemental sorption, namely an effect on the solubility and speciation of the ions in

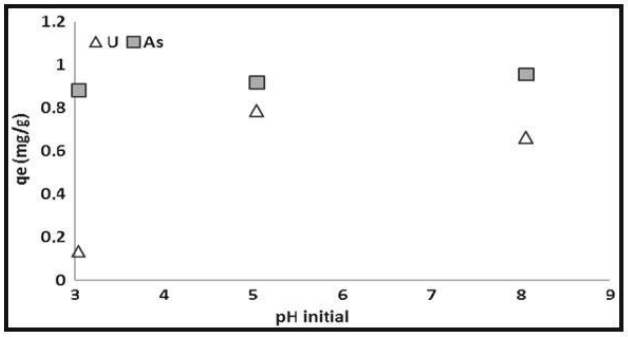


Fig. 3 Effect of pH on the adsorption of U and As on IOCZ (temp = 25 °C, C_i = 20 mg L^{-1}, contact time = 5 h) (n = 3 and RSD <10%)

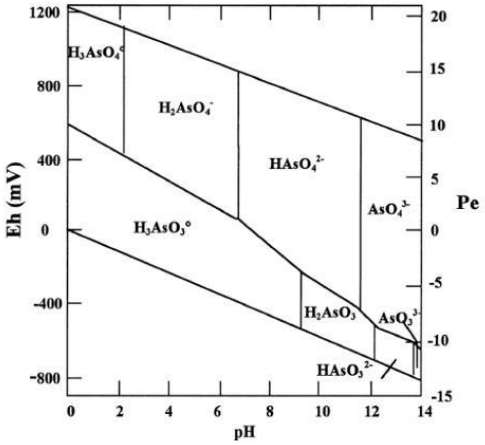


Fig. 4 Eh–pH diagram for aqueous arsenic species in the system AsO_2–H_2O at 25 °C (re-printed with permission from Smedley and Kinniburgh 2002)

solution and on the overall charge of the adsorbent. The adsorption of U and As was studied at pH 3, 5, and 8, which is the pH regime of most of gold mine waters in the Witwatersrand. The results of the effect of pH are shown in Fig. 3.

As seen in Fig. 3, the adsorption efficiency of As(III) on IOCZ was not much affected by the solution pH (pH 3 to 8). In fact, arsenic exists as oxyanions across pH ranges 2 to 8, as represented by the speciation diagram in Fig. 4. The diagram depicted $H_2AsO_4^-$ as the only dissolved species from pH 3 to 7 and $H_2AsO_4^{-2}$ at pH >7. Therefore, $(H_2AsO_4)^-$ being the most abundant species of As at the pH range studied, this explained the trend seen in the Fig. 3, almost no variation in adsorption capacity with the variation of solution pH. Similar trend was observed by Jeon et al. (2009) when adsorbing arsenic on iron-coated zeolite. As explained in the previous paragraph, the adsorption of arsenic on IOCZ followed an ion exchange process. This means that the surface charge of the adsorbent had no effect on the adsorption. Thus, it was concluded that adsorption of arsenic from aqueous solutions is independent of pH.

The relative abundance of various uranium(VI) species is a strong function of pH and composition of solution. The strong dependence of adsorption on pH can be explained by changes in the IOCZ surface charge and U speciation with pH. The pH_{PZC} of 10.4 means that at the pH range of the experiments, the surface charge of the IOCZ was positive. Thus, the predominance of U species will greatly influence its adsorption. The distribution of uranium species as a function of pH is presented in Fig. 5. At low pH (3–5), the UO_2^{2+} was predominant. Since both the uranyl ion and the adsorbent have net positive charges, the repulsion by the positive surface could explain the low removal of uranium by IOCZ. At pH 5–6, the neutral $UO_2(OH)_2{\cdot}H_2O$ (schoepite) was the most abundant species. This would likely precipitate on the adsorbent, and thus, the observed increase in adsorption may be a combination of precipitation and adsorption. At pH >6, negatively charged species, i.e., $UO_2(OH)_3^-$ and $UO_2(OH)_3^{2-}$, were dominant. More U would have been expected to be adsorbed, but the contrary was observed. This could suggest that the positively charged sites begin to

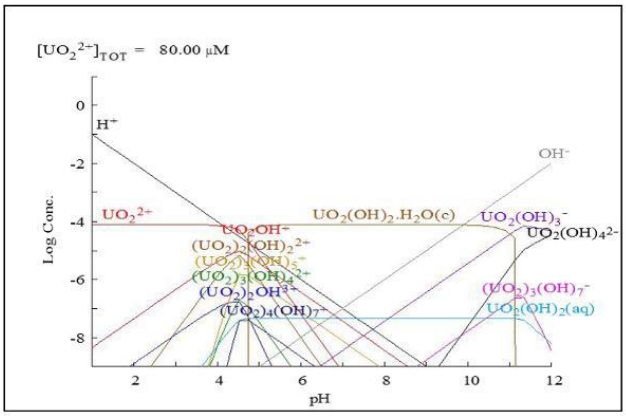


Fig. 5 Speciation of uranium in a uranium–water system at 25 °C and $I = 0$ M calculated using Hydra and MEDUSA speciation modeling freeware versions (Bakatula et al. 2015)

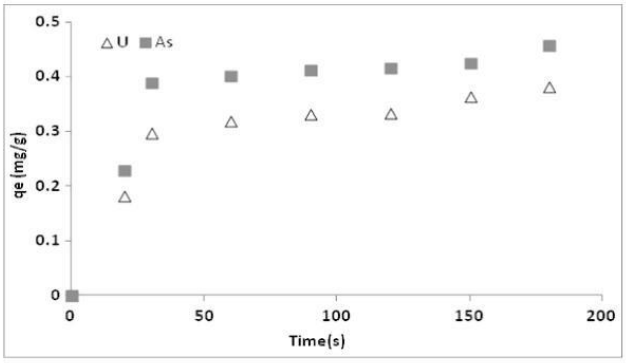


Fig. 6 Adsorption kinetics of U(VI) and As(III) onto IOCZ (temp = 25 °C, C_i = 20 mg L^{-1}, pH = 3) (n = 3 and RSD <10%)

decrease at those higher pH values that are close to the pH_{PZC}, leading to decreased adsorption of negatively charged U species.

Further work involving surface complexation modeling would have to be conducted to comprehensively understand the mechanism behind U adsorption as pH changes.

3.2.4 Adsorption Kinetics

Figure 6 illustrates adsorption kinetics of uranium and arsenic onto IOCZ. Adsorption kinetic studies showed a rapid removal of U(VI) and As(III) within the first 30 s to achieve equilibrium. The adsorption kinetics can be divided into two linear stages: (i) the rapid adsorption phase and (ii) the second stage of steady state, where the adsorption reached a plateau.

The change in the adsorption rate during adsorption could be explained by the availability of a large number of free adsorption sites on the surface of the adsorbent in the beginning of the reaction.

Kinetic Parameters The pseudo first-order and pseudo second-order models were applied to the kinetic data of uranium and arsenic adsorption onto IOCZ to investigate the mechanism of the adsorption process and determine the rate controlling step in the overall adsorption process. The kinetic parameters and correlation coefficients (R^2) for the two kinetic models were calculated from the linear plots of $\log(q_e - q_t)$ vs. t and t/q_t vs. t, respectively, and are listed in Table 3.

Based on the correlation coefficients, the pseudo second-order kinetic model represented the uranium and arsenic uptake best. The plots of q_t/t vs. t showed good linearity (Fig. 7) with high correlation coefficients (0.989 for U(VI) 0.991 and for As(III)). In addition, the equilibrium uptake calculated from the kinetic plots ($q_{e,cal}$) agreed well with the experimental values ($q_{e,exp}$, 0.363 and 0.421 mg/g for U(VI) and As(III), respectively.

Therefore, the sorption kinetics was well described by the pseudo second-order kinetics, which implied that the uranium and arsenic uptake by IOCZ was due to chemisorption.

The pseudo second-order kinetic model has been used to describe uranium and arsenic uptake by other iron containing adsorbents (Gu and Deng 2007; Guo and Chen 2005; Fierro et al. 2009).

Table 3 Kinetic parameters of the adsorption of U and As on IOCZ

Metal	Pseudo first-order				Pseudo second-order			
	k_1 min^{-1}	$q_{e(calc)}$ mg g^{-1}	R^2	Δq [%]	k_2 [mol (kg min)$^{-1}$]	$q_{e(calc)}$ mg g^{-1}	R^2	Δq [%]
U	0.151	1.208	0.864	88.35	49.48	0.348	0.989	13.14
As	0.129	1.149	0.736	86.23	17.06	0.459	0.995	14.67

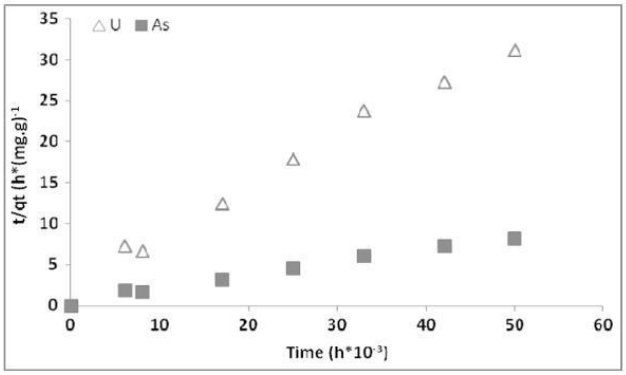


Fig. 7 Pseudo second-order kinetic model for the adsorption of uranium and arsenic on IOCZ

3.2.5 Effect of Temperature

The adsorption of U(VI) and As(V) was assessed at two different temperatures: 297.15 and 303.15 K. Thermodynamic parameters, i.e., enthalpy change (ΔH^{o}), free energy change (ΔG^{o}), and entropy change (ΔS^{o}), were calculated from the experimental data and the results are presented in Table 4. Raising the temperature of the metal solutions led to a decrease of the adsorption capacity of 8.5 and 27.5% for U and As, respectively. These results were confirmed by the negative values of enthalpy change, suggesting that the adsorption of both elements was exothermic. The ΔH° for the present process was found to be negative (−124.9 and −16.25 kJ mol^{-1}, for U and As, respectively), which proves the exothermic nature of the sorption reaction. The standard free energies ΔG^{o} for the sorption of uranium, obtained from Eq. (8), were −4.429 and 1.787 kJ mol^{-1} at 297.15 and 303.15 K, respectively. The negative value of ΔG^{o} depicts a spontaneous adsorption process. The standard free energy ΔG^{o} for As was close to 0 (0.138 kJ mol^{-1}), implying that the removal of As was spontaneous. A more positive ΔG^{o} with the increment of temperature implies a non-favorable reaction at higher temperature, which is a characteristic of exothermic surface process. The entropy changes (ΔS^{o}) were positive for both U and As, suggesting a high affinity of the elements for the IOCZ. This also confirms the increased randomness at the solid–solution interface during adsorption.

3.2.6 Effect of Competing Ions

The presence of competing ions, such as Cd^{2+}, Cr^{3+}, and Cu^{2+}, can have a significant effect on uranium and arsenic adsorption onto IOCZ. The results of the effect of competing ion studies are presented in Table 5. The presence of Cd^{2+}, Cr^{3+}, and Cu^{2+} decreased the percentage of U(VI) adsorption by 13.77%, whereas adsorption of As(III) increased slightly by 9.21%.

The concentrations of competing ions in this study are those likely to be encountered in wastewater from some mining areas in South Africa (Bakatula et al. 2015). Thus, IOCZ is able to remove uranium and arsenic even at the presence of competing ions investigated in this study.

Table 4 Thermodynamic parameters of U and As on IOCZ

Metal	*qe*		*Ea*	ΔH	ΔS	ΔG	
	mg g^{-1}		kJ mol^{-1}	kJ mol^{-1}	kJ (mol K)$^{-1}$	kJ mol^{-1}	
	297.15 K	303.15 K				297.15 K	303.15 K
U	0.992	0.907	129.8	−124.9	0.376	−4.429	1.787
As	0.946	0.686	107.2	−16.25	4.812	0.138	0.933

Table 5 Effect of the presence of competing ions (Cd^{2+}, Cr^{3+}, and Cu^{2+})

	Multi-ions solution q_e (mg g^{-1})	Single-ion solution q_e (mg g^{-1})
U	0.457	0.530
As	0.498	0.456
Cd	0.249	
Cu	0.248	
Cr	0.250	

4 Conclusion

In this study, iron oxide-coated zeolite (IOCZ) was synthesized and used for the removal of U(VI) and As(V) from aqueous solutions. The equilibrium of adsorption was suitably described by the Freundlich models, depicting that adsorption on a heterogeneous surface. The process of adsorption was relatively rapid and was best described by the pseudo second-order kinetic model. The thermodynamic models showed that the adsorption of U and As was spontaneous and followed exothermic processes. Furthermore, IOCZ was able to adsorb uranium and arsenic in the presence of competing ions such as Cd^{2+}, Cr^{3+}, and Co^{2+}.

Further work should focus on comprehensively understanding the adsorption at various pH values as surface complexation may be an important process. The findings of the study can be used to design and understand systems applying zeolite for contaminant removal from industrial and mine-polluted water.

Acknowledgements The authors express their sincere gratitude to the University Research Committee (URC) Postdoc Fellowship and the National Research Foundation for financial support.

References

Agency for Toxic Substances and Disease Registry (ATSDR). (2000). *Toxicological profile for arsenic TP-92/09*. Georgia: Center for Disease Control, Atlanta.

Aksu, Z. (2002). Determination of the equilibrium, kinetic and thermodynamic parameters of the batch biosorption of lead(II) ions onto Chlorella vulgaris. *Process Biochemistry, 38*, 89–99.

Badruzzaman, M., Westerhoff, P., & Knappe, D. (2004). Intraparticle diffusion and adsorption of arsenate onto granular ferric hydroxide (GFH). *Water Research, 38*(18), 4002–4012.

Bakatula, E.N. (2012). *Development of a biophysical system based on bentonite, zeolite and micro-organisms for remediating gold mine wastewaters and tailings ponds*. Thesis, University of the Witwatersrand, 7–12.

Bakatula, E. N., Cukrowska, E. M., Weiersbye, I. M., Mihaly-Cozmuta, L., Peter, A., & Tutu, H. (2014). Biosorption of trace elements from aqueous systems in gold mining sites by the filamentous green algae (*Oedogonium* sp.). *Journal of Geochemical Exploration*. doi:10.1016/j.gexplo.2014.02.017.

Bakatula, E. N., Mosai, A. K., & Tutu, H. (2015). Removal of uranium from aqueous solutions using ammonium-modified zeolite. *South African Journal of Chemistry, 68*, 165–171.

Centeno, J.A., Tchounwou, P.B., Patlolla, A.K, Mullick, F.G., Murakat, L., & al. (2005). Environmental pathology and health effects of arsenic poisoning: a critical review. In: Naidu R, Smith E, Smith J, Bhattacharya P, (eds.) *Managing arsenic in the environment: from soil to human health*. Adelaide.

Dada, A. O., Olalekan, A. P., & Olatunya, A. M. (2012). Langmuir, Freundlich, Temkin and Dubinin–Radushkevich isotherms studies of equilibrium sorption of Zn^{2+} unto phosphoric acid modified rice husk. *Journal of Applied Chemistry, 3*(1), 38–45.

Department of water affairs and forestry (DWAF). https://www.dwaf.gov.za/iwqs/wq_guide/domestic.pdf Accessed on 19 May, 2015.

Feather, C. E., & Koen, G. M. (1975). The mineralogy of the Witwatersrand reefs. *Minerals Science and Engineering, 7*, 189–224.

Ferguson, J. F., & Gavis, J. (1972). A review of the arsenic cycle in natural waters. *Water Research, 6*, 1259–1274.

Fierro, V., Muiz, G., Gonzalez-Sánchez, G., Ballinas, M., & Celzard, A. (2009). Arsenic removal by iron-doped activated carbons prepared by ferric chloride forced hydrolysis. *Journal of Hazardous Materials, 168*(1), 430–437.

Freundlich, H. M. F. (1906). Over the adsorption in solution. *The Journal of Physical Chemistry, 57*, 385–470.

Fungaro, D. A., Yamaura, M., & Craesmeyer, G. R. (2012). Uranium removal from aqueous solution by zeolite from fly ash-iron oxide magnetic nanocomposite. *International Review of Chemical Engineering, 4*(3), 353–358.

Gillman, G. P., & Sumpter, E. A. (1986). Modification to the compulsive exchange method for measuring exchange characteristics of soils. *Australian Journal of Soil Research, 24*, 61–66.

Gu, Z., & Deng, B. (2007). Use of iron-containing mesoporous carbon (IMC) for arsenic removal from drinking water. *Environmental Engineering Science, 24*(1), 113–121.

Guo, X., & Chen, F. (2005). Preparation and evaluation of GAC-based iron-containing adsorbents for arsenic removal. *Environmental Science and Technology, 39*, 6808.

Hakonson-Hayes, A. C., Fresquez, P. R., & Whicker, F. W. (2002). Assessing potential risks from exposure to natural uranium in well water. *Journal of Environmental Radioactivity, 59*, 29–40.

Ho, Y. S., Wase, D. A. J., & Forester, C. F. (1999). Kinetic studies of competitive heavy metal adsorption by sphagnum peat. *Environmental Technology, 17*, 441–443.

Hsu, J. C., Lin, C. J., Liao, C. H., & Chen, S. T. (2008). Removal of As(V) and As(III) by reclaimed iron-oxide coated sands. *Journal of Hazardous Materials, 153*, 817–826.

Jeon, C. S., Baek, K., Park, J. K., Oh, Y. K., & Lee, S. D. (2009). Adsorption characteristics of As(V) on iron-coated zeolite. *Journal of Hazardous Materials, 163*, 804–808.

Kesunathan, G., M. Tumelo, M., & Moodley, K.G. (2006). *Paper for the COST Action 37 Workshop,* Berlin.

Langmuir, I. (1918). The adsorption of gases on plane surfaces of glass, mica and platinum. *Journal of the American Chemical Society, 40*, 1361–1403.

Lumsdon, D. G., Fraser, A. R., Russell, J. D., & Livesey, N. T. (1984). New infrared band assignments for the arsenate ion adsorbed on synthetic goethite (a-FeOOH*). Journal of Soil Science, 35*, 381–386.

Mahmood, T., Saddique, M. T., Naeem, A., Westerhoff, P., Mustafa, S., et al. (2011). Comparison of different methods for the point of zero charge determination of NiO. *Industrial & Engineering Chemistry Research, 50*, 10017–10023.

McCarthy, T.S., & and Pretorius, K. (2009). Coal mining on the Highveld and its future water quality in the Vaal river system. *International Mine Water Association*, ISBN Number: 978-0-9802623-5-3.

Mondal, P., Mohanty, B., Majumder, C., & Bhandari, N. (2009). Removal of arsenic from simulated groundwater by GAC-Fe: a modeling approach. *AICHE Journal, 55*(7), 1860–1871.

National Research Council. Arsenic in drinking water. (2001) Update. On line http://www.nap.edu/books/0309076293/html/.

Osborne, S. H., & Ehrlich, H. L. (1976). Oxidation of arsenite by a soil isolate of Alcaligenes. *Journal of Applied Bacteriology, 41*, 295–305.

Özer, A., Ekiz, I. H., Özer, D., Kutsul, T., & Caglar, A. (1997). A comparative study of the biosorption of cadmium(II) ions to S. leibleinil and R. arrhizis. *Chimica Acta Turica, 25*(1), 63–67.

Puigdomenech, I. (1999). *MEDUSA: make equilibrium diagrams using sophisticated algorithms, version 2. Inorganic Chemistry*. Stockholm7 Royal Institute of Technology (KTH). http://www.inorg.kth.se.

Reimold, W. U., & Gibson, R.J. (2006). *Processes on the early earth, geological society of America*, pp 354.

Robb, L. J., & Robb, V. M. (1998). Gold in the Witwatersrand basin. In M. G. C. Wilson & C. R. Maske (Eds.), *The mineral resources of South Africa* (6th ed., pp. 294–349). Pretoria: Council of Geoscience.

Sami, K. & Druzynski, A.L. (2003). *Final report to the water research commission for the project* "*mapping of naturally occurring hazardous trace constituents in groundwater*". WRC Report No. 1236/1/03, South Africa.

Smedley, P. L., & Kinniburgh, D. G. (2002). A review of the source, behaviour and distribution of arsenic in natural waters. *Applied Geochemistry, 17*(5), 517–568.

Smedley, P.L. & Kinniburgh, D.G. (2003). *Source and behaviour of arsenic in natural waters, chapter 1, Arsenic report*, WHO, pp 60, British Geological Survey, Wallingford, Oxon OX10 8BB, U.K.

Sun, X., & Doner, H. E. (1996). An investigation of arsenate and arsenite bonding structures on goethite by FTIR. *Soil Science, 161*, 865–872.

Taffarel, R. S., & Rubio, J. (2010). Removal of Mn^{2+} from aqueous solution by manganese oxide coated zeolite. *Minerals Engineering, 23*, 1131–1138.

Tan, W. F., Lu, S. J., Liu, F., Feng, X. H., He, J. Z., & Koopal, L. K. (2008). Determination of the point of zero charge of manganese oxides with different methods including an improved salt titration method. *Soil Science, 173*, 277.

Tchounwou, P. B., Patlolla, A. K., & Centeno, J. A. (2003). Carcinogenic and systemic health effects associated with arsenic exposure—a critical review. *Journal of Toxicologic Pathology, 31*, 575–588.

Tchounwou, P. B., Centeno, J. A., & Patlolla, A. K. (2004). Arsenic toxicity, mutagenesis and carcinogenesis—a health risk assessment and management approach. *Molecular and Cellular Biochemistry, 255*, 47–55.

Thirunavukkarasu, O., Viraraghavan, T., Subramanian, K., & Tanjore, S. (2002). Organic arsenic removal from drinking water. *Urban Water, 4*(4), 415–421.

Thirunavukkarasu, O. S., Viraraghavant, T., & Subramanian, K. S. (2003). Arsenic removal from drinking water using iron oxide-coated sand. *Water, Air, and Soil Pollution, 142*, 95–111.

Tutu, H. (2006). *Determination and geochemical modeling of the dispersal of uranium in gold-mine polluted land on the Witwatersrand*. PhD Thesis, University Witwatersrand, Johannesburg.

Tutu, H., McCarthy, T. S., & Cukrowska, E. M. (2008). The chemical characteristics of acid mine drainage with particular reference to sources, distribution and remediation: the Witwatersrand Basin, South Africa, as a case study. *Applied Geochemistry, 23*, 3666–3684.

Tutu, H., McCarthy, T. S., Cukrowska, E. M., Hart, R., & Chimuka, L. (2009). Radioactive disequilibrium and geochemical modelling as evidence of uranium leaching from gold tailings dumps in the Witwatersrand Basin. *International Journal of Environmental Analytical Chemistry, 89*(8–12), 687–703.

Unlu, N., & Ersoz, M. (2007). Removal of heavy metal ions by using dithiocarbamated-sporopollenin. *Separation and Purification Technology, 52*, 461.

Wang, J., & Chen, C. (2006). Biosorption of heavy metals by Saccharomyces cerevisiae: a review. *Biotechnology Advances, 24*(5), 427–451.

Wang, J., Li, X., Scott, J. I., Yue, Z., & Economy, J. (2010). Iron oxide-coated on glass fibers for arsenic removal. *Separation Science and Technology, 45*(8), 1058–1065.

Waychunas, G. A., Rea, B. A., Fuller, C. C., & Davis, J. A. (1993). Surface chemistry of ferrihydrite. 1. EXAFS studies of the geometry of coprecipitated and adsorbed arsenate. *Geochimica et Cosmochimica Acta, 57*(15), 2251–2269.

Winde, F. (2002). Uranium contamination in fluvial systems—mechanisms and processes. Part I: geochemical mobility of uranium along the water path—the Koekemoerspruit (South Africa) as a case study. *Cuardernos de Investigacion Geografica, 28*, 49–57. ISSN 0211–6820.

Winde, F. (2010). U pollution in the Wonderfonteinspruit: 1997–2008 part I: U-toxicity, regional background and mining-related sources of U-pollution. *Water SA, 36*(3), 239–256.

Winde, F. & Sandham, L.A. (2004). Uranium pollution of South African streams—an overview of the situation in gold mining areas of the Witwatersrand. Sustainable Water Management

in Africa-Chances and Barriers. Supplement volume, *GeoJournal*, *61*, 131–149.

World Health Organization (WHO) (2005). Uranium in drinking water: background document for development of WHO guidelines for drinking water quality (WHO/SDE/WSH/03.04/118). *World Health Organization*, 26 pp.

Yean, S., Cong, L., Yavuz, C. T., Mayo, J. T., Yu, W. W., et al. (2005). Effect of magnetite particle size on adsorption and desorption of arsenite and arsenate. *Journal of Materials Research, 20*(12), 3255–3264.

Yuan, T., Hu, J. Y., Ong, S. L., Luo, Q. F., & Ng, W. J. (2002). Arsenic removal from household drinking water by adsorption. *Journal of Environmental Science and Health, Part A: Toxic/Hazardous Substances & Environmental Engineering, 37*(9), 1721–1736.

Chapter 5

General conclusion and future work

In this section, conclusions based on experimental findings are discussed. The recommended future work is also presented in this section.

"Any new fact or insight that I may have found has not seemed to me as a 'discovery' of mine, but something that has been there and that I had chanced to pick up". ~ Subrahmanyan Chandrasekhar

5.1 Conclusion

Natural zeolite (i.e. clinoptilolite-containing material) has the capacity to effectively treat acid mine drainage by removing dissolved metal content. This research aimed at gaining insight on the influence the hydroxides and oxides of Fe coating on zeolite during field application will have on the adsorptive properties as the zeolite surfaces become modified and can be viewed as mixtures of zeolitic and Fe hydroxide and/or oxide surfaces.

The selectivity of iron (hydr) oxide modified zeolite towards As(V) was demonstrated in **paper I**. The removal of As(V) from both synthetic and real AMD was insignificantly affected by the solution pH indicating that adsorption likely followed a surface complexation process and was thus independent of pH. Speciation models for arsenic depicted $H_2AsO_4^-$ as the most abundant and dissolved species in the pH range studied. The pH_{PZC} of sorbent did not have an influence on the extraction of As(V), since no change was observed on the adsorption capacity beyond the pH_{PZC} (5.6 ±0.1).

In **paper II**, the same adsorbent was evaluated for its extraction capabilities for U(VI) from synthetic solution. The results demonstrated that the removal efficiency for U(VI) was strongly reliant on the solution pH. The extraction efficiency increased with an increase in solution pH until the pH_{PZC} of the adsorbent and then declined slowly with a further increment in pH. This was attributed to repulsion between the negatively charged U(VI) species and the negative charge on surface of the sorbent.

A novel nanocomposite iron-oxide coated zeolite sorbent was synthesized (**paper III**); in-order to gain insight into the effect of the maturation of amorphous Fe hydroxide to crystalline iron oxide in the form of Fe_2O_3 will have on the sorption of U(VI) and As(III). The results demonstrated that the sorption efficiency of As(III) was insignificantly influenced by the solution pH, whereas the opposite was observed for the extraction of U(VI). This study clearly established that coating of zeolite by Fe hydroxide/oxide plays a vital role in the adsorption of U(VI), As(III)

and As(V) from AMD, a phenomenon that will have a significant bearing on a large-scale remediation situation based on zeolite.

The adsorption capacities of As onto zeolite modified with iron hydroxide/oxide were found to be higher than for natural zeolite while those of U were found to be lower. The implications of these observations in a field application are that the performance of natural zeolite will decrease over time for U following quotation by iron hydroxide/oxide while that for As will increase. Thus, breakthroughs and subsequent increase in U concentrations would be expected in a zeolitic system that has been deployed for longer and has had sufficient modification of its surface through precipitation of iron hydroxides/oxides.

5.2 Future work

The future work can focus on performing column studies using modified zeolite. These will give a better perspective of the point made in the last paragraph in the preceding text. Column studies will draw from the batch studies that have been conducted and will enable the establishment of actual field parameters to be used e.g. bed length, breakthrough volumes (and essentially replacement times) and flow rate among others. With these established, it will be possible to use the modified zeolite system in a variety of contexts, the main one being a permeable reactive barrier integrated into the flow path of the contaminated water.

References

Adler, R.A., Claassen, M., Godfrey, L. and Turton, A.R. (2007) Water, mining, and waste: an historical and economic perspective on conflict management in South Africa, *The economics of peace and security journal*, 2, 32-41.

Akcil, A. and Koldas, S. (2006) Acid Mine Drainage (AMD): causes, treatment and case studies, *Journal of Cleaner Production*, 14, 1139-1145.

Bell, F.G., Bullock, S.E.T., Hälbich, T.F.J. and Lindsay, P. (2001) Environmental impacts associated with an abandoned mine in the Witbank Coalfield, South Africa, *International Journal of Coal Geology*, 45, 195-216.

Blowes, D.W., Ptacek, C.J., Jambor, J.L. and Weisener, C.G. (2003) The geochemistry of acid mine drainage, *Treatise on geochemistry*, 9, 612.

Bowman, R.S. (2003) Applications of surfactant-modified zeolites to environmental remediation. *Microporous and Mesoporous Materials*, 61, 43-56.

Cawthorn, R.G. (2010) The platinum group element deposits of the Bushveld Complex in South Africa, Platinum Metals Review, 54, 205-215.

Chutia, P., Kato, S., Kojima, T. and Satokawa, S. (2009) Arsenic adsorption from aqueous solution on synthetic zeolites. *Journal of Hazardous Materials*, 162, 440-447.

Erdem, E., Karapinar, N. and Donat, R. (2004) The removal of heavy metal cations by natural zeolites. *Journal of colloid and interface science*, 280, 309-314.

Enslin, F., Van der Mey, L. and Waanders, F. (2010) Acid leaching of heavy metals from bentonite clay, used in the cleaning of acid mine drainage, *Journal of The Southern African Institute of Mining and Metallurgy*, 110, 187-191.

Espana, J.S., Pamo, E.L., Santofimia, E., Aduvire, O., Reyes, J. and Barettino, D. (2005) Acid mine drainage in the Iberian Pyrite Belt (Odiel river watershed, Huelva, SW Spain): geochemistry, mineralogy and environmental implications, *Applied geochemistry*, 20, 1320-1356.

Febrianto, J., Kosasih, A.N., Sunarso, J., Ju, Y.H., Indraswati, N. and Ismadji, S. (2009) Equilibrium and kinetic studies in adsorption of heavy metals using biosorbent: a summary of recent studies. *Journal of hazardous materials*, 162, 616-645.

Gitari, M.W., Petrik, L.F., Etchebers, O., Key, D.L., Iwuoha, E. and Okujeni, C. (2006) Treatment of acid mine drainage with fly ash: removal of major

contaminants and trace elements, *Journal of Environmental Science and Health Part A*, 41, 1729-1747.

Gray, N.F. (1997) Environmental impact and remediation of acid mine drainage: a management problem, *Environmental Geology*, 30, 62-71.

http://www.southafrica.info/travel/advice/climate.htm#.WElMm9V96M8 (Accessed on 8 December 2016; 02:07)

Hubicki, Z. and Kołodyńska, D. (2012) Selective removal of heavy metal ions from waters and waste waters using ion exchange methods. INTECH Open Access Publisher.

Johnson, D.B. and Hallberg, K.B. (2005) Acid mine drainage remediation options: a review, *Science of the total environment*, 338, 3-14.

Li, L.Y., Tazaki, K., Lai, R., Shiraki, K., Asada, R., Watanabe, H. and Chen, M. (2008) Treatment of acid rock drainage by clinoptilolite—adsorptivity and structural stability for different pH environments. *Applied Clay Science*, 39, 1-9.

Martinson, C.A. and Reddy, K.J. (2009) Adsorption of arsenic (III) and arsenic (V) by cupric oxide nanoparticles. *Journal of Colloid and Interface Science*, 336, 406-411.

Martí-Calatayud, M.C., Buzzi, D.C., García-Gabaldón, M., Ortega, E., Bernardes, A.M., Tenorio, J.A.S. and Pérez-Herranz, V. (2014) Sulfuric acid recovery from acid mine drainage by means of electrodialysis. *Desalination*, 343, 120-127.

Masindi, V., Gitari, M.W., Tutu, H. and De Beer, M. (2016) Fate of inorganic contaminants post treatment of acid mine drainage by cryptocrystalline magnesite: Complimenting experimental results with a geochemical model, *Journal of Environmental Chemical Engineering*, 4, 4846-4856.

Matlock, M.M., Howerton, B.S. and Atwood, D.A. (2002) Chemical precipitation of heavy metals from acid mine drainage. *Water research*, 36, 4757-4764.

Mendez, M.O., Glenn, E.P. and Maier, R.M. (2007) Phytostabilization potential of quailbush for mine tailings, *Journal of Environmental Quality*, 36, 245-253.

Mendez, M.O. and Maier, R.M. (2008) Phytostabilization of mine tailings in arid and semiarid environments-an emerging remediation technology, *Environmental Health Perspectives*, 116, 278.

Motsi, T., Rowson, N.A. and Simmons, M.J.H. (2009) Adsorption of heavy metals from acid mine drainage by natural zeolite. *International Journal of Mineral Processing*, 92, 42-48.

Motsi, T. (2010). Remediation of acid mine drainage using natural zeolite (Doctoral dissertation, University of Birmingham).

Neculita, C.M., Zagury, G.J. and Bussière, B. (2007) Passive treatment of acid mine drainage in bioreactors using sulfate-reducing bacteria, *Journal of Environmental Quality*, 36, 1-16.

Naicker, K., Cukrowska, E. and McCarthy, T.S. (2003) Acid mine drainage arising from gold mining activity in Johannesburg, South Africa and environs. *Environmental pollution*, 122, 29-40.

Nganje, T.N., Adamu, C.I., Ntekim, E.E.U., Ugbaja, A.N., Neji, P. and Nfor, E.N. (2010) Influence of mine drainage on water quality along River Nyaba in Enugu South-Eastern Nigeria, *African Journal of Environmental Science and Technology*, 4.

Oke, I.A., Olarinoye, N.O. and Adewusi, S.R.A. (2008) Adsorption kinetics for arsenic removal from aqueous solutions by untreated powdered eggshell. *Adsorption*, 14, 73-83.

Peng, J.F., Song, Y.H., Yuan, P., Cui, X.Y. and Qiu, G.L. (2009) The remediation of heavy metals contaminated sediment. *Journal of hazardous materials*, 161, 633-640.

Polat, E., Karaca, M., Demir, H. and Onus, A.N. (2004) Use of natural zeolite (clinoptilolite) in agriculture. *Journal of fruit and ornamental plant research*, 12, 183-189.

Pokhrel, D. and Viraraghavan, T. (2008) Arsenic removal from an aqueous solution by modified A. niger biomass: batch kinetic and isotherm studies. Journal of Hazardous Materials, 150, 818-825.

Rösner, T. and Van Schalkwyk, A. (2000) The environmental impact of gold mine tailings footprints in the Johannesburg region, South Africa, *Bulletin of Engineering Geology and the Environment*, 59, 137-148.

Rosario, K., Iverson, S.L., Henderson, D.A., Chartrand, S., McKeon, C., Glenn, E.P. and Maier, R.M. (2007) Bacterial community changes during plant

establishment at the San Pedro River mine tailings site, *Journal of environmental quality*, 36, 1249-1259.

Saada, A., Breeze, D., Crouzet, C., Cornu, S. and Baranger, P. (2003) Adsorption of arsenic (V) on kaolinite and on kaolinite–humic acid complexes: role of humic acid nitrogen groups. *Chemosphere*, 51, 757-763.

Simate, G.S. and Ndlovu, S. (2014) Acid mine drainage: Challenges and opportunities. *Journal of Environmental Chemical Engineering*, 2, 1785-1803.

Stumm, W. and Morgan, J.J. (1996) Aquatic Chemistry: Chemical Equilibria and Rates in Natural Waters {*Environmental Science and Technology*}. Wiley.

Sprynskyy, M., Buszewski, B., Terzyk, A.P. and Namieśnik, J. (2006) Study of the selection mechanism of heavy metal (Pb 2+, Cu 2+, Ni 2+, and Cd 2+) adsorption on clinoptilolite, *Journal of colloid and interface science*, 304, 21-28.

Tutu, H., McCarthy, T.S. and Cukrowska, E. (2008) The chemical characteristics of acid mine drainage with particular reference to sources, distribution and remediation: The Witwatersrand Basin, South Africa as a case study, *Applied Geochemistry*, 23, 3666-3684.

Tutu, H., Cukrowska, E.M., McCarthy, T.S., Hart, R. and Chimuka, L. (2009) Radioactive disequilibrium and geochemical modelling as evidence of uranium leaching from gold tailings dumps in the Witwatersrand Basin. *International Journal of Environmental and Analytical Chemistry*, 89, 687-703.

Ye, Z.H., Shu, W.S., Zhang, Z.Q., Lan, C.Y. and Wong, M.H. (2002) Evaluation of major constraints to revegetation of lead/zinc mine tailings using bioassay techniques, *Chemosphere*, 47, 1103-1111.

Yavuz, Ö., Altunkaynak, Y. and Güzel, F. (2003) Removal of copper, nickel, cobalt and manganese from aqueous solution by kaolinite. *Water research*, 37, 948-952.

Zhong, C.M., Xu, Z.L., Fang, X.H. and Cheng, L. (2007) Treatment of acid mine drainage (AMD) by ultra-low-pressure reverse osmosis and nanofiltration. *Environmental Engineering Science*, 24, 1297-1306.

Wang, S. and Peng, Y. (2010) Natural zeolites as effective adsorbents in water and wastewater treatment. *Chemical Engineering Journal*, 156, 11-24.

Wei, X., Viadero Jr, R.C. and Buzby, K.M. (2005) Recovery of iron and aluminum from acid mine drainage by selective precipitation. *Environmental Engineering Science*, 22, 745-755.

Wingenfelder, U., Hansen, C., Furrer, G. and Schulin, R. (2005) Removal of heavy metals from mine waters by natural zeolites. *Environmental Science & Technology*, 39, 4606-4613.